

# OPTICAL PROPERTIES AND VISUAL EFFECTS OF SMOKE-STACK PLUMES

A Cooperative Study:

Edison Electric Institute and U.S. Public Health Service

William D. Conner  
National Environmental Research Center, RTP

J. Raymond Hodkinson  
Department of Physics, Virginia State College

ENVIRONMENTAL PROTECTION AGENCY  
Office of Air Programs  
Research Triangle Park, N. C.  
Revised May 1972

---

**Allow \_\_\_\_\_ picas**  
**Margin to trim**

The AP series of reports is issued by the Environmental Protection Agency to report the results of scientific and engineering studies, and information of general interest in the field of air pollution. Information presented in this series includes coverage of intramural activities involving air pollution research and control technology and of cooperative programs and studies conducted in conjunction with state and local agencies, research institutes, and industrial organizations. Copies of AP reports are available free of charge - as supplies permit - from the Office of Technical Information and Publications, Office of Air Programs, Environmental Protection Agency, Research Triangle Park, North Carolina 27711.

2nd printing May 1972

1st printing 1967

Office of Air Programs Publication No. AP-30

For sale by the Superintendent of Documents, U.S. Government Printing Office  
Washington, D.C. 20402 - Price 45 cents  
Stock Number 5503-0037

## FOREWORD

In 1961, the Edison Electric Institute on the recommendations of its Prime Movers Committee and the National Center for Air Pollution Control (formerly the Division of Air Pollution), Public Health Service, U.S. Department of Health, Education, and Welfare initiated a study of the optical properties and visual effects of smoke plumes. The cooperative project, which was originally proposed by the Pacific Gas and Electric Company, was established to provide technical information on the evaluation of smoke plumes from a distance. Such information will be helpful to agencies and organizations concerned with regulating plume emissions to control air pollution. The study was conducted with the guidance of a joint steering committee from the Prime Movers Committee of the Edison Electric Institute and Public Health Service. EEI members of the Committee were:

- V. F. Estcourt, Chairman, Pacific Gas and Electric Co.,  
1961-64
- P. Matthew, Chairman, Pacific Gas and Electric Co.,  
1964-67
- T. M. Hotchkiss, Southern California Edison Co.,  
1961-63
- J. U. Baley, Baltimore Gas and Electric Co., 1963-67
- E. M. Parrish, Duquesne Light Co., 1961-65
- V. L. Stone, Commonwealth Edison Co., 1961-67

Public Health Service members from the National Center for Air Pollution Control were:

- J. H. Ludwig, Associate Director for Control Technology  
Research and Development, 1961-67
- R. A. McCormick, Chief, Meteorology Program, 1961-67
- J. S. Nader, Chemical and Physical Research and Development Program, 1961-67
- A. C. Stern, Assistant Director of the Center, 1961-63
- J. J. Schueneman, Chief, Control Development Program,  
1963-67

The work was conducted with three main objectives. One objective was to analyze the visual effects of smoke plumes to determine whether a measure of these effects is a logical method for evaluating smoke plumes. A second objective was to determine which optical property or visual effect of a smoke plume is a measurable inherent characteristic of the plume, independent of environmental illuminating conditions and most closely related to its particulate content. A third objective of the study was to establish an objective instrumental method (or methods) of evaluating plumes and to evaluate the methods with experimental and natural plumes.

# CONTENTS

	Page
ABSTRACT . . . . .	ix
INTRODUCTION . . . . .	1
APPARATUS . . . . .	2
VISUAL EFFECTS OF SMOKE PLUMES . . . . .	10
OPTICAL PROPERTIES OF SMOKE PLUMES . . . . .	29
INSTRUMENTAL TECHNIQUES FOR EVALUATING SMOKE PLUMES. . . . .	49
CONCLUSIONS . . . . .	58
ACKNOWLEDGMENTS . . . . .	60
REFERENCES . . . . .	61
APPENDIX A: ANALYSES OF THE ANGULAR SCATTERING PATTERNS OF THE EXPERIMENTAL PLUMES . . .	65
APPENDIX B: DATA ON PLUME CONTRAST AND OBSCURATION OF CONTRAST FOR EXPERIMENTAL BLACK AND WHITE PLUMES . . .	73
GLOSSARY OF PHOTOMETRIC TERMS . . . . .	89

## ABSTRACT

Two experimental smoke stacks were constructed to provide test plumes for studies of optical properties and visual effects over a wide range of illuminating and viewing conditions. Contrast reduction between objects viewed through plumes was used as an index of vision obscuration, and contrast between plumes and their background was used as an index of visual appearance. Results indicate that visual effects are not intrinsic properties of the plumes but vary with the background of the plume and with illuminating and viewing conditions. Variation was much greater with white plumes than with black. Tests conducted with trained smoke inspectors showed that their evaluations of nonblack smoke plumes were significantly influenced by these variations.

The angular scattering and transmission characteristics of the experimental plumes were measured and estimates of particle size derived therefrom.

The study shows that the quantity of aerosols in a plume is best evaluated optically by its transmittance. Special methods for measuring the transmittance of smoke plumes objectively are discussed. The methods involve telephotometry, photography, and photometry of targets; the use of smoke guides; and laser measurements.



## Vision Obscuration as a Specification for the Acceptability of Non-Black Plumes

If the smoke is not black, then evaluation by comparing its luminance with filters or Ringelmann charts becomes unrealistic. The plume luminance due to transmitted sky-light may be augmented considerably by the scattering of light the plume receives from the rest of the sky and from the sun. If the smoke is white, its luminance may equal that of "Ringelmann O," a white card with no grid, or exceed that of the adjacent sky seen through a filter with 100 percent transmittance, the more so as the smoke density increases. In the absence of any recognized method of evaluating white plumes, a concept of vision obscuration is sometimes used.<sup>5</sup> In California plumes are illegal if they obscure vision as much or more than did a black smoke of Ringelmann shade No. 2.

For a given plume, the plume-scattered light and the contrast reduction caused by the plume vary with the strength of the illuminating light and the angle between light source, plume, and observer. Therefore, vision obscuration for a given plume varies considerably according to the lighting and observing conditions. Also, it is often impossible to measure the vision obscuration by a plume from a smoke stack under the limitations of routine evaluation in the field. In practice, inspectors are trained to recognize white test-smokes, whose obscuration of vision is known by previous calibrations to be equivalent to the obscuration of vision of black smokes of various Ringelmann shades. On the basis of this experience, the inspectors then allocate equivalent Ringelmann shades to white smokes seen in the field.<sup>6,7</sup>

*Handwritten note:*  
A. For a given plume, the plume-scattered light and the contrast reduction caused by the plume vary with the strength of the illuminating light and the angle between light source, plume, and observer.

## APPARATUS

For study of these phenomena under controlled conditions, facilities for generating and measuring smoke were established.<sup>8</sup> At the Robert A. Taft Sanitary Engineering Center of the U.S. Public Health Service, an experimental outdoor stack (Figure 1) was constructed so that a 31-cm-high, 20-cm-thick, 60-cm-long horizontal black or white plume could be maintained at uniform concentration and at a uniform velocity of about 16 km/hr. To attain a uniform, nondiffusing plume around 60 cm long when the ambient wind direction and speed deviates only slightly from those of the plume, an air sheath 5 cm thick surrounding the smoke plume was made to travel at the same velocity as the smoke. A narrow-angle transmissometer (Figure 2) was mounted in the stack for monitoring the transmittance of the plumes. The stack and all associated apparatus were mounted on a base that can be easily rotated to allow plume observation in any direction relative to plume travel and sun position.

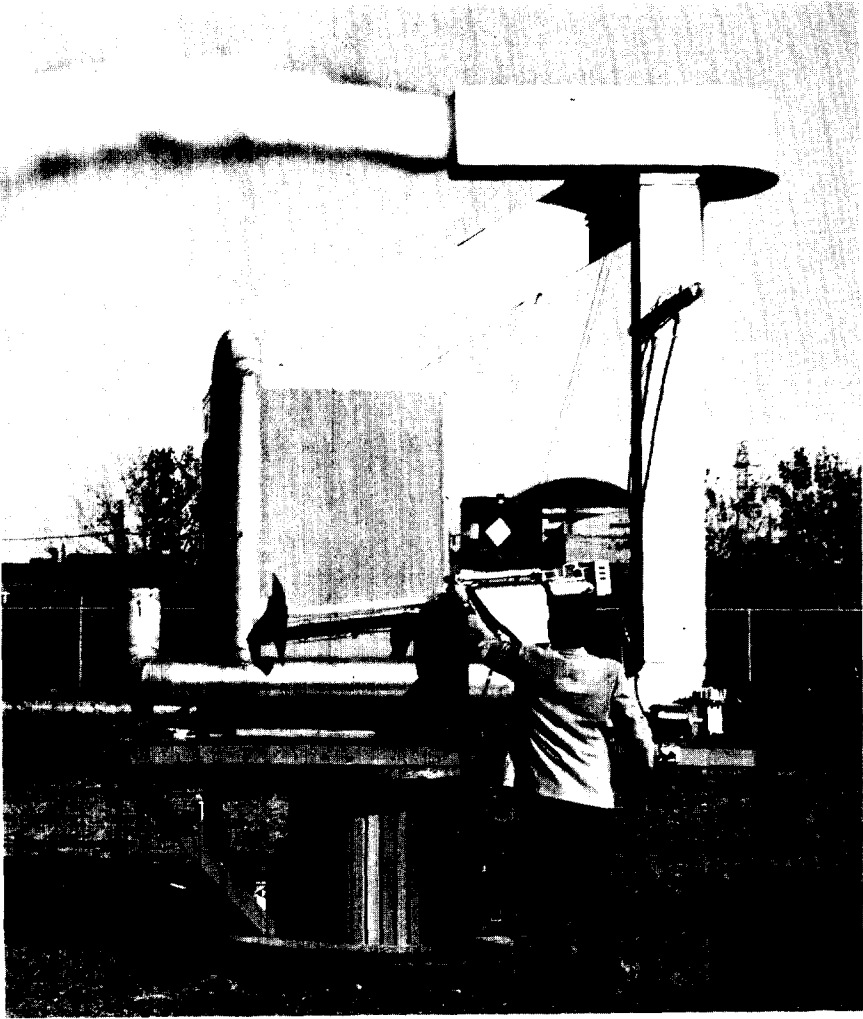


Figure 1. Laboratory smoke stack.

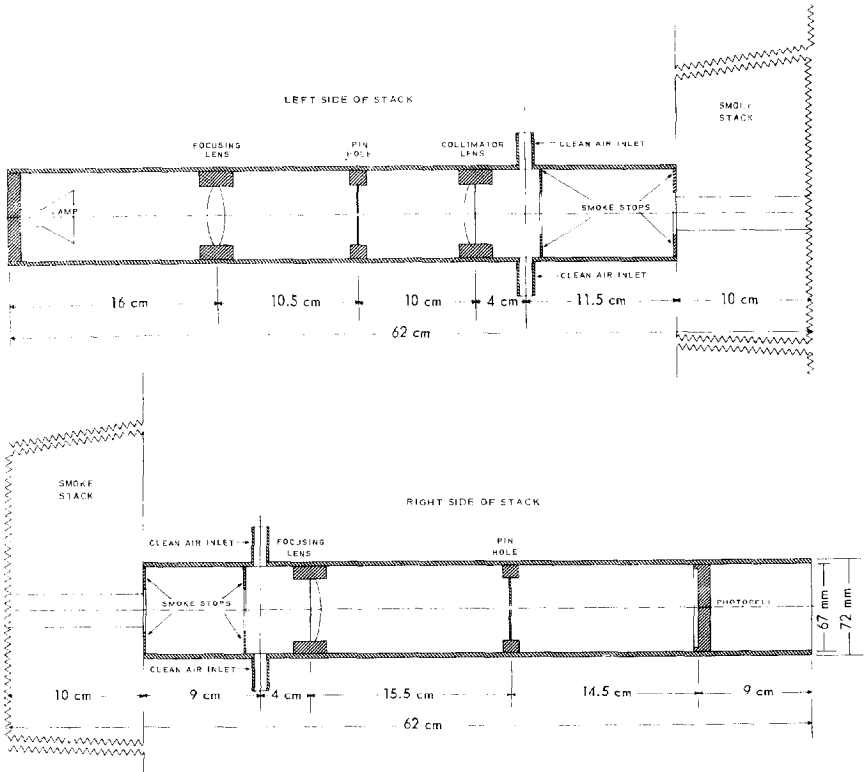


Figure 2. Smoke stack transmissometer.

The black smoke was produced with a domestic oil furnace by choking off the air supply to cause incomplete combustion of the oil; the white smoke was produced from fuel oil by an insecticide fogger.<sup>9</sup> The transmittance of both smoke sources was adjustable from 100% to below 20%.

An experimental smoke stack was also constructed at a gas- and oil-burning steam electric plant of the Pacific Gas and Electric Company at Morro Bay, California. Part of the effluent to the main stack was diverted at the base of the stack to a convenient place on the roof of the plant, where it was accessible for study both in the duct and after discharge to the air. The experimental duct was designed and constructed to simulate real stack conditions of retention time, temperature gradient, turbulence, and discharge velocity so that the concentration and size distribution of the particulates within the plume would match those in the real plume as closely as possible. The duct was 31 cm in diameter at the exit. Figure 3 is a view of the plant showing the take-off on the induced-draft-fan suction duct, the discharge above the roof, and the location of the observation towers on the roof.

To measure the luminance of distant objects, a narrow-angle telephotometer was developed. The complete unit (Figure 4) consisted of a photo-multiplier-photometer<sup>10</sup> and a pair of telescope lens systems (Figure 5) mounted parallel to each other, one for viewing and aiming and the other for focusing an image of the target on the entrance pupil of the photomultiplier tube. The effective focal length of the telephotometer was 1.324 meters and its angular field of view was 0.28°.

During the latter part of the study, a commercial telephotometer (Figure 6) was purchased<sup>11</sup> for the field work. This unit was battery operated and its angular field of view was 0.50°.

### **Spectral Responses of the Telephotometer and Transmissometer**

The spectral responses of the 0.28° telephotometer and in-stack transmissometer with "visual correction" filters were measured with the aid of a calibrated, tungsten-filament, quartz-envelope, iodine-filled lamp<sup>12</sup> and a grating monochromator to disperse its spectrum. The responses ( $P_i$ ) of the instruments to light of wavelength  $\lambda_i$  were calculated using the relation  $P_i = O_i/L_i$ , where  $O_i$  was the observed response of the sensors to the standard lamp at  $\lambda_i$  and  $L_i$  was the lamp irradiance at  $\lambda_i$ . The relative response curves are shown in Figure 7 along with the desired relative luminosity curve for the human eye.

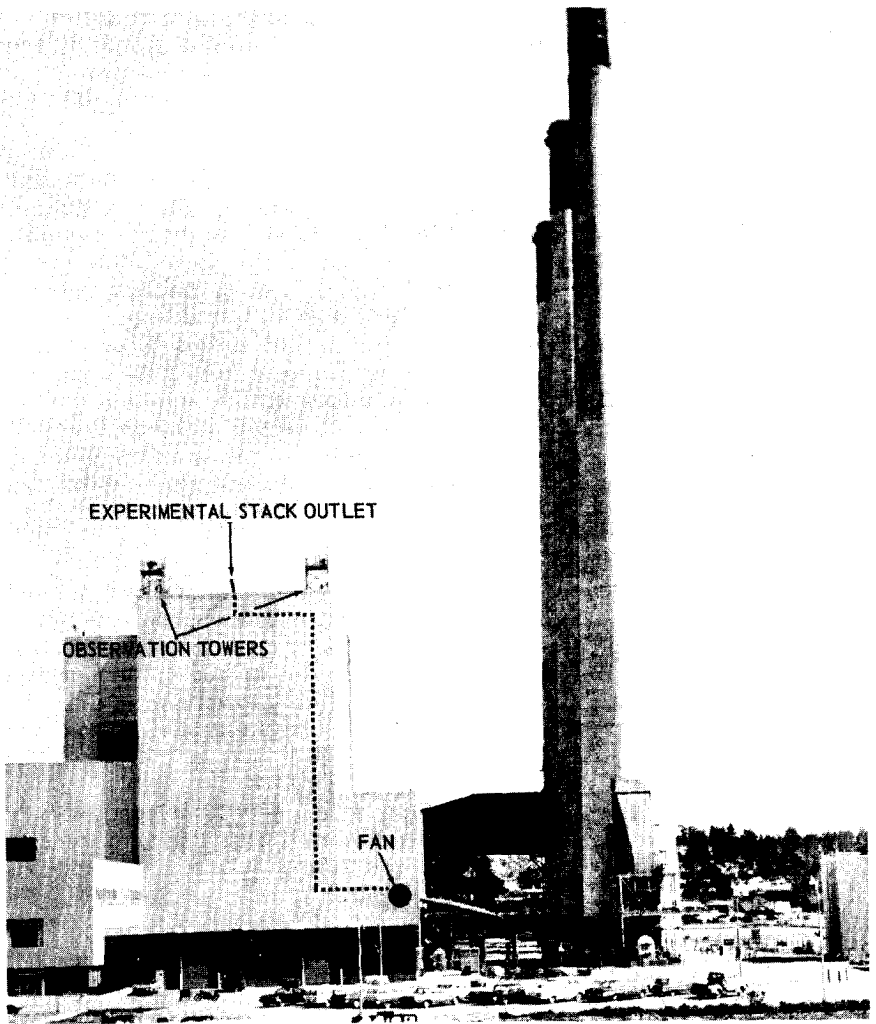


Figure 3. Experimental smoke stack at a power plant.

### Telephotometer Calibration

For calibration of the telephotometer, a self-luminous laboratory target was constructed and its luminance was determined with the aid of a Weston Model 614 illumination meter. This laboratory target was used to determine the effective luminance of a field light source, which was placed on the front of the telephotometer for periodic checks of calibration in the field.

The laboratory target was composed of a 61-cm-long, 31-cm-diameter cylindrical container, two sheets of ground glass, and a 350-

watt flood lamp. The double layer of ground glass diffusing screens was placed over the open end of the cylinder, and the flood lamp was placed at the opposite closed end of the cylinder to illuminate them.

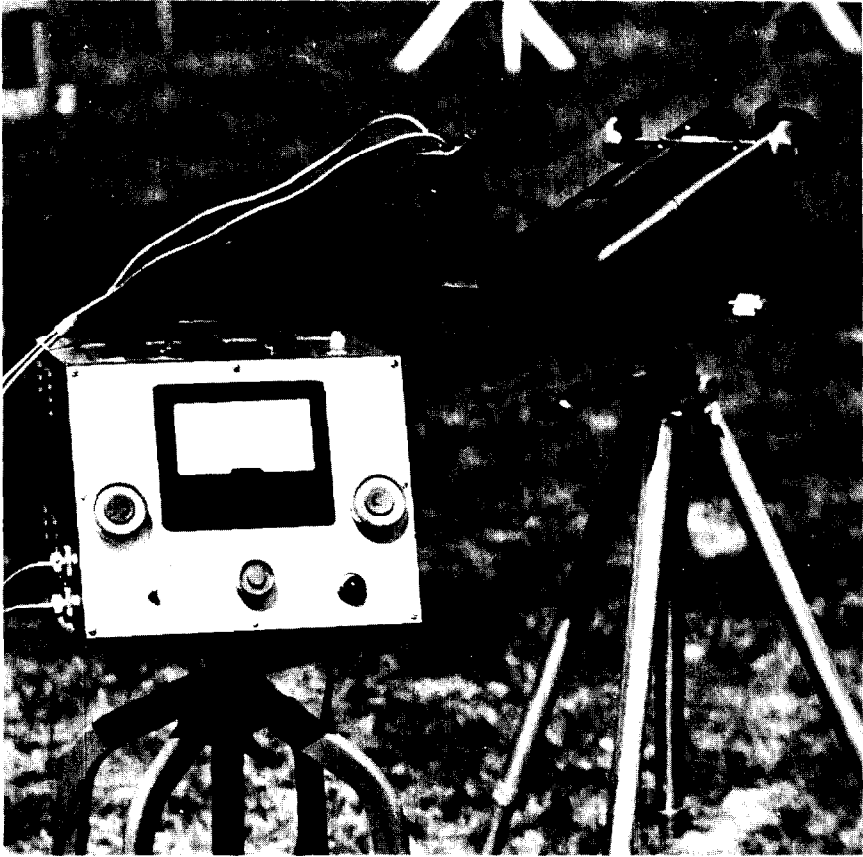


Figure 4. Telephotometer assembly.

After it was determined that the ground glass was evenly illuminated by the flood lamp, it was masked down until a  $64\text{-cm}^2$  area was exposed at the center. The intensity of this area was determined by measuring the illumination received at various distances from the source with the illumination meter. A curve of the illumination versus meter distance from the light source is shown in Figure 8. Where the slope of this curve was linear and equal to  $-2$ , the illumination was varying with distance as though the  $64\text{-cm}^2$  light source was a point source. The intensity of the source can be determined from any point on the linear part of the curve by multiplying the illumination at this point by the square of the corresponding distance. The intensity of the target was 320 candles. The luminance of the target, which is defined

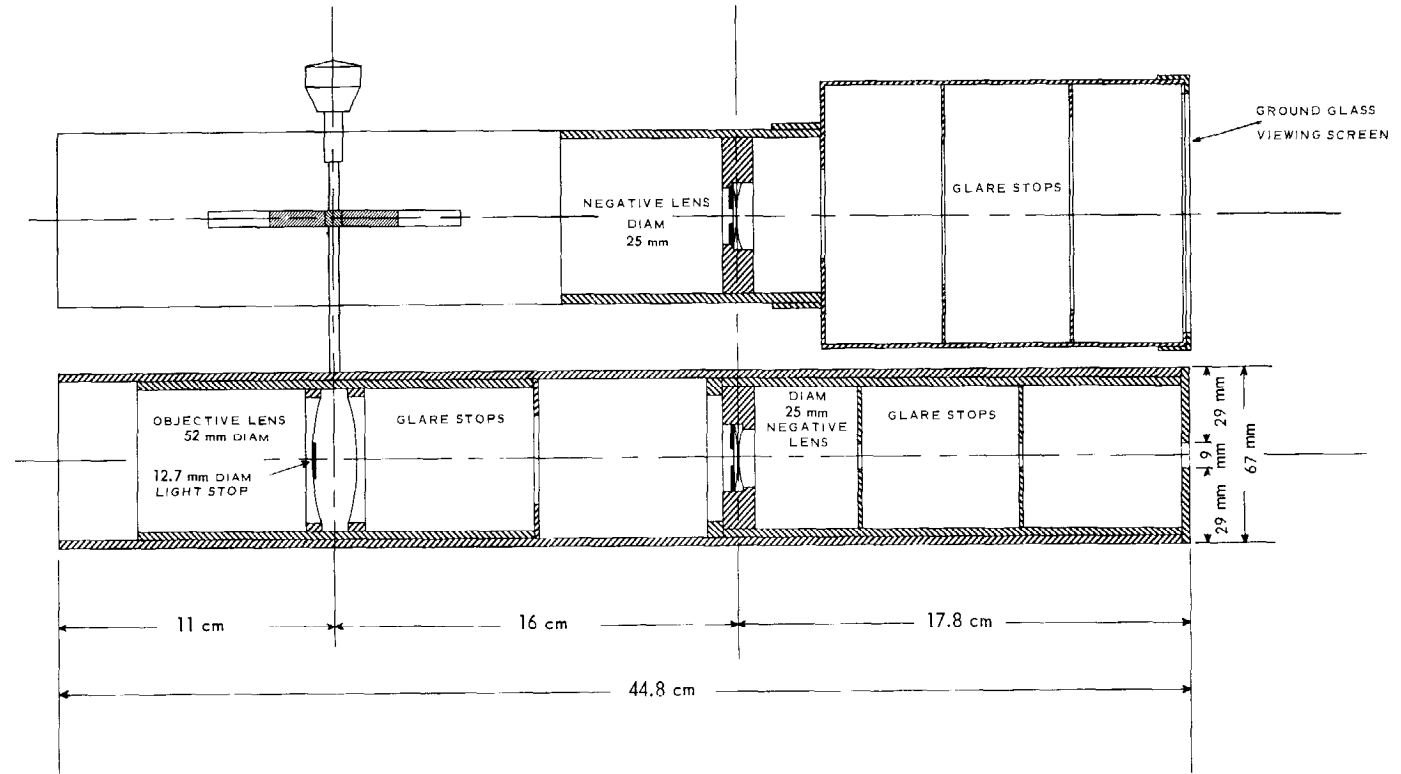


Figure 5. Telescope lens system for telephotometer.

as the intensity of the target divided by the target area, was  $50 \times 10^3$  candles/meter<sup>2</sup>. Although the luminance of the target was higher than the luminances that will be encountered in the field, by a factor of about 10, the extra brightness was needed so that the illumination measurements could be taken at a distance great enough for the intensity of the source to be determined. A neutral density filter with a transmittance of 10% was placed in front of the telephotometer objective to give an apparent luminance of 5000 candles/meter<sup>2</sup> for calibrating.

The field light-calibrating source was built into a cylindrical container 7.6 cm in diameter and about 25 cm long. A ground-glass diffusing screen located about 7.6 cm from the open end of the tube



Figure 6. Telephotometer.

was illuminated by a 40-watt incandescent lamp with voltage regulation located at the closed end of the tube. The effective luminance of this field calibrating source was found to be 5200 candles/meter<sup>2</sup> when compared with the laboratory target.

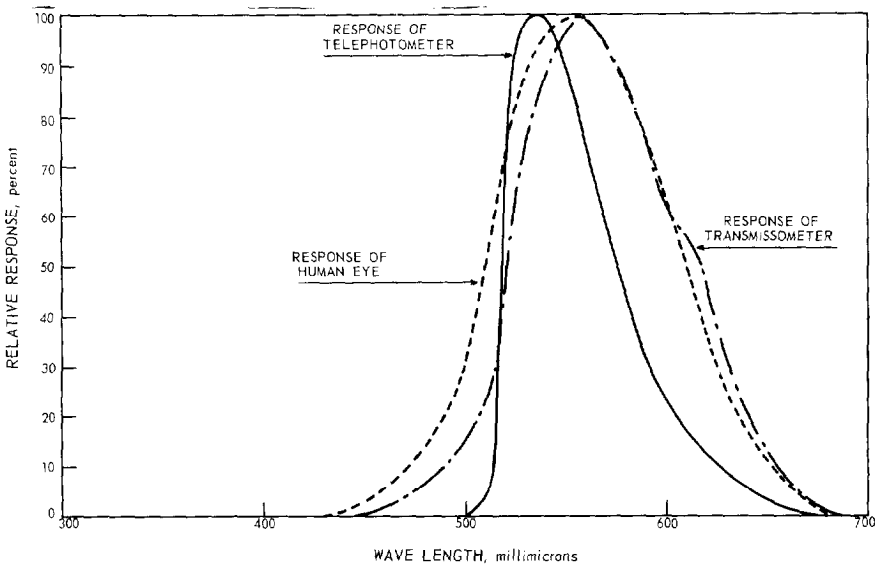


Figure 7. Spectral response of telephotometer and smoke stack transmissometer.

## VISUAL EFFECTS OF SMOKE PLUMES

Vision involves physiological factors and cannot be defined by physical measurements alone; however, in the absence of color contrasts, visibility of objects depends among other things on the perception of luminance contrasts between the objects and their surroundings. For scenes of normal brightness in daylight, the eye can usually distinguish an object from its background when their relative contrast (defined below) exceeds  $\pm 0.02$  to 0.05; in general, the greater the contrast of the object with its background, the greater its visibility.<sup>13</sup> In this study we take photometric measurements of contrast between plumes and their background (usually the sky) as an index of the visibility of the plumes themselves; and we take the reduction in contrast between objects viewed through plumes as an index of obscuration by the plumes. The relationships can be expected to be simplest when the plumes are viewed with a restricted field of view as in a telescope. For normal unrestricted vision, perception of contrasts between parts of the field can be influenced significantly by the brightness of the field as a whole.

The other common criterion of vision obscuration is the reduction in meteorological visual range. This range is usually defined as the

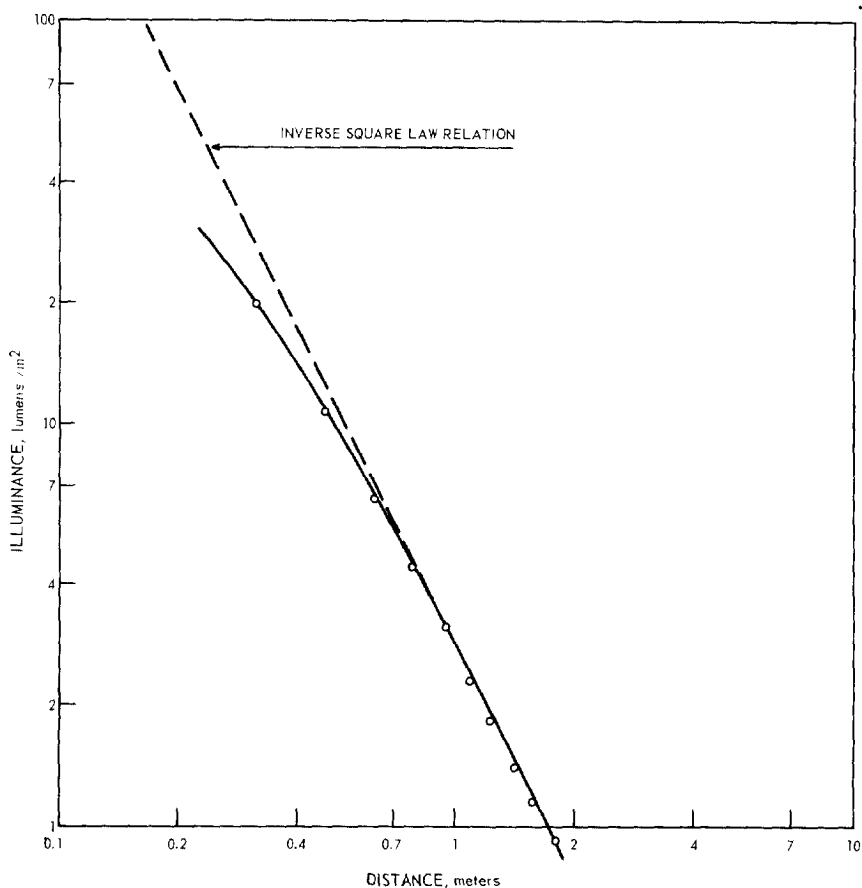


Figure 8. Illuminance as a function of distance from the telephotometer calibration target.

distance at which the contrast of a black object, relative to the horizon sky, is 0.02 and its value is  $3.9/K$ , where  $K$  is the atmospheric turbidity coefficient defined below. This criterion is more appropriate as a measure of the visual nuisance of the smoke plume after it has been dispersed in the atmosphere. Since the relationships involved in visibility through the atmosphere are more complex than in the contrast reduction between objects seen at a shorter distance, where natural atmospheric attenuation and scattering may be neglected in comparison with the smoke, evaluation by contrast-reduction is preferable for our present purpose.

### Contrast Between Targets Viewed Through Smoke Plumes

The luminance contrast between two equal-size targets with luminances of  $B_1$  and  $B_2$  ( $B_1 > B_2$ ) may be defined as

$$C = \frac{B_1 - B_2}{B_1} \quad (1)$$

If the targets are not self-luminous, their luminances depend on their reflectances ( $R_1$  and  $R_2$ ), and on the illuminance ( $E$ ) such that

$$B_1 = k_1 R_1 E$$

and  $B_2 = k_2 R_2 E$  (2)

where  $k_1$  and  $k_2$  are factors depending on the diffusing characteristics of the target surfaces and viewing direction. For perfectly diffuse surfaces (that obey Lambert's law)  $k = 1/\pi$  and their luminances are independent of viewing direction, a good approximation for the behavior of many surfaces. If the targets have similar, even if not perfectly diffusing surfaces and are illuminated in the same way  $k_1 = k_2$  and  $C$  becomes

$$C_i = \frac{R_1 - R_2}{R_1} \quad (3)$$

an intrinsic property of the targets independent of ambient lighting conditions.

When the targets are viewed through a light-scattering plume, their luminance will appear to change because of the attenuation of light being transmitted through the plume and to the addition of air-light resulting from the scattering of ambient light by the plume in the direction of the viewer. If, in addition to the foregone assumptions, the plume transmittance and the scattered light are the same along both lines of sight, then the apparent luminances of the targets ( $B'_1$  and  $B'_2$ ) may be written

$$B'_1 = B_a + B_1 T$$

and  $B'_2 = B_a + B_2 T$  (4)

where  $B_1$  and  $B_2$  are the luminances of the targets viewed clear of the plume,  $T$  is the plume transmittance, and  $B_a$  is the plume air-light. Plume air-light is defined here as the limiting apparent luminance of a black target viewed through the plume as its size goes to zero. The apparent contrast ( $C_a$ ) between the targets is

$$C_a = \frac{B'_1 - B'_2}{B'_1} \quad (5)$$

which becomes

$$C_a = \frac{(B_1 - B_2) T}{B_a + B_1 T} \quad (6)$$

by substitution of (4). For targets with similar diffusing properties, substituting relations (2) with  $k_1 = k_2 = k$  reduces (6) to

$$C_a = C_i \frac{A}{A + B_a} \frac{1}{ET} \quad (7)$$

where  $B_a$  is the plume air-light,  $E$  is the illumination on the targets,  $T$  is the plume transmittance, and  $A$  is a constant equal to  $kR_1$ . Thus the luminance contrast between targets will always be reduced when they are viewed through a plume that scatters light. If the plume scatters a negligible amount of light,  $B_a \approx 0$  and the target contrast remains unchanged. Equation (7) also shows that the apparent contrast between the targets, besides being a function of plume air-light ( $B_a$ ), is now a function of the target illumination ( $E$ ) and the plume transmittance ( $T$ ). An increase in air-light results in a decrease in contrast, whereas an increase in target illumination or plume transmittance results in an increase in the apparent contrast between the targets.

### Contrast Between Smoke Plumes and Their Background

The contrast  $C_p$  between a plume of luminance  $B_p$  viewed against an extended background of luminance  $B_b$  is

$$C_p = \frac{B_p - B_b}{B_b} \quad (8)$$

but by relations (4), the luminance  $B_p$  of a light-scattering plume viewed against a background of luminance  $B_b$  is

$$B_p = B_a + B_b T \quad (9)$$

where  $B_a$  is the plume air-light and  $T$  the plume transmittance. Substitution of (9) into (8) gives

$$C_p = \frac{B_a}{B_b} + (T-1) \quad (10)$$

for the contrast between a plume and its background. Thus, the plume air-light also plays an important role in determining plume-to-background contrast. For a plume that scatters a negligible amount of light,  $B_a \approx 0$  and  $C_p = T-1$ .

## Contrast Reduction by the Experimental Black and White Plumes

To illustrate how the contrast between objects can vary when the objects are viewed through plumes from different directions relative to the sun on clear days, the apparent contrast between targets was measured through the experimental black and white plumes on clear and overcast days for periods of 6 to 7 hours from fixed plume-viewing positions. The viewing directions chosen were east and west, since extremes in the angle between plume, viewer, and sun occur when plumes are viewed throughout the day in these directions. Runs were conducted from about 9:00 a. m. to 4:00 p. m. with plumes having in-stack transmittances of 60 and 40 percent. The plume directions were south or north, according to the wind. The targets were located about 3 meters behind the plumes, and the telephotometer was located about 12 meters east or west of the plumes. Measurements of the inherent contrast between the targets and of intensity of solar radiation on a horizontal surface, as indicated by an Eppley globe pyrheliometer,<sup>14</sup> were taken concurrently during each run. Tests were also conducted to illustrate how the apparent contrast between targets can vary with plume transmittance when the targets are viewed through plumes under illuminating conditions that result in high and low plume-air-light luminances.

Two types of target-pairs were used. The first pair of targets consisted of 31- by 62-cm black and white panels. The surfaces of these targets were of matte finish and exhibited similar diffusing characteristics. Consequently, the contrast between them showed little variation when they were illuminated from different directions as the day progressed, even though their luminances varied considerably.

The targets in the second pair were self-luminous; each consisted of a circular, 13-cm-diameter frosted-glass sheet located in the back of a cylindrical 93-cm-long, 31-cm-diameter "black box target." The luminance of the frosted glass was controlled by illuminating it from behind with four 100-watt lamps and one 25-watt lamp. Its luminance was 10700 candles/meter<sup>2</sup> with all lamps on and 800 candles/meter<sup>2</sup> with the 25-watt lamp on; it served as a black box target with the lamps off. The lamp housing was cooled with a small blower. The luminances of these targets, unlike those of the panel targets, were independent of ambient illumination and remained constant as the day progressed.

The apparent contrasts between the panel targets were measured through white and black plumes with 60 and 40 percent transmittance during clear days from both east and west (Figures 9a and 9b), and during overcast days from the east only (Figure 10). The apparent contrasts between the self-luminous targets were measured through white and black plumes with 60 and 40 percent transmittance during clear days from the east (Figures 11a and 11b). Measurements of plume air-light were taken concurrently during the latter runs by using the target as a black box to eliminate transmitted light from the background.

The different contrasts between both sets of targets were measured through black and white plumes of various in-stack transmittances late in the afternoon from the east (high plume air-light) and from the west (low plume air-light). The measurements were taken within a period of about 45 minutes, between 3:30 and 4:15 p. m. Figure 12a shows the results for white plumes; Figure 12b, for black plumes.

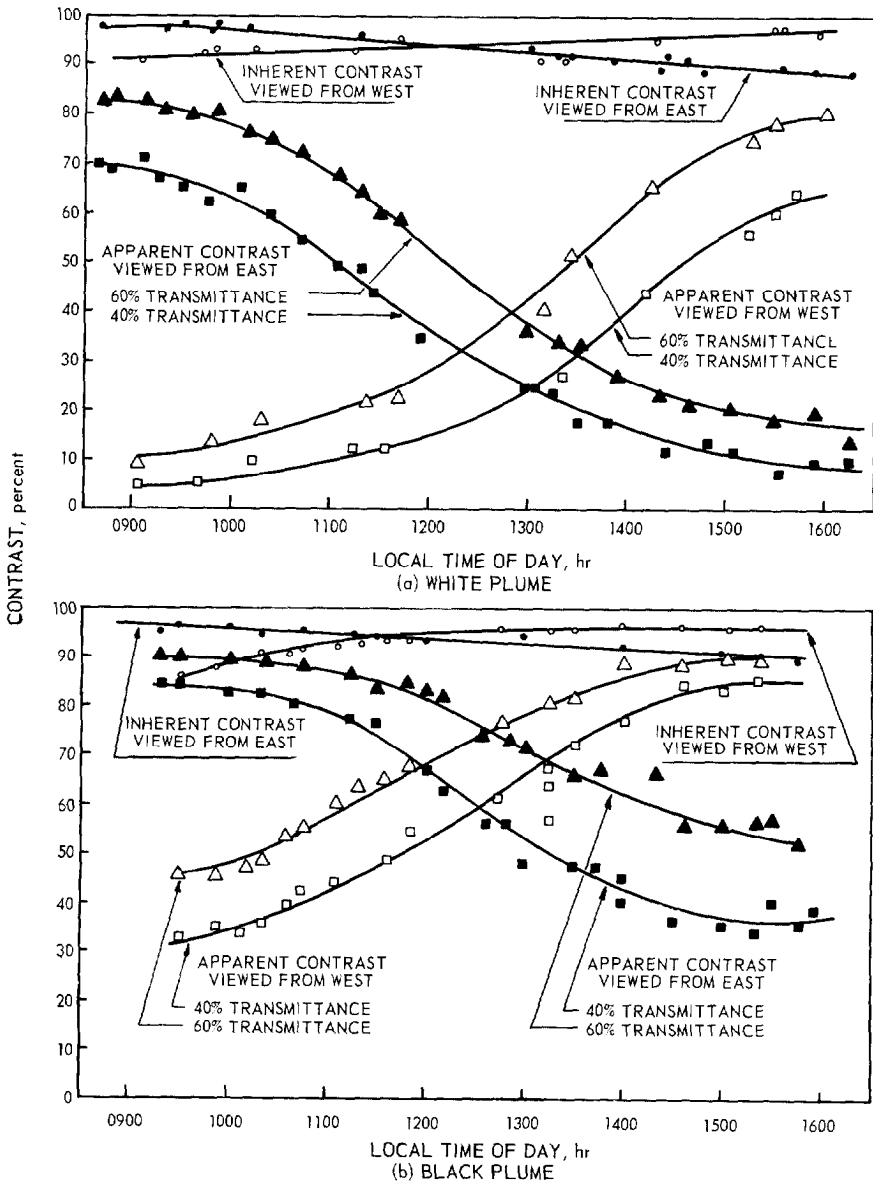


Figure 9. Variation throughout the day of apparent contrast between panel targets viewed from east and west through experimental plumes on clear days.

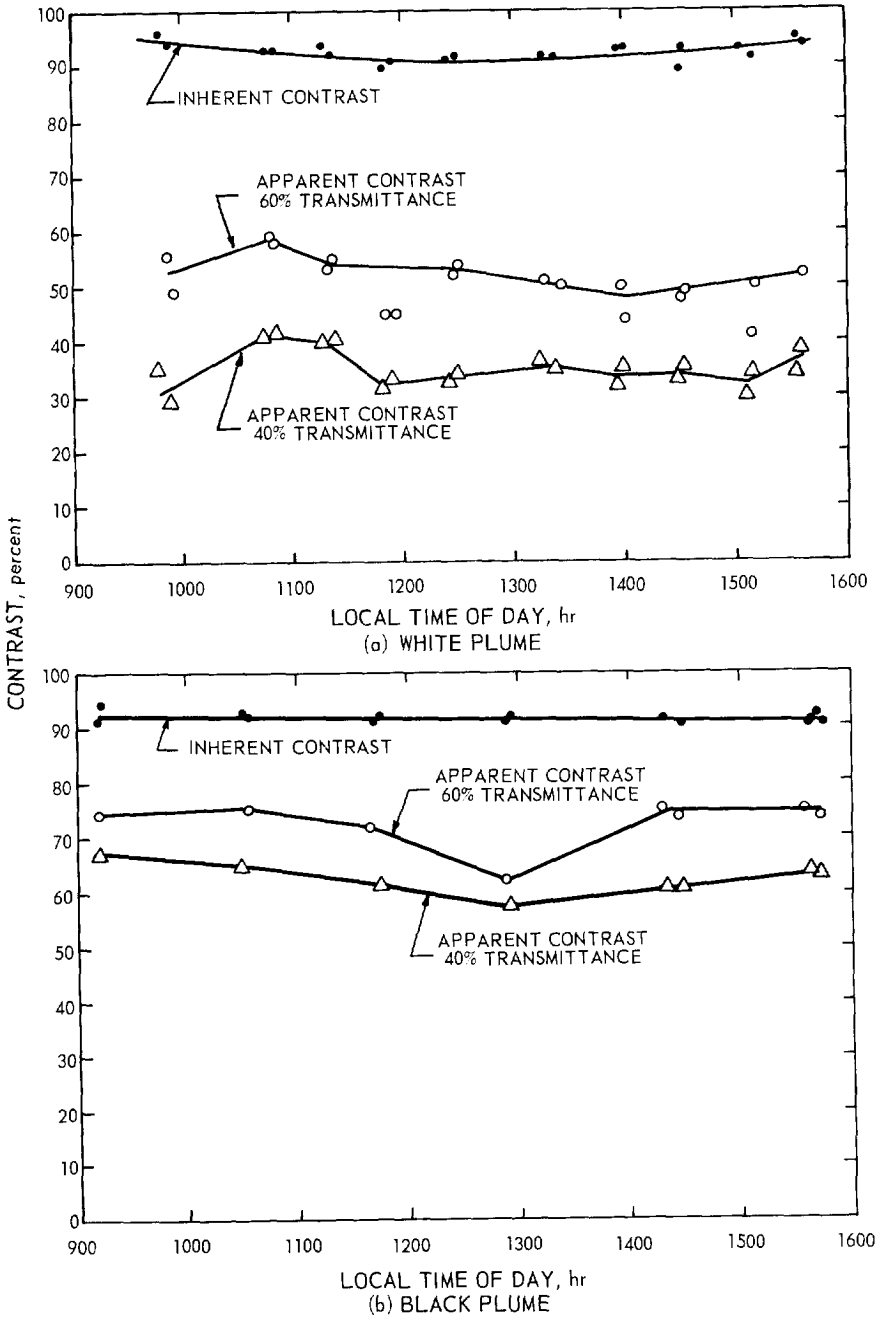


Figure 10. Variation throughout the day of apparent contrast between panel targets viewed from the east through experimental plumes on overcast days.

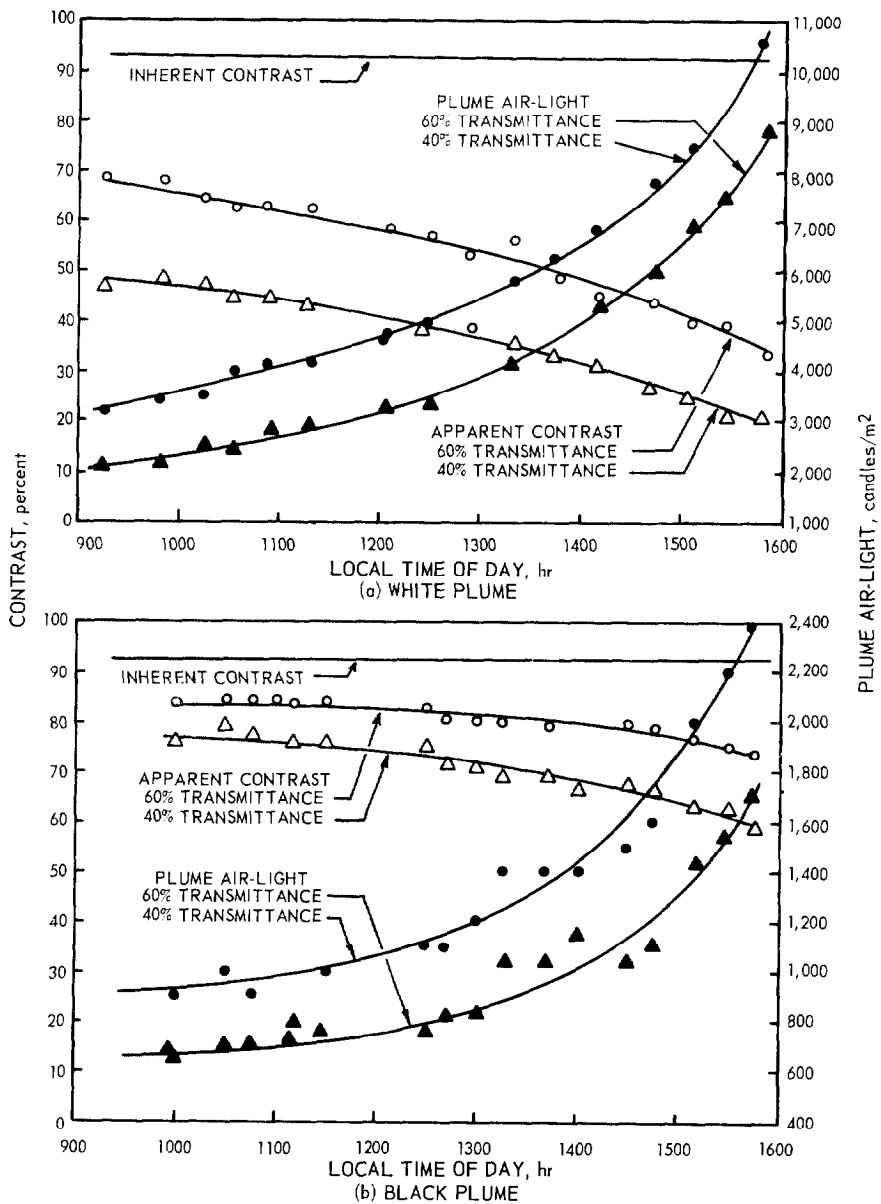


Figure 11. Variation throughout the day of apparent contrast between self-luminous targets viewed from the east through experimental plumes on clear days.

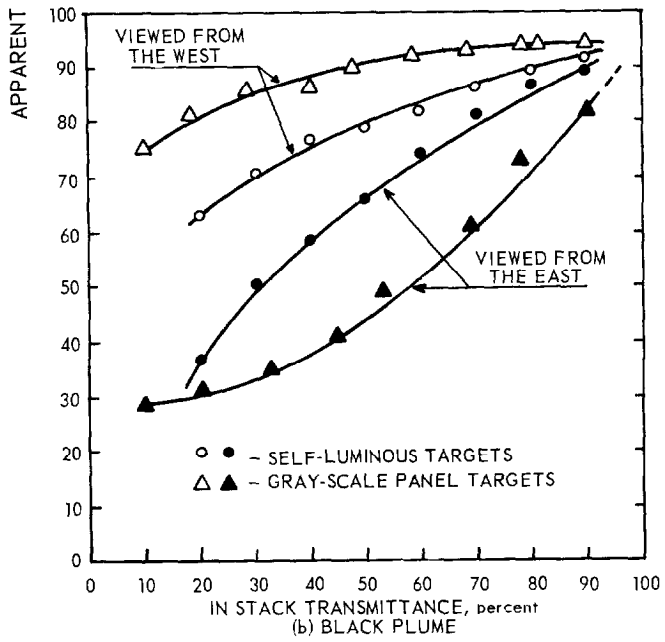
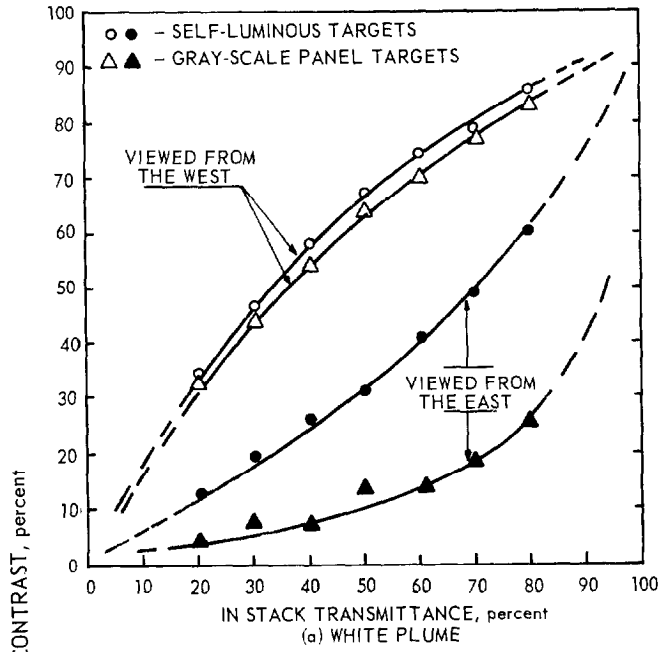


Figure 12. Apparent contrast between panel and self-luminous targets viewed from east and west through experimental plumes on clear days (3:30 - 4:15 p.m.), as a function of plume transmittance.

## **Contrast Between the Experimental Black and White Plumes and Their Sky Backgrounds**

To illustrate how the contrast between black and white plumes and their sky background can vary when viewed from different directions relative to the sun on a clear day, tests similar to the contrast-reduction experiments were conducted. Here the contrast between plumes with transmittances of 60 percent and the sky behind them were measured over 6- to 7-hour periods on clear days from the east and west. The results are shown in Figure 13a for white plumes and Figure 13b for black plumes. The low plume-to-sky contrast measurements from the west early in the morning in Figure 13a resulted from atmospheric haze, which gives a high plume background luminance particularly when the observer is viewing in the direction of the sun. The hazy condition cleared by about 11:00 a. m. The contrast between black and white plumes with a range of in-stack transmittances and their sky backgrounds were measured late in the afternoon from the east and from the west between 3:30 and 4:15 p. m. (Figures 14a and 14b), and from the west on overcast days (Figures 15a and 15b). The figures also show values of plume air-light, measured concurrently by using a black box target to eliminate directly transmitted light.

The results of the contrast obscuration and plume-to-sky contrast experiments showed that, as expected, the contrast between objects viewed through a white plume and the contrast between a white plume and its background are both highly variable with respect to the viewer, plume, and sun increased, the light scattered by the plume in the direction of the viewer increased. The increase in scattered light caused a decrease in contrast between objects viewed through the plume and an increase in contrast between the plume and its sky background. If the objects were not self-luminous, and most objects are not, the contrast between them was further affected because the illumination of the object decreased as the viewer-plume-sun angle increased.

The contrast obscuration experiments with black plumes showed that this obscuration of contrast was also variable with respect to plume-viewing direction on clear days. The variation was similar to that found with white plumes, but less pronounced. The plume-to-sky contrast experiments with black plumes, unlike those with white plumes, showed that the contrast between black plumes and their sky background varied little with respect to plume-viewing direction on a clear day.

This is to be expected with an ideal black plume, whose luminance is a constant percentage (the transmittance) of the sky behind it; however, a perfectly non-scattering plume cannot exist. An analysis of these data by Stoeber<sup>15</sup> suggests that with this black plume, the light it scatters forward toward the observer from the area of sky seen adjacent to the plume, predominates over sunlight, which must be scattered through a wider angle to reach the observer when the sun is not seen near the plume. Thus luminance of the plume light will change in proportion as luminance of its sky background changes. This result is

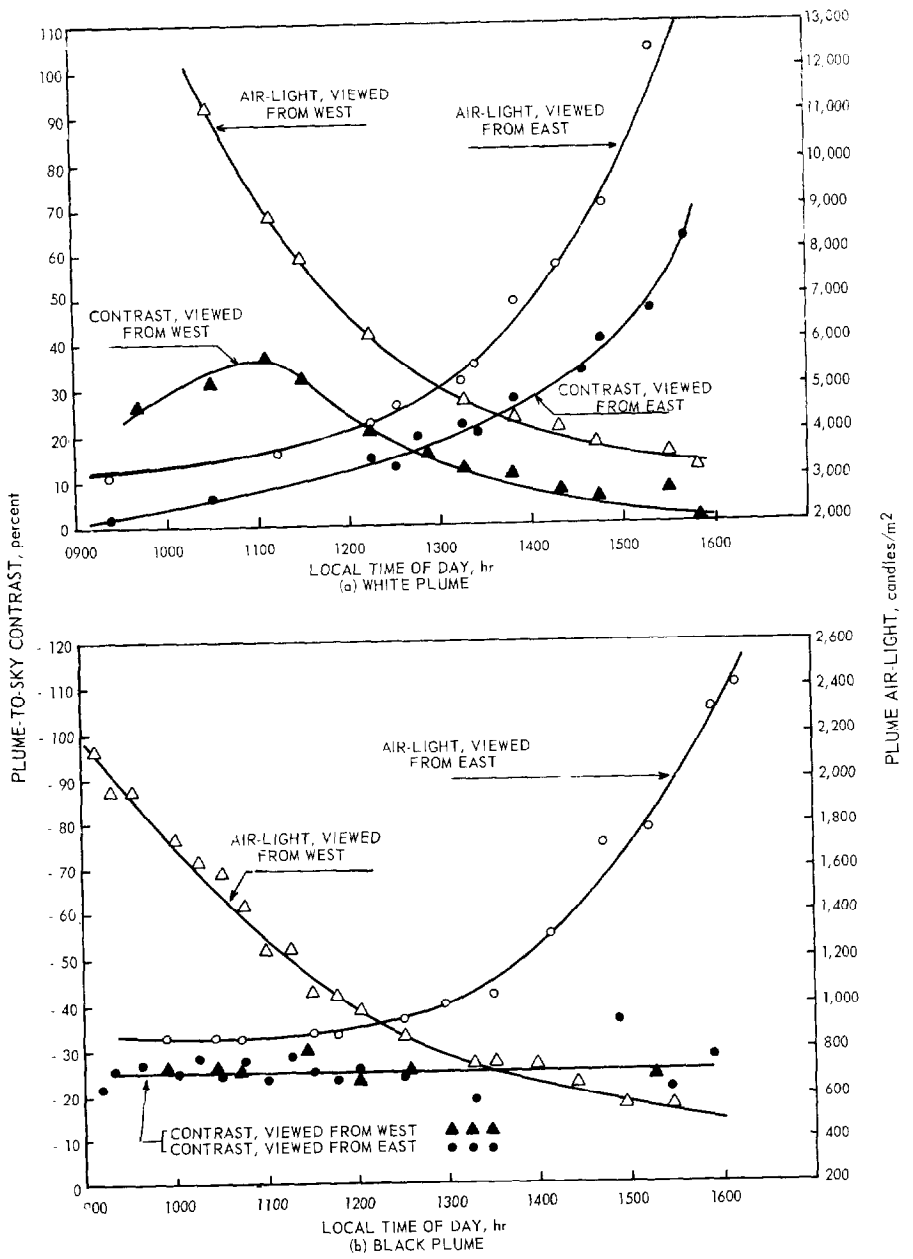


Figure 13. Air-light and plume-to-sky contrast of experimental plumes with 60 percent transmittance viewed from east and west on clear days, as a function of time.

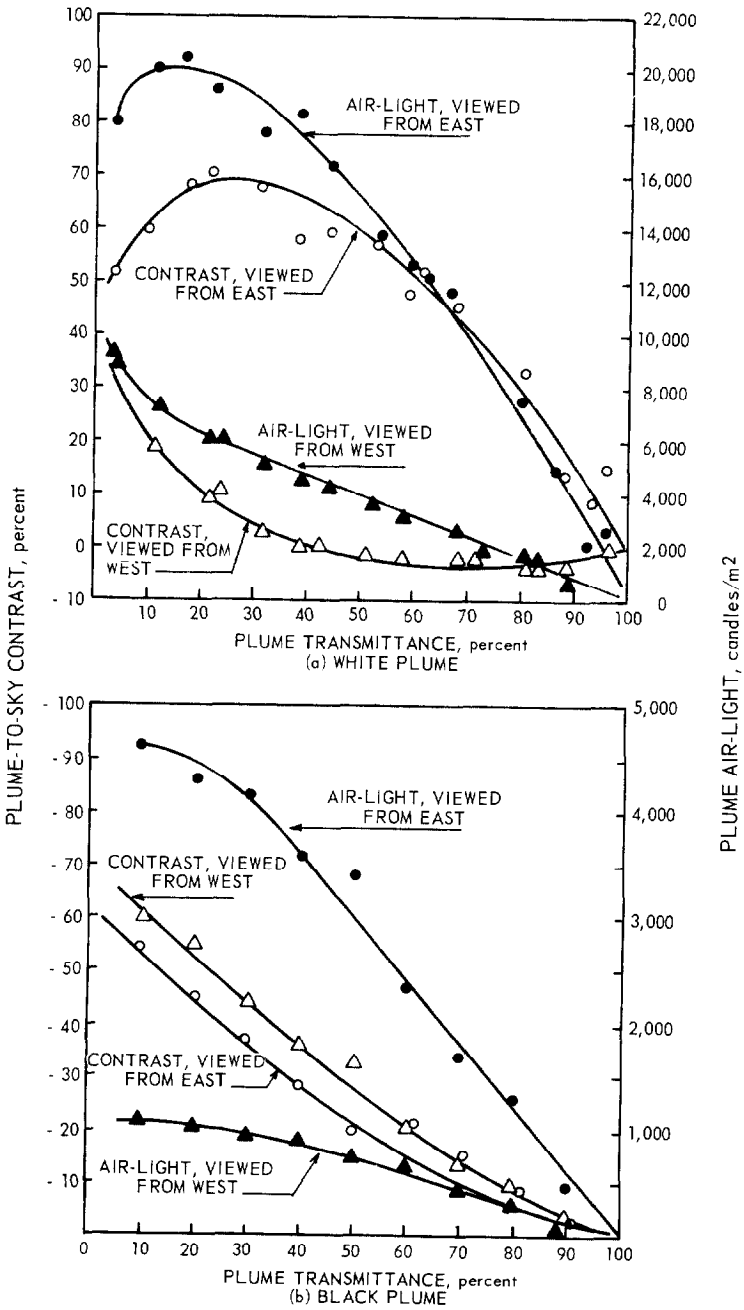


Figure 14. Air-light and plume-to-sky contrast of experimental plumes viewed from east and west on clear days, (3:30 - 4:15 p.m.), as a function of plume transmittance.

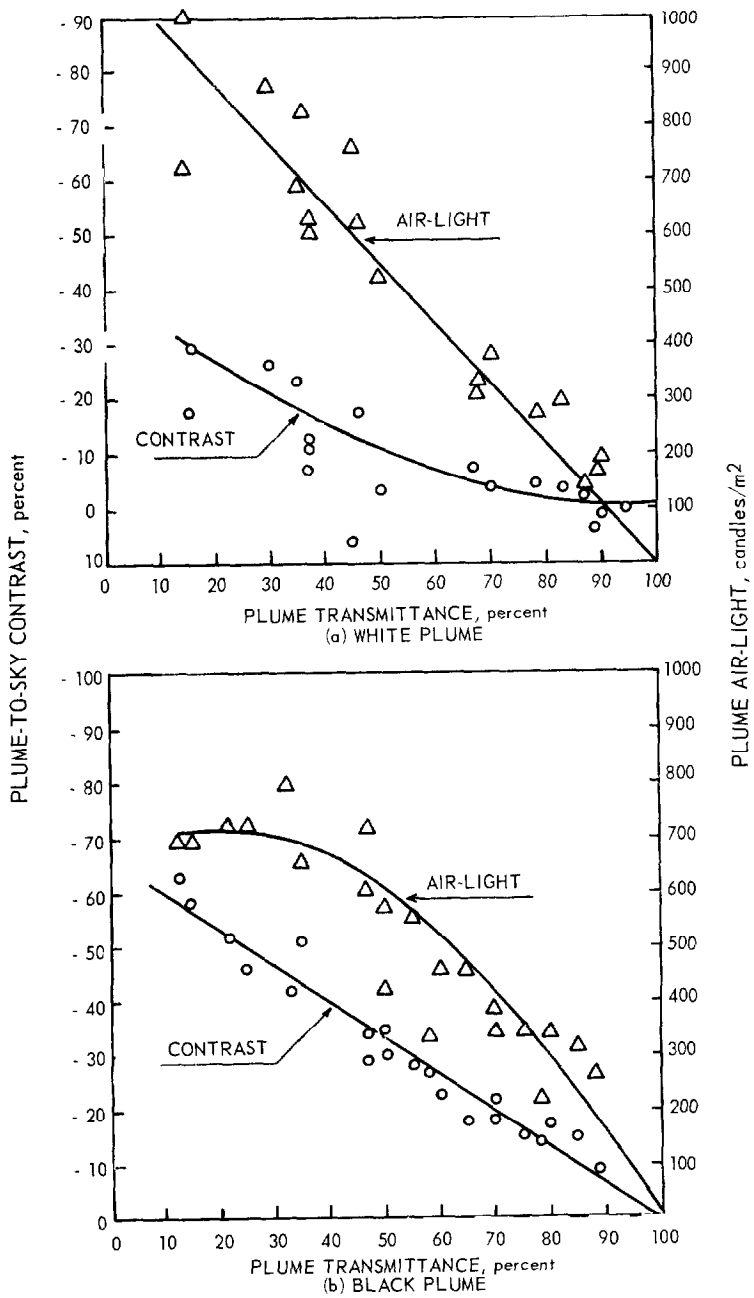


Figure 15. Air-light and plume-to-sky contrast of experimental plumes viewed on overcast days.

physically reasonable because the scattering by absorbing particles differs from that by transparent particles chiefly in the reduction in scattering at angles outside the main forward lobe in the scattering pattern. This effect would not be expected if the plume background were a dark object.

On overcast days when illumination of plumes was by diffused light and not strongly directional, the contrast between objects viewed through black and white plumes and the contrast between the plumes and their background did not show the extreme variation with viewing direction that was apparent on clear days; rather, the contrasts fluctuated randomly as overcast areas of varying density passed in front of the sun. The plume-to-background contrast of a white plume and its obscuration of contrast on an overcast day can be extremely complex and vary in no predictable manner as overcast conditions vary from day to day and minute to minute.

### **Evaluation of Plumes by Trained Observers**

Since tests have shown that the visual appearance of a plume as measured instrumentally by telephotometer varies with direction of view relative to the sun, we must ask whether the subjective evaluation of plumes by trained observers also varies with direction of view relative to sun. Or can the trained observer compensate for the observed variation in the luminance contrast of plumes with viewing direction?

Evaluation tests were made at the smoke school of an air pollution control district. A group of five observers was positioned about 18 meters east of the training stacks and a group of four observers was positioned about 18 meters west of the stacks. The observers were requested to allot Ringelmann numbers to the plumes in accordance with their training and to allow for any variation in plume appearance due to viewing direction. A telephotometer was stationed with both groups. The observers had been trained to recognize plumes of a given Ringelmann number as indicated by appropriate readings of the in-stack transmittance under various lighting conditions. Both black and white plumes with in-stack transmittances of 15, 35, 50, 65, and 85 percent were generated in random sequences. On signal, the observers assessed the plumes and the telephotometer operators measured the plume and background luminances.

Eight runs were made with the groups located east and west of the stacks, four runs with dark plumes and four with white plumes. Six of the runs were made with alternating dark and white plumes between 9:30 and 11:00 a. m. The other runs were made between 12:30 and 1:15 p. m. A run consisted of 10 assessments, with each of the transmittance levels occurring twice in each run. Each run lasted about 15 minutes. The average assessments by the observers for the five transmittances of each run are shown in Figures 16 and 17, for white and dark plumes, respectively. The assessments were made in terms of Ringelmann numbers for the dark plumes and equivalent Ringelmann

numbers for the white plumes. The calibration scheme (Ringelmann number: in-stack transmittance) by which the observers were trained is described by Yocum and Coons<sup>6, 7</sup> and is shown on the ordinates of Figures 16 and 17. The concurrent plume-to-sky contrast measurements from east and west of the plume are shown for each run in Figure 18.

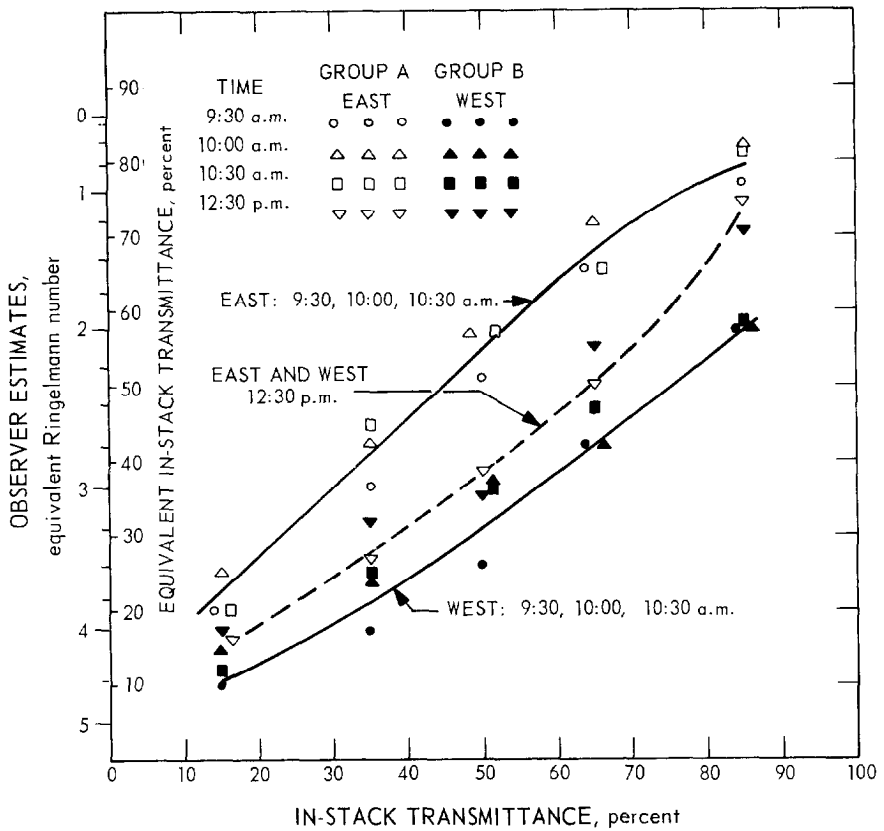


Figure 16. Variation in evaluations of white plumes by groups of trained observers viewing from east and west on a clear day.

Plans to continue assessing the plumes with the group positioned east and west of the stacks were abandoned shortly after 1:00 p.m. because clouds began to form on the eastern horizon and a change in the wind direction shifted the plume direction from south to east. During the afternoon, runs were made with each plume with both panels combined and positioned north and south of the stacks. The results are shown in Figures 19a and 19b for white and dark plumes, respectively.

Additional tests were conducted with trained observers to determine how accurately they could evaluate smoke plumes when allowed to choose their own viewing conditions. For these tests a panel of six

observers were shown black and white plumes with in-stack transmittances of 15, 30, 45, 60, 75, and 90 percent. As before, the plumes were generated in random sequence and on signal the observers assessed the plumes. Five runs were made, each consisting of 12 assessments with each of the transmittance levels occurring twice in each run. No restriction was placed on viewing direction. The tests were conducted near noon. Results are given in Tables 1 and 2, which show the mean of the 10 estimates by each inspector for the six transmittances assessed with both plumes, the standard deviation of the estimates from the mean, and the error of the mean.

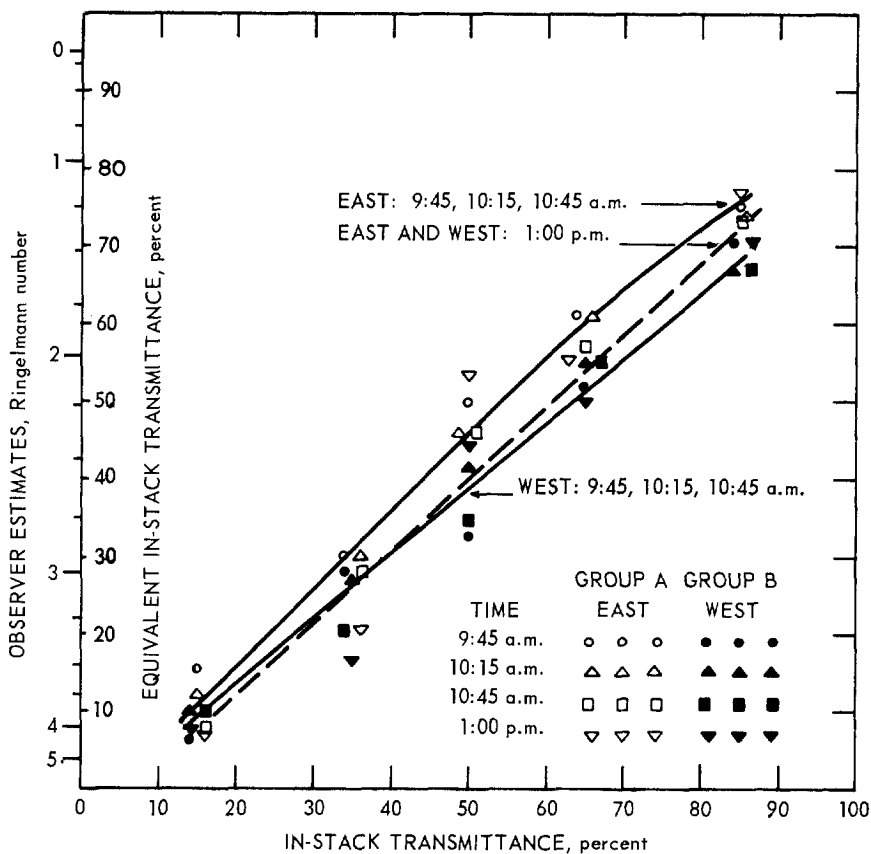


Figure 17. Variation in evaluations of black plumes by groups of trained observers viewing from east and west on a clear day.

These tests of trained observers show that the observers that viewed white plumes on a clear day facing the sun assessed the plumes at a higher Ringelmann number (lower transmittance) than did observers that viewed the plumes with the sun to their backs. For darker plumes, the effect was less pronounced. Group assessments showed good agreement for similar sun-plume-viewer geometries.

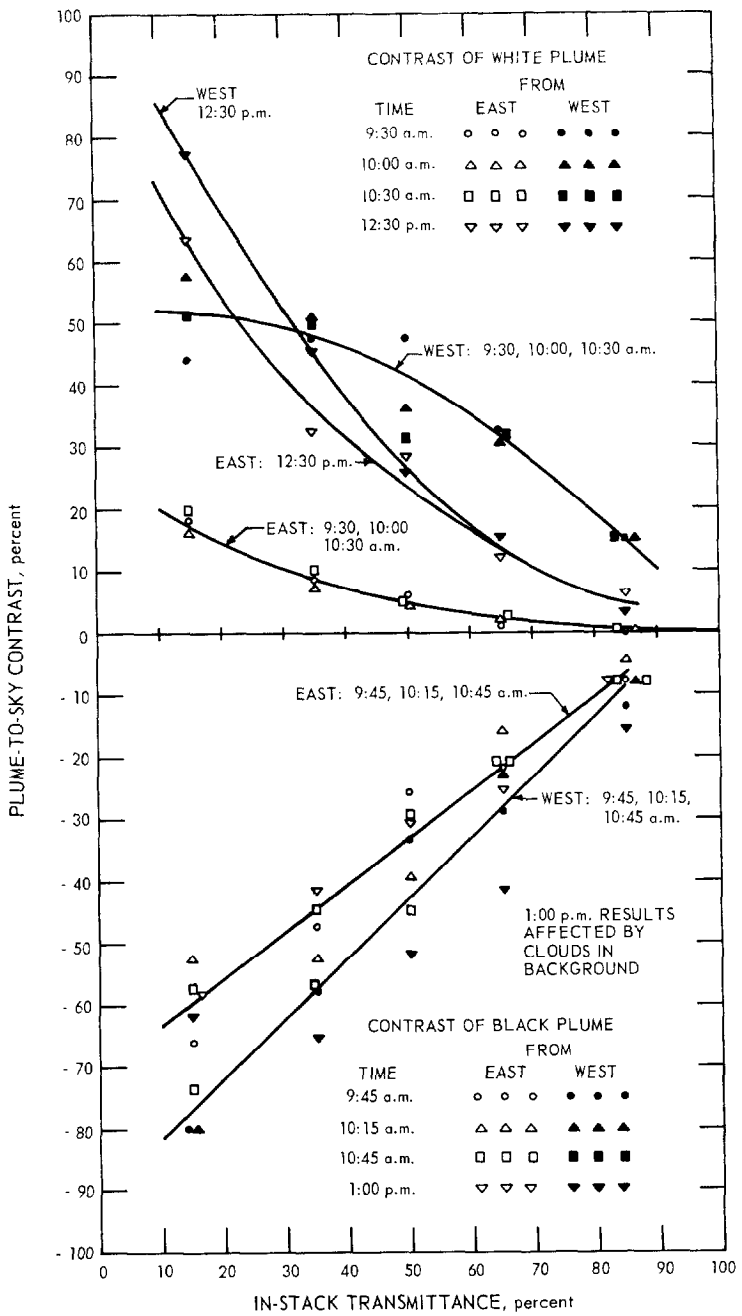


Figure 18. Variation in plume-to-sky contrast of plumes from east and west on a clear day during evaluation by trained observers.

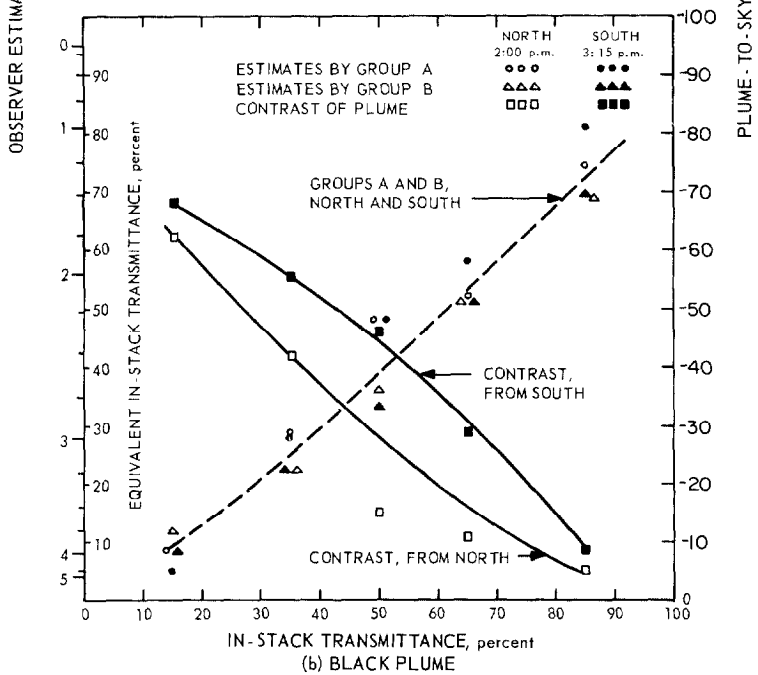
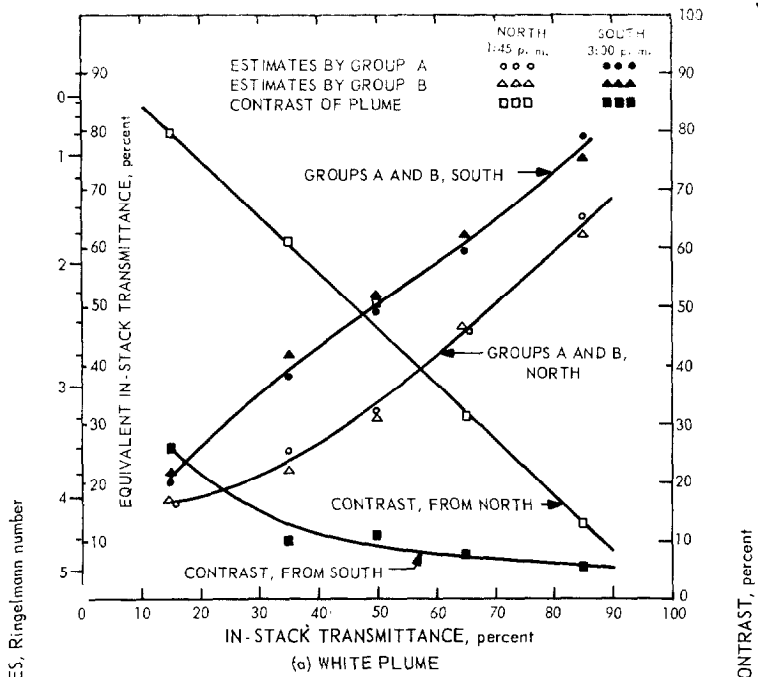


Figure 19. Variation in evaluations of plumes by groups viewing from north and south on a clear day.

**Table 1. EVALUATION OF BLACK TRAINING PLUMES BY TRAINED SMOKE INSPECTORS**

In-stack trans, % Equiv. Ring. No.	15	30	45	60	75	90
Insp. No. 1	3.68	3.08	2.65	2.14	1.65	1.20
Std. Dev.	0.34	0.34	0.37	0.24	0.33	0.38
Error	+ 0.18	+ 0.08	+ 0.25	+ 0.24	+ 0.35	+ 0.70
Insp. No. 2	3.58	2.95	2.53	2.03	1.55	1.10
Std. Dev.	0.32	0.35	0.31	0.34	0.24	0.37
Error	+ 0.08	- 0.05	+ 0.13	+ 0.13	+ 0.25	+ 0.60
Insp. No. 3	3.58	3.00	2.67	2.30	1.68	1.23
Std. Dev.	0.24	0.35	0.33	0.29	0.34	0.39
Error	+ 0.08	0	+ 0.27	+ 0.40	+ 0.38	+ 0.73
Insp. No. 4	3.38	2.70	2.10	1.75	1.45	0.84
Std. Dev.	0.42	0.33	0.30	0.19	0.31	0.24
Error	- 0.12	- 0.30	- 0.30	- 0.15	+ 0.15	+ 0.34
Insp. No. 5	3.70	2.94	2.43	1.78	1.35	1.03
Std. Dev.	0.50	0.28	0.32	0.26	0.20	0.21
Error	+ 0.20	- 0.06	+ 0.03	- 0.12	+ 0.05	+ 0.53
Insp. No. 6	3.50	3.00	2.35	1.98	1.43	1.10
Std. Dev.	0.34	0.29	0.33	0.26	0.24	0.12
Error	0	0	- 0.05	+ 0.08	+ 0.13	+ 0.60

**Table 2. EVALUATION OF WHITE TRAINING PLUMES BY TRAINED SMOKE INSPECTORS**

In-stack trans, % Equiv. Ring. No.	15	30	45	60	75	90
Insp. No. 1	4.20	3.30	2.60	1.80	1.00	0
Insp. No. 1	3.90	2.94	2.42	1.70	1.03	0.03
Std. Dev.	0.28	0.10	0.40	0.33	0.34	0.09
Error	- 0.30	- 0.36	- 0.18	- 0.10	+ 0.03	+ 0.03
Insp. No. 2	3.92	2.83	2.59	1.78	1.13	0.16
Std. Dev.	0.31	0.30	0.41	0.20	0.41	0.21
Error	- 0.28	- 0.47	- 0.01	- 0.02	+ 0.13	+ 0.16
Insp. No. 3	3.73	2.97	2.47	1.70	0.97	0.17
Std. Dev.	0.42	0.38	0.46	0.42	0.56	0.17
Error	- 0.47	- 0.33	- 0.13	- 0.10	- 0.03	+ 0.17
Insp. No. 4	4.28	3.55	3.15	2.55	1.98	1.18
Std. Dev.	0.31	0.44	0.28	0.37	0.21	0.23
Error	+ 0.08	+ 0.25	+ 0.55	+ 0.75	+ 0.98	+ 1.18
Insp. No. 5	4.18	3.58	2.78	2.38	1.80	1.06
Std. Dev.	0.23	0.35	0.24	0.32	0.29	0.11
Error	- 0.02	+ 0.28	+ 0.18	+ 0.52	+ 0.80	+ 1.06
Insp. No. 6	4.08	3.58	3.08	2.53	1.90	1.10
Std. Dev.	0.37	0.46	0.30	0.51	0.30	0.17
Error	- 0.12	+ 0.28	+ 0.48	+ 0.73	+ 0.90	+ 1.10

A similar series of tests conducted with white plumes on an overcast day did not show any variation with plume-viewing direction. This was to be expected, since on an overcast day the plume illumination is not directional.

## OPTICAL PROPERTIES OF SMOKE PLUMES

### A Brief Outline of Scattering by Fine Particles

The optical properties of smokes could be studied to some extent without reference to their connection with the size, composition, and concentration of the constituent smoke particles; however, some knowledge of this connection is of great practical interest, and can aid in interpreting and understanding the observations.

If in the presence of an interposed aerosol the observing eye or instrument receives a flux  $F$  direct from a source of light (which can be a portion of sky or an object such as a lamp) and in the absence of the aerosol a flux  $F_0$ , then the aerosol transmittance  $T$  is given by Bouguer's law (often called the Lambert-Beer law), which may be written

$$T \equiv \frac{F}{F_0} = \exp(-naQt)$$

where  $n$  = the number of particles per unit volume of air in the light path of length  $t$  through the aerosol;  $a$  = the projected area of one of these particles;  $Q$  = the particle extinction coefficient or extinction-efficiency factor defined as

$$Q \equiv \frac{\text{total flux scattered and absorbed by a particle}}{\text{flux geometrically incident on the particle}}$$

If particles of different sizes and extinction coefficients are present then a summation over all values of  $a$  and  $Q$  must be taken, or alternatively, appropriately taken average values  $\bar{a}$  and  $\bar{Q}$  must be taken, so the law may be written

$$T \equiv \exp(-t \sum_i n_i a_i Q_i) \equiv \exp(-n \bar{a} \bar{Q} t).$$

The product  $n\bar{a}\bar{Q} \equiv K$  is sometimes called the turbidity coefficient or the extinction coefficient of the aerosol as a whole, and has the dimensions (length)<sup>-1</sup>.

The particle extinction coefficient or extinction efficiency factor  $Q$  depends on the particle refractive index relative to the surrounding medium, its shape, and its size relative to the wavelength usually expressed as  $\alpha \equiv \frac{\pi d}{\lambda}$ , where  $d$  is the particle diameter and  $\lambda$  is the wavelength of light in the medium surrounding it.

Particles of transparent materials, i. e., materials with negligible electrical conductivity, have real values for the refractive index, e. g., 1.33 for water, 1.55 for quartz. Absorbing materials, i. e., those having appreciable conductivity, have a complex refractive index, e. g.,  $(2 - i)$  for carbon (moderately absorbing) in much of the visible spectrum<sup>16</sup> or  $(0.89 - 2.23i)$  for copper at 5,500 Å.<sup>17</sup>

In visible light, in air,  $Q \propto d^4$  when  $d < 0.05$  microns. This is the Rayleigh or dipole scattering regime for very small particles in which  $Q$  seldom exceeds  $10^{-2}$ . When  $d = 2$  microns,  $Q$  exceeds by less than 50 percent, sometimes by less than 10 percent, the limiting value 2 to which it tends at larger diameters. At larger diameters the total extinction by the particle, regardless of how it is divided between scattering and absorption and regardless of particle composition and shape, is simply proportional to its projected area. If the particle is a transparent sphere, then as  $d$  increases above 0.05 micron,  $Q$  rises, attains a maximum value about 3 or 4 somewhere between  $2/3$  and 1 micron diameter, and settles after some oscillation to the limiting value 2 (Figure 20, curves A and B). With an irregular transparent particle averaged over all orientations (rotational Brownian motion physically accomplishes this), the  $Q$  curve settles to 2 after passing through a simple maximum whose position and size depend on the particle shape. For an absorbing particle of any shape,  $Q$  settles to 2 without oscillation and with only a weak maximum or none, completing the rise when  $\alpha \simeq 1/2$  to 1 (Figure 20, curve C).

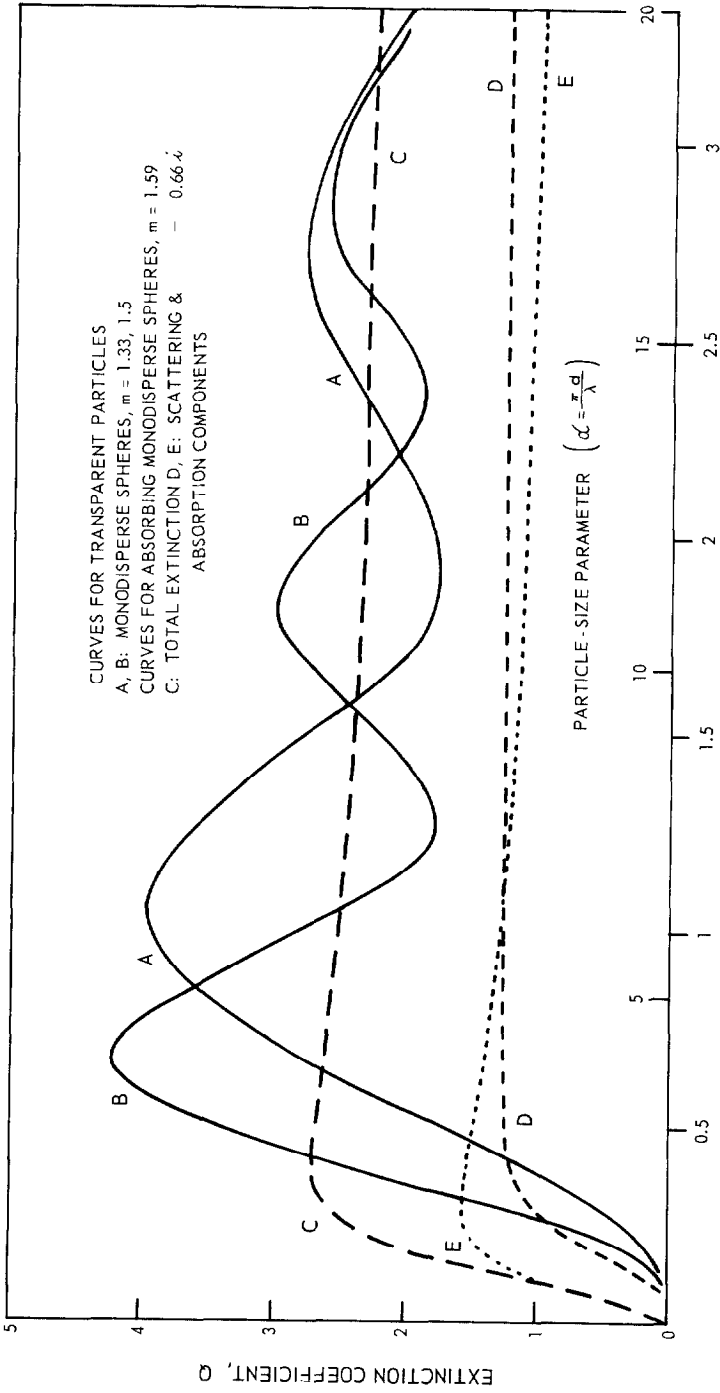
The  $Q$  curves for transparent, non-spherical particles averaged over all orientations resemble those for absorbing particles, except that the rise is slower than with transparent spheres. The maximum is less marked the more irregular the particle shape.<sup>18</sup>

Thus, if the aerosol transmittance is found not to vary with wavelength, its projected-area-concentration  $na$  or  $n\bar{a}$  can be deduced from Bouguer's law taking  $Q = 2$  without serious error, and without needing to know its particle size or composition. If the transmittance does vary with wavelength, then an estimate of size and area-concentration can be derived by fitting measurement at two wavelengths to the theoretical curves of  $Q$ ; the better the particle composition is known, the more accurate the estimate.

It is interesting to express the Bouguer law also in terms of the mass concentration of the particles,  $C_M = n\pi\rho d^3/6$ , where  $\rho$  and  $d$  are the density and diameter of the particles in consistent units, giving for monodisperse particles

$$T = \exp(-3C_M Q t / 2\rho d).$$

Even when  $Q = 2$  and the mass-concentration is constant, the transmittance will decrease with decreasing particle size. A family of curves showing the relation between plume transmittance and mass concentration in a plume 3 meters in diameter with black and white particles of different sizes is shown in Figure 21.



AREA - MEAN PARTICLE DIAMETER FOR WAVELENGTH OF 0.52 MICRON, microns

Figure 20. Particle extinction coefficients for various aerosols, calculated from Mie theory.

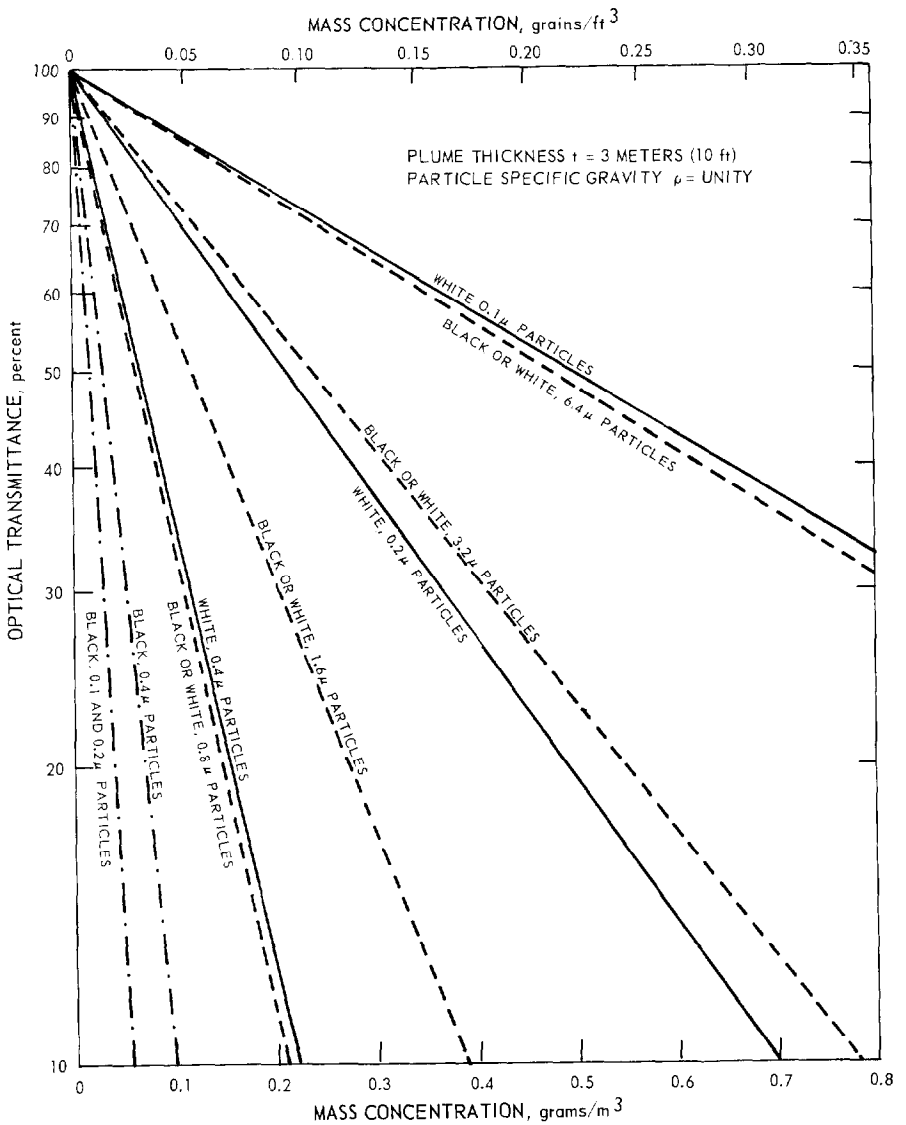


Figure 21. Relationship of transmittance and mass concentration for plumes containing particles of various diameters and irregular shapes.

In preparing this figure we assumed that the particles were irregular in shape, and of unit specific gravity; that those in the white smoke were transparent with refractive index 1.5 (many common transparent materials); and those in the black smoke were like carbon with complex refractive index about  $2(1-0.5i)$ . Values for the extinction coefficient  $Q$ , assuming a mean wavelength 0.5 micron, were as follows, taken from values established by one of the authors. <sup>19</sup>

$d, \mu$	:	0.1	0.2	0.4	0.8	1.6	3.2	6.4
$\alpha = \pi d/\lambda$	:	0.63	1.26	2.52	5.04	10.8	21.6	43.2
Q (white):		0.03	0.14	0.88	1.87	2	2	2
Q (black):		0.88	1.87	2	2	2	2	2

Black smokes and white smokes yield different curves for particles smaller than 0.8 micron diameter because the light extinction by black particles below this size is greater than by white.

The white smoke shows a maximum extinction per unit mass concentration at about 0.6 micron particle size, because below this size the particle extinction coefficient decreases faster than its surface per unit mass increases. The black smoke shows this minimum at about 0.15 micron. Transparent spheres smaller than about 2 microns extinguish more light than irregular particles of the same projected area. So if the particles in the plume are polydisperse spheres, as with mists, the read mass concentration will be 2 or 3 times too high for white plumes between 0.2 and 1.6 microns in mean particle-size, but not appreciably different for black plumes.

The angular distribution of light scattered by particles smaller than 0.05 micron diameter does not change with size; only the total amount changes. The scattering for both polarizations combined is equal in the forward and backward directions and is only 50 percent less at 90°. With increasing size above 0.05 micron the pattern becomes more forward-directed, and in visible light the scattering patterns of particles larger than 1 micron show a strong forward lobe of angular half-width about 35/d degrees, the particle diameter d being expressed in microns. At the same time subsidiary lobes appear in the scattering pattern, by number approximately 2 $\alpha$ . This evolution of the scattering pattern with increasing particle size, for transparent spherical particles of refractive index 1.5 in monochromatic light, is illustrated in Figure 22. The particle diameters for light of wavelength about 0.5 micron have been marked as well as the  $\alpha$ -values.

The strong forward scattering that all particles develop as their size increases above 0.5 micron is much the same for all materials, but transparent particles scatter much more strongly than absorbing ones at all angles outside the forward lobe just mentioned. There is, in fact, no such thing as a black smoke-particle in the sense of a particle that scatters no light whatever. In fact, particles of absorbing material (e.g., carbon) that are smaller than about 0.1 micron, as well as absorbing light, can at the same time scatter in all directions as much and sometimes more light than transparent particles of the same size. A smoke of absorbing particles can only appear black, i.e., not scattering significantly, either when it is not seen close to the sun, or not against a dark background (as from an aircraft above it), or when it is so dense that most of the light entering it is eventually absorbed from repeated encounters with particles, being part scattered and part absorbed at each encounter.

In white light the oscillations in the angular scattering pattern of a spherical particle (Figure 22) would be diminished because of the smoothing over a range of  $\alpha$ -values, and a range in particle size would have the same effect. The angular scattering patterns for an assembly of irregular particles in random orientation are similar to those of an assembly of spheres of similar size-range in white light. Even with such smoothing, there remain large differences between the patterns of particles with different refractive indices. Figures 23 and 24 show how the intensities of scattering through  $45^\circ$  and  $90^\circ$ , respectively, by single spheres vary with particle size and refractive index.<sup>20</sup> The curve for the complex refractive index  $(2 - i)$  would be appropriate for carbon; a curve for water, 1.33, may be interpolated between the curves for 1.2 and 1.4; and many transparent minerals, such as quartz, have a refractive index about 1.6.

The angular scattering pattern of an assembly of particles, such as portion of a smoke plume, is given by the sum of the patterns of the individual particles in it only so long as its transmittance exceeds at least 80 percent. The lower the transmittance, the greater is the proportion of light that is scattered more than once before emerging from the plume. This secondary scattering modifies the overall scattering pattern, reducing the angular variation and especially the forward lobe. The scattering process at the individual particles in the plume is not affected by increasing particle concentration until the mean inter-particle distance is reduced to a few particle diameters; these conditions could not persist in an aerosol because of the rapid coagulation that would ensue even if it arose.

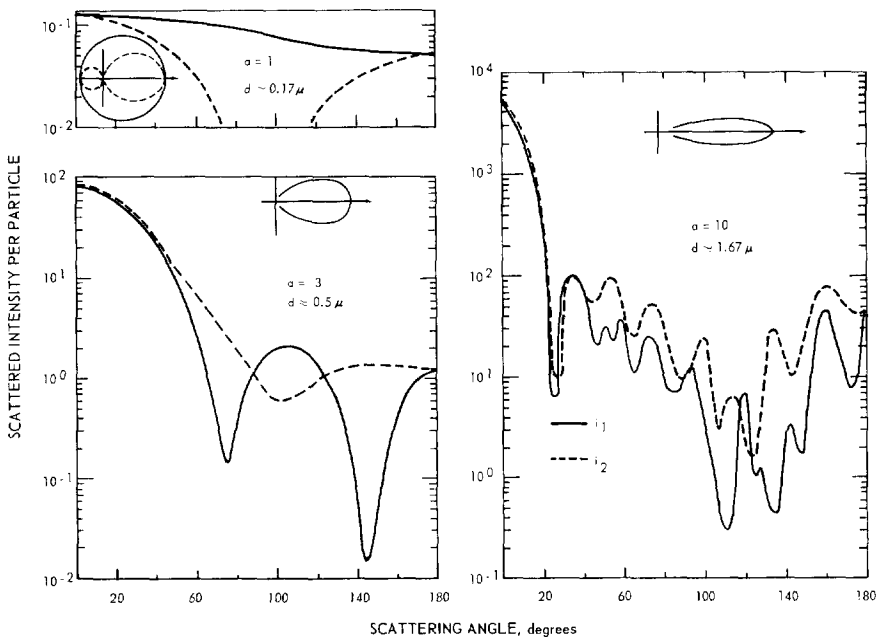


Figure 22. Scattering by transparent spheres, calculated from Mie theory.

For a fuller account of light scattering, one may refer to the review by Hodgkinson<sup>18</sup> and the theoretical treatise of Van de Hulst.<sup>17</sup> Because the angular scattering phenomena are much more complex than the extinction phenomena, it is considered impracticable to evaluate plumes by measurements of scattered light, whether from natural or artificial sources.

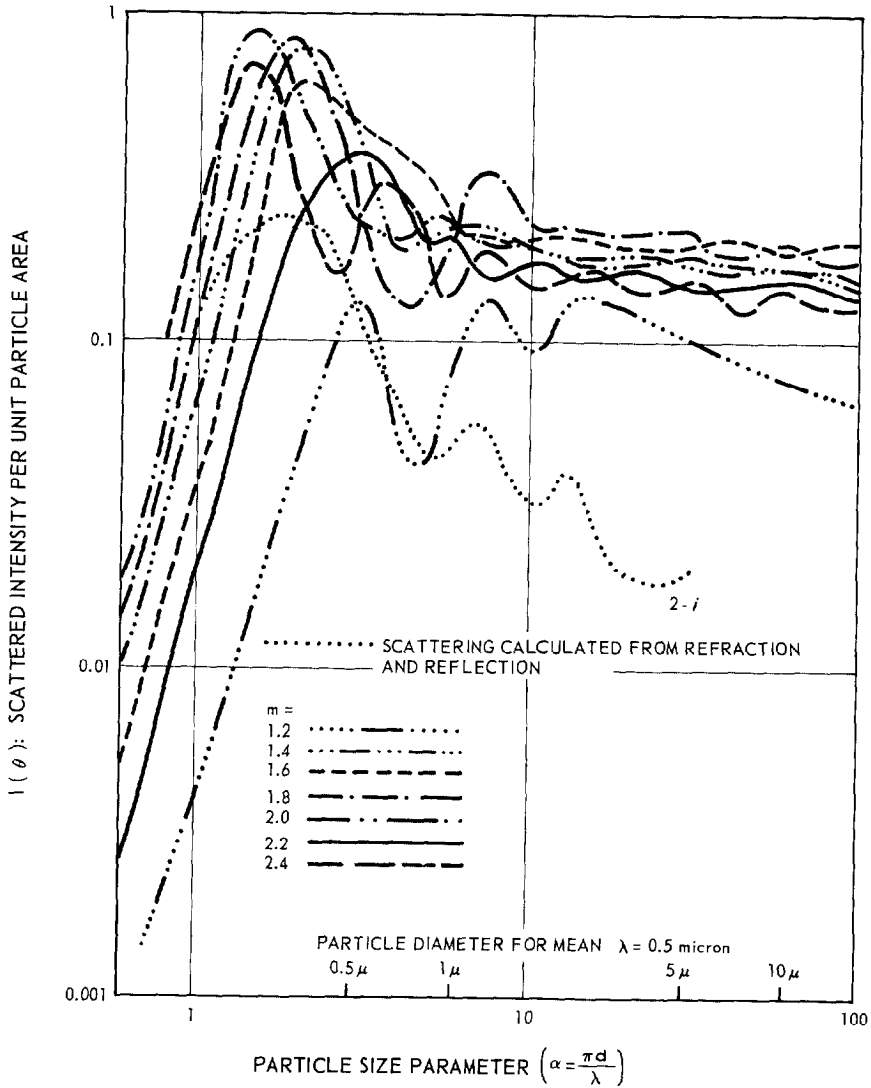


Figure 23. Scattering at 45 degrees by transparent spheres in white light, calculated from Mie theory.

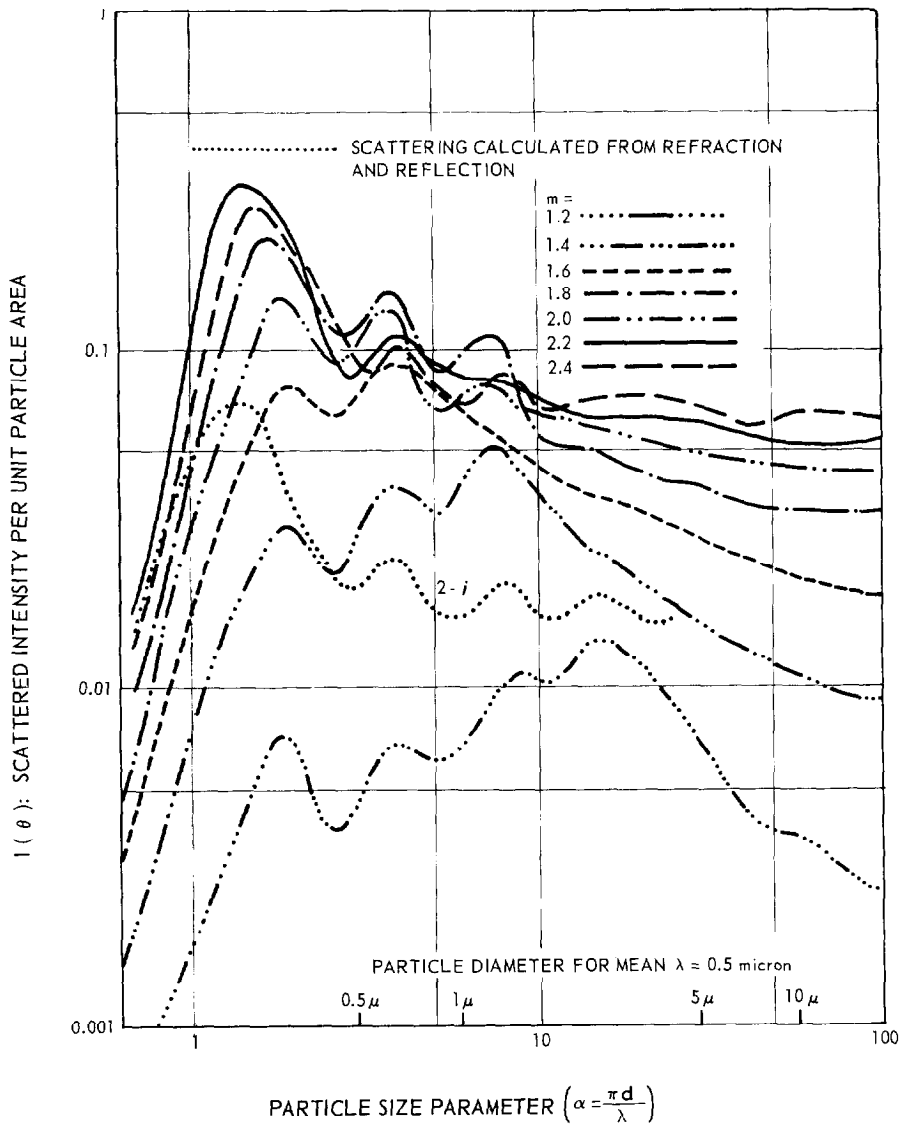


Figure 24. Scattering at 90 degrees by transparent spheres in white light, calculated from Mie theory.

### Transmittance-Wavelength Characteristics of the Experimental Plumes

The out-of-stack transmittances of the plumes were determined by viewing a 500-watt incandescent reflecting flood lamp through the

plumes with the telephotometer. This procedure permitted direct out-of-stack transmittance measurements in daylight because the intensity of the lamp was high enough that the light scattered by the plume was negligible when the sun was not directly behind the plumes. Without interference from scattered light, the transmittance is given by the ratio of the telephotometer reading of the lamp sighted through the plume to the telephotometer reading of the lamp sighted clear of the plume. The transmittance measurements were made for white light by using the telephotometer with the visual correction filter and for blue (No. 47), green (No. 58), and red (No. 29).

The effective overall spectral distribution of the telephotometer with the color filters and lamp was measured with the aid of the monochromator by using the telephotometer 1P22 phototube with each of the three filters. The relative distributions are shown in Figure 25. The mean responses ( $\bar{\lambda}$ ) of the distributions were calculated from the relation

$$\bar{\lambda} = \frac{\sum_i R_i \lambda_i}{\sum_i R_i}$$

where  $R_i$  is the spectral response at the corresponding wavelength  $\lambda_i$ . The mean responses of the telephotometer to the flood lamp with blue, green, and red filters were at the wavelengths 0.438, 0.531, and 0.651 micron, respectively.

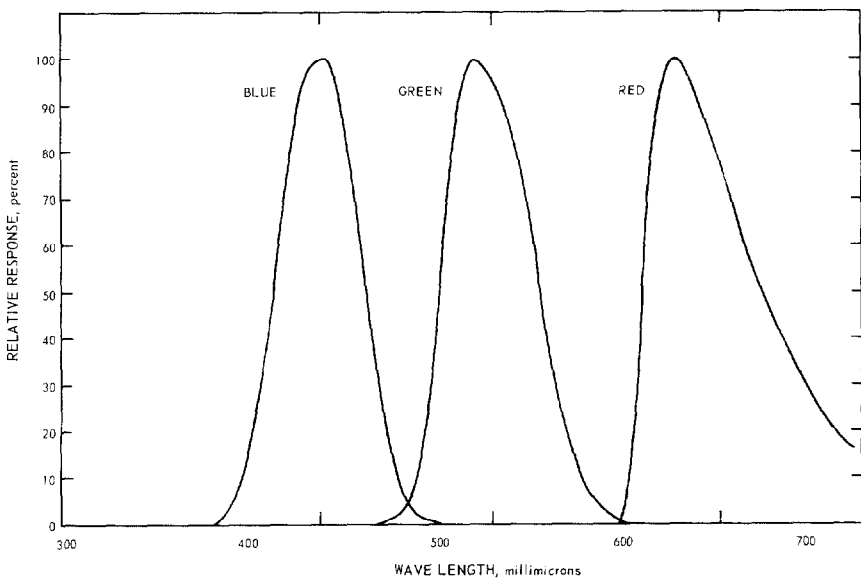


Figure 25. Effective spectral response of telephotometer-filter-lamp combinations used for plume transmittance measurements.

For the measurements on the black and white experimental plumes, the lamp (12-cm diameter) was placed about 3 meters behind the plumes and the telephotometer was placed about 12 meters in front of the plumes. The out-of-stack transmittances of red, blue, green, and white light through the experimental white and black plumes are compared to concurrent measurements of in-stack white light transmittance in Figures 26 and 27, respectively.

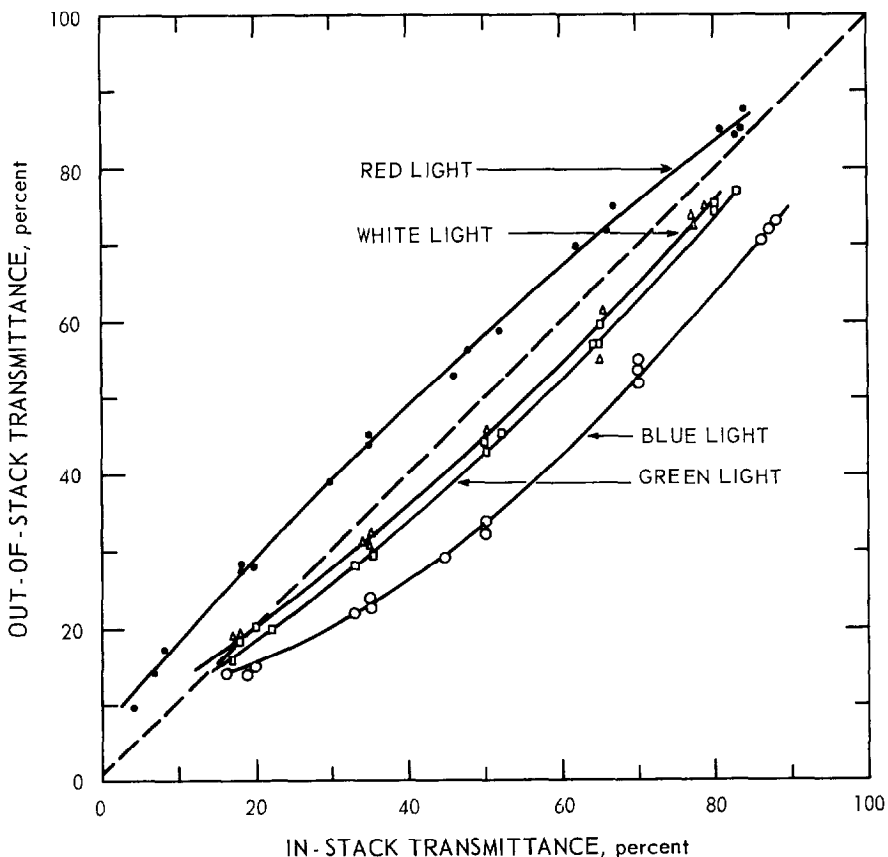


Figure 26. White plume: transmittance measurements by transmissometer inside stack and telephotometer with color filters sighted on lamp outside stack.

The variation in transmittance with wavelength observed with these plumes shows that the particles are so small that the particle extinction coefficient ( $Q$ ) varies with wavelength, i. e., they are on average smaller than about 1 micron.

Linear plots, as in Figures 26 and 27, give curved lines passing through the points (100%, 100%) and (0%, 0%). A straight line (slope = 1) in Figures 26 and 27 results only when  $T_2 = T_1$ , which is when  $\lambda_1 = \lambda_2$ , or when  $Q$  is independent of wavelength, i. e., for polydisperse smokes of particle-size exceeding about 1 micron.

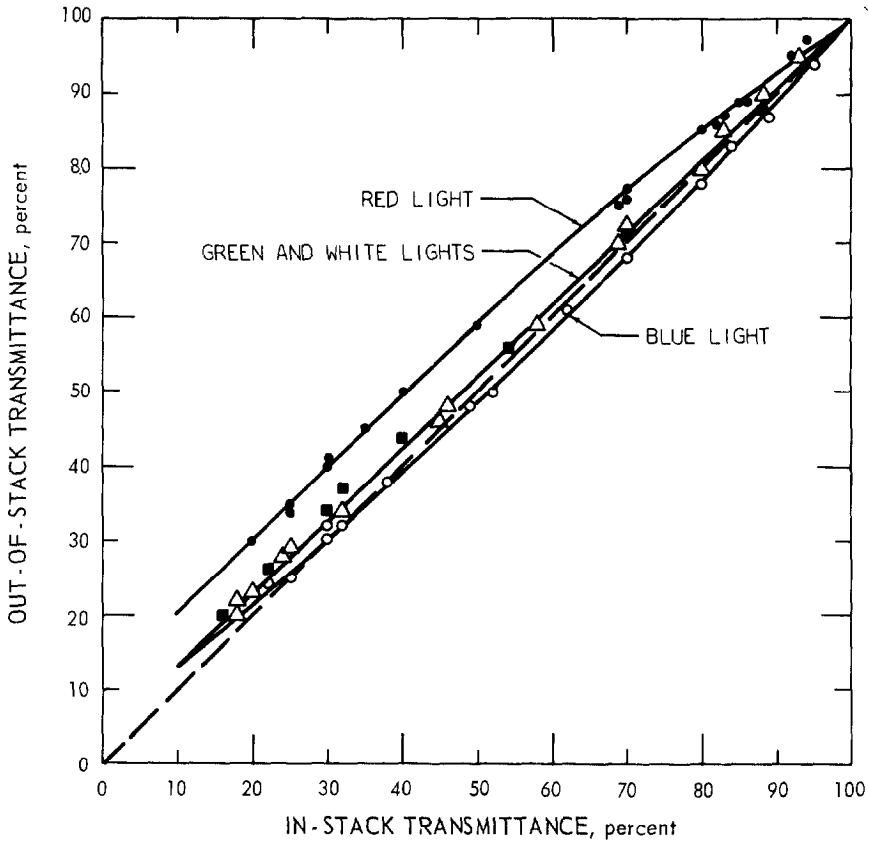


Figure 27. Black plume: transmittance measurements by transmissometer inside stack and telephotometer with color filters sighted on lamp outside stack.

The correlation between in- and out-of-stack transmittances, both measured in white light, for the experimental plumes showed that the in-stack transmittance of the white plume was higher by as much as 6 percent and the relation was not linear. This deviation from the ideal 1:1 relation for the white light curve and the failure of all the curves to pass through the (0, 0) point is probably due to a difference in the conditions of air flow between the in- and out-of-stack measurement positions.

For the transmittance measurements on the experimental power station plume, an experimental arrangement was devised to permit measurement through a greater thickness of the effluent because the transmittance of the 30-cm-diameter plume was around 98 percent. The effluent from the stack exit was diverted into a horizontal duct 30 cm in diameter and 4.9 meters long. The effluent entered the duct near one end through a side arm; because of the angle and high velocity at which the effluent entered the duct, it continued to flow through the

duct and out at the far end. By viewing the lamp through the duct, the observers measured transmission through a section of the effluent 5 meters long or more. The average transmittance measurements for four runs with blue, green, and red filters were 81.5, 86.0, and 93.0 percent, respectively.

### Angular Scattering Characteristics of the Experimental Plumes

The angular scattering patterns of the plumes were measured at night by viewing the plumes with the telephotometer while rotating a lamp around them. A lamp-holding mechanism was attached to the stack exits to permit the lamp to be rotated at a fixed distance from the center of the plumes in a plane normal to the direction of the plumes. The plumes were viewed along the lamp rotation plane and as close to the plumes as practicable to eliminate interference from light scattered by the intervening air between the telephotometer and plumes.

Before the angular scattering of the black and white plumes was measured, it was necessary to attach a 23-cm-diameter, 46-cm-length of duct to the stack exit to change its rectangular cross section to a circular one. For these measurements, a 500-watt flood lamp was rotated at a distance of 1.2 meters from the center of the plumes and the telephotometer was located about 50 cm from the plumes. The angular scattering patterns of black and white experimental plumes with transmittances of 60 and 90 percent were measured in white light. Because of the low plume density of the experimental power plant plume, it was necessary to rotate two 250-watt spot lamps around the 30-cm-diameter plume at a distance of 1.1 meters from its center. The scattering patterns are shown in Figure 28.

### Optical Properties and Particle Sizes of Experimental Plumes

The mean particle sizes of the experimental plumes were estimated by fitting the ratios of the mean particle extinction coefficients of the plumes for red, green, and blue light to theoretical extinction curves plotted from Mie-theory computations for the correct refractive index. If the plume transmittances are  $T_1$  and  $T_2$  when measured at two different wavelengths  $\lambda_1$  and  $\lambda_2$ , it follows from Bouguer's law that

$$\log_e T_2 = \frac{Q_2}{Q_1} \log_e T_1$$

where  $Q_1$  and  $Q_2$  are the mean particle extinction coefficients at  $\lambda_1$  and  $\lambda_2$ . Consequently, as the particle concentration is varied a log-log plot of  $T_2$  versus  $T_1$  would give a straight line of slope  $Q_2/Q_1$  through the point 1, 1 (100%, 100%).

If  $T_r$ ,  $T_g$ , and  $T_b$  are the measured transmittances for red, green, and blue light, then from Bouguer's law

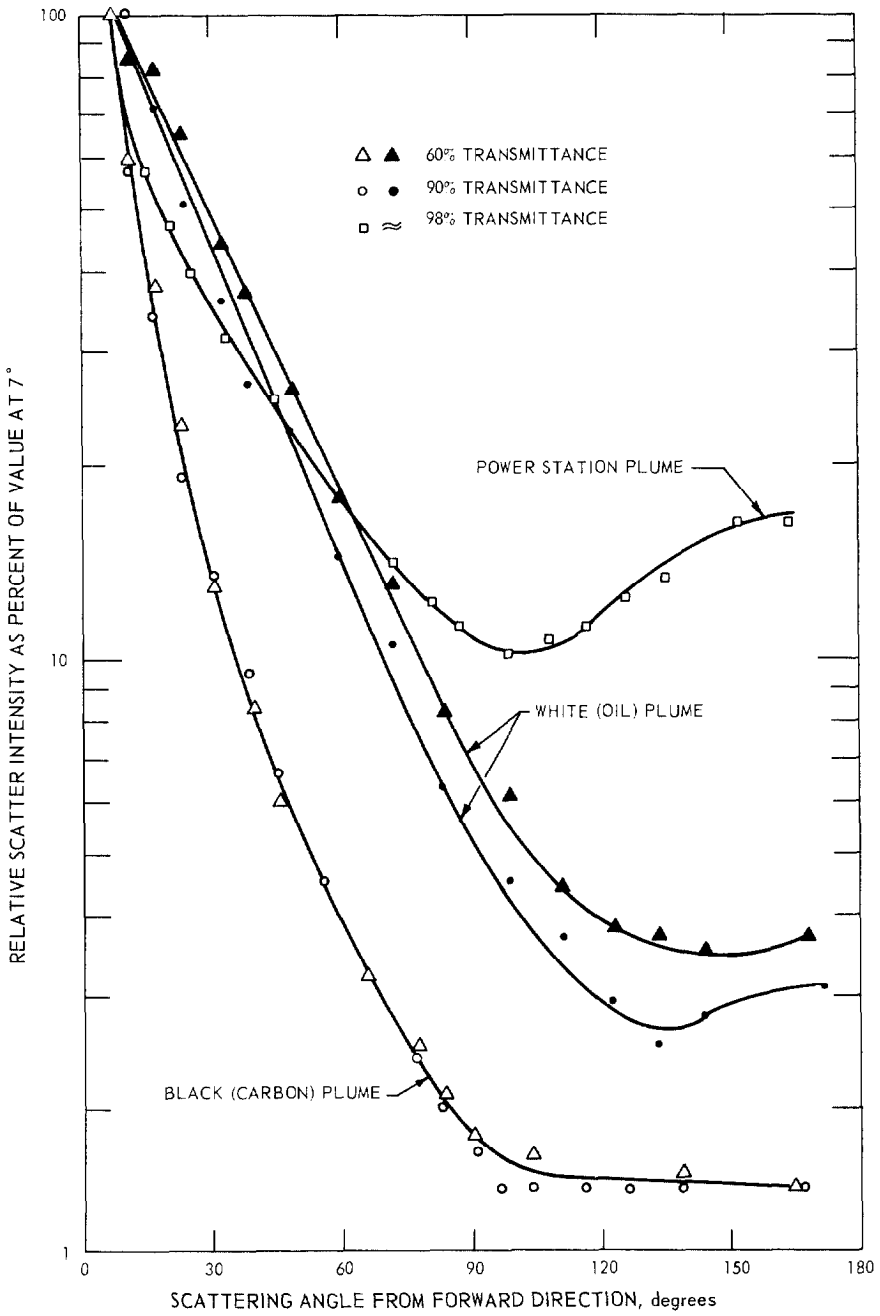


Figure 28. Angular scattering measurements of experimental plumes.

$$Q_r : Q_g : Q_b = \log_e T_r : \log_e T_g : \log_e T_b$$

where  $Q_r$ ,  $Q_g$ , and  $Q_b$  are the corresponding particle extinction coefficients. The corresponding ratios of the particle size parameters  $\alpha_r$ ,  $\alpha_g$ , and  $\alpha_b$  are

$$\alpha_r : \alpha_g : \alpha_b = \lambda_r^{-1} : \lambda_g^{-1} : \lambda_b^{-1}$$

where  $\lambda_r$ ,  $\lambda_g$ , and  $\lambda_b$  are the mean spectral responses of the tele-photometer and filter combinations used for the measurement.

To obtain the estimate, the theoretical curve of particle extinction coefficient  $Q$  against particle size parameter  $\alpha = \pi d/\lambda$  is plotted on a log-log scale; on an identical graph sheet are plotted the points  $(\log T_r/\log T_r = 1, \pi/\lambda_r)$ ,  $(\log T_g/\log T_r, \pi/\lambda_g)$ , and  $(\log T_b/\log T_r, \pi/\lambda_b)$ ; the second sheet is slid over the first, with the axes kept parallel until the three points are fitted to the portion of the theoretical curve with the appropriate curvature; then the correspondence of the logarithmic abscissae of  $\pi d/\lambda$  and  $\pi/\lambda$  gives the value of particle diameter  $d$ . With this value of  $d$  the actual value of  $Q$  for any of the wavelengths may be read from the theoretical curve for the appropriate  $\alpha$  and hence the projected-area concentration also derived, from Bouguer's equation.

A second estimate of the particle sizes of the plumes was obtained by comparing the angular scattering patterns of the plumes with theoretical patterns for different particle sizes plotted from Mie-theory computations (Appendix A).

### Transmittance-Wavelength Characteristics and Particle-Size of the White (Oil) Plume

The published Mie-theory extinction computations for spherical particles that came nearest to the refractive index of the oil, approximately 1.45, were those for 1.44 by Penndorf<sup>21</sup> and are plotted as the dashed curve in Figure 29. Since the droplets were not monodisperse but ranged in size, a sliding average of this extinction curve was taken over a 2-to-1 range in diameter for an equal number frequency of particles through this range. If the range is considered to run from  $2D/3$  to  $4D/3$  with a frequency of 1 particle per unit size-range, then the area-mean particle diameter is given by

$$d_a^2 = \int_{2D/3}^{4D/3} D^2 dD \div \int_{2D/3}^{4D/3} dD = \frac{28}{27} D^2,$$

$$d_a = 1.02D \approx D.$$

The area-mean diameter is the appropriate measure of mean particle size because the particle extinction coefficient  $Q$  is defined with respect

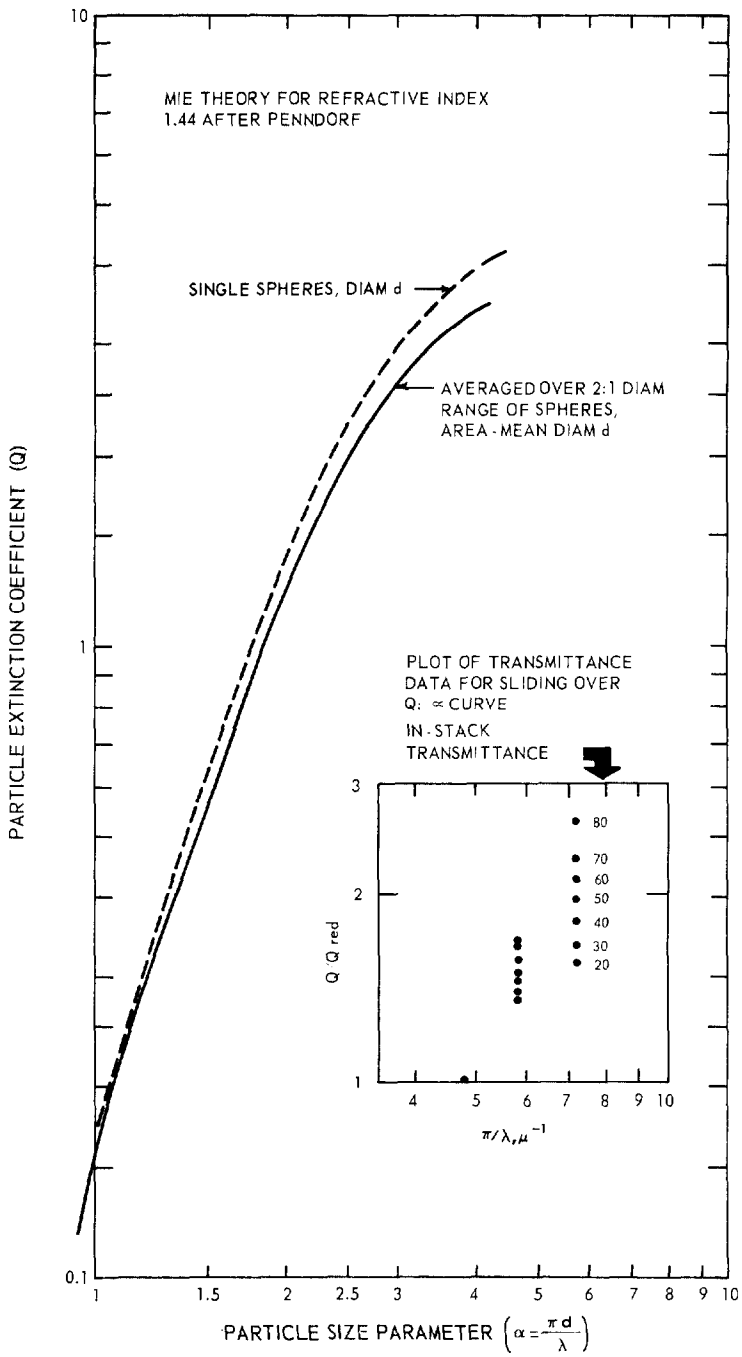


Figure 29. White plume: transmittance measurements fitted to Mie-theory extinction curve.

to the particle area. The solid curve in Figure 29 represents this sliding average, the  $\alpha$  values corresponding to  $\pi d/\lambda$ . It differs very little from the monodisperse curve and so, although the size distribution on which it is based represents the oil drops only approximately, a sliding average using the actual distribution would result in a curve not very different.

The transmittance measurements (Figure 26) were used to compute the extinction ratios of the particles in the experimental white (oil) plume for light of mean wavelengths 0.651, 0.531, and 0.438 micron. The ratios between extinction coefficients (Table 3) are plotted in the insert of Figure 29, providing three points on the sliding graph since three wavelengths were used. Each trio of points was fitted in two ways, using the red and blue points only and using all three; but the resulting estimates of area-mean particle diameter (Table 3) do not differ significantly. The increase in particle size with increasing smoke concentration is consistent with reports on the performance of such smoke generators; it may be due to increased coagulation of droplets in the generator or to reduced evaporation of droplets caused by increased oil vapor pressure in the smoke, or to both.

**Table 3. EXTINCTION COEFFICIENT RATIOS AND PARTICLE SIZE ESTIMATES OF THE EXPERIMENTAL WHITE (OIL) PLUME**

In-stack transmittance, %	$Q_r : Q_g : Q_b$	Area-mean particle diameter, microns	
		3-point Fit	2-point Fit
80	1 : 1.69 : 2.60	0.32	0.32
70	1 : 1.67 : 2.28	0.37	0.39
60	1 : 1.58 : 2.10	0.44	0.43
50	1 : 1.50 : 1.93	0.47	0.47
40	1 : 1.47 : 1.80	0.48	0.49
30	1 : 1.39 : 1.56	0.54	0.54
20	1 : 1.34 : 1.56	0.58	0.57

### **Transmittance-Wavelength Characteristics and Particle-Size of the Black (Carbon) Plume**

Complex refractive indexes of 1.90 (1-0.36i) for wavelength 0.436 micron and 2.00 (1-0.33i) for 0.623 micron are cited for carbon particles by McDonald.<sup>22</sup> At these two wavelengths, McDonald has also published Mie extinction efficiency factors for carbon spheres with particle size parameters from  $0.2 < \alpha < 8$ . The extinction curve (Figure 30) was constructed from an average of the extinctions at the two wavelengths. For particle size parameters greater than about 3, the extinction factor was not different at the two refractive indexes and

was only slightly different below 3. As with the white plume the extinction curve was averaged over a 2:1 range in particle diameters.

The extinction coefficients of the particles in the black plume - computed from the transmittance measurements of Figure 27 - did not vary with plume density as did the coefficients of the white plume. Consequently, an average of the extinction ratios at in-stack transmittance intervals of 10 percent gave 1:1.23:1.37 as the extinction ratios of the particles in the black plume for light of wavelengths 0.651, 0.531, and 0.438 micron. The extinction size parameter ratios are plotted in the insert of Figure 30. The points were fitted to the averaged Mie-theory curve in the manner described above and gave an area-mean particle diameter estimate of 0.23 micron for the black experimental plume.

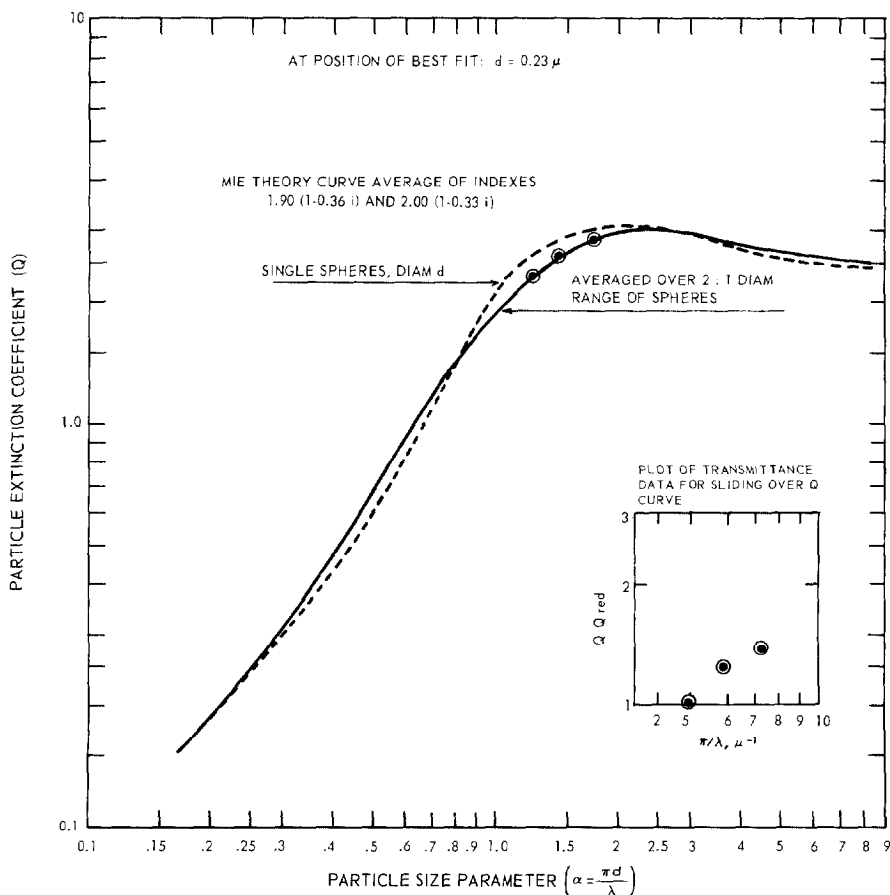


Figure 30. Black plume: transmittance measurements fitted to Mie-theory extinction curve.

## Comparison of Particle-Size Estimates with Direct Mass-Concentration Measurements

The mass concentration of an aerosol with monodisperse spherical particles of diameter  $d$ , specific gravity  $\rho$ , and number concentration  $n$  is  $C_m = n\pi d^3 \rho/6$ , and the projected area of the particles is  $a = \pi d^2/4 = 3C_m/2nd$ . Consequently, the mass concentration of a plume of spherical particles may be written from Bouguer's law as

$$C_m = \frac{2 \bar{d} \rho}{3 \bar{Q} t} \log_e \frac{1}{T} \left[ \frac{\text{grams}}{\text{meter}^3} \right]$$

where  $t$  is the thickness of the plume in meters,  $\bar{d}$  is the mean diameter of the particles in microns, and  $\bar{Q}$  and  $T$  are the mean particle extinction coefficient and transmittance of the plume, both functions of wavelength.

For calculation of the mass concentration of the white and black experimental plumes, their transmittance data (Figures 26 and 27) were fitted by the procedure described above, to the Mie-theory curves of Figures 29 and 30 to obtain  $\bar{d}$  and  $\bar{Q}$ . The thickness of the plumes was 0.2 meter, and the specific gravity of the fuel oil used in the white smoke generator was 0.87. A specific gravity of 1.95 was used for particles in the black plume since a specific gravity 1.8 to 2.1 is reported for amorphous carbon.

To obtain direct measurements of the mass concentration of the plumes, isokinetic samples of the effluents were collected on membrane filters and weighed with an analytical balance. Samples were collected at plume transmittance intervals of about 10 percent. The comparisons are shown in Figures 31 and 32.

The measured mass concentration of the white plume was higher than the calculated concentration by 44 percent at 70 percent transmittance, and 25 percent at 20 percent transmittance. This agreement is as close as can be expected, since much mass may be contributed by a few large particles (mass  $\propto d^3$ ). In terms of the particle size estimate from light extinction, this agreement implies an error of only 8 to 15 percent over the range of transmittances.

Almost perfect agreement was obtained between the measured and calculated weight concentration of the black plume. Such an agreement is undoubtedly coincidental and is probably due to a fortuitous compensation of the effects of using both a high extinction coefficient and a high area-mean diameter in the computation due to matching the transmittance data to a Mie extinction curve for spheres. Irregular particles less than about 1 micron extinguish less light than spheres with the same projected area, and the volume to area diameter for irregular particles will be less than for spheres. Nevertheless, the agreement again illustrates how the transmittance of a plume can be related to the amount of nongaseous material in the plume.

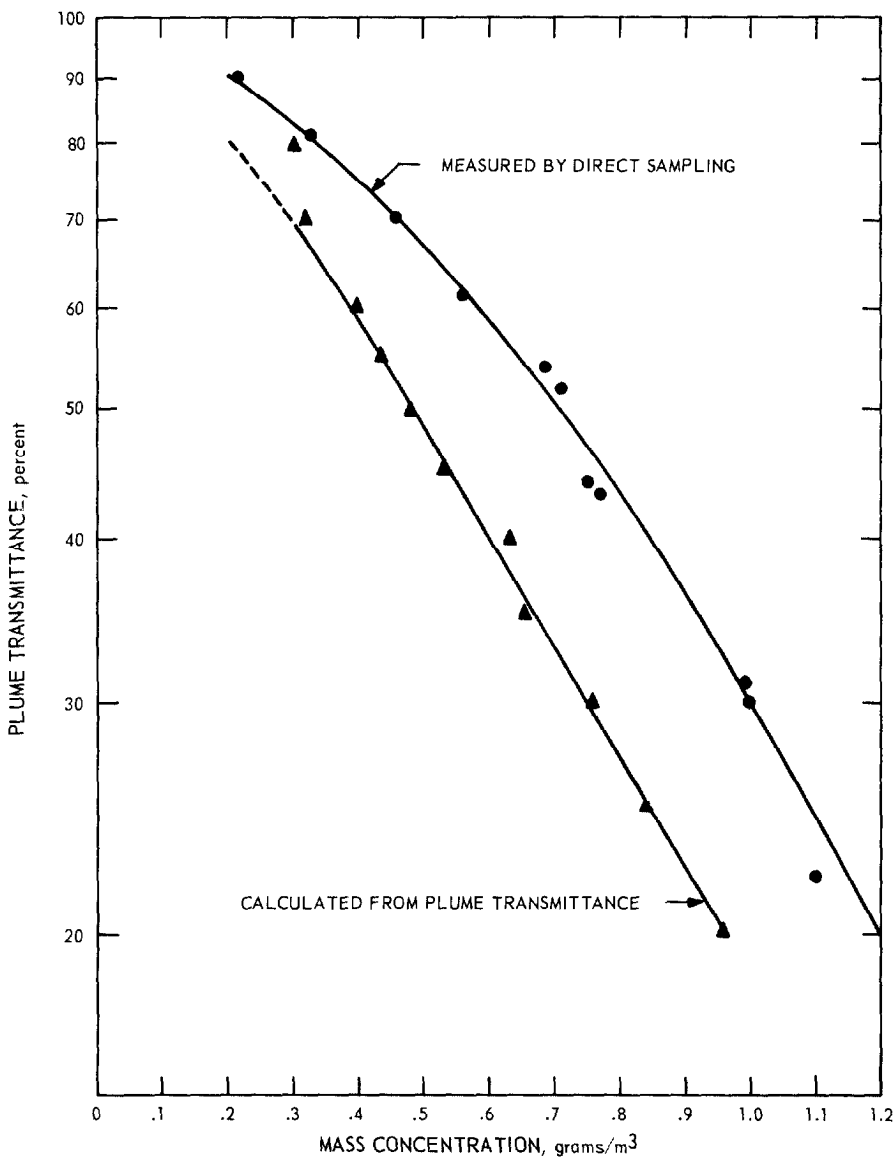


Figure 31. Mass concentration of white plume as calculated from transmittance and measured by direct sampling.

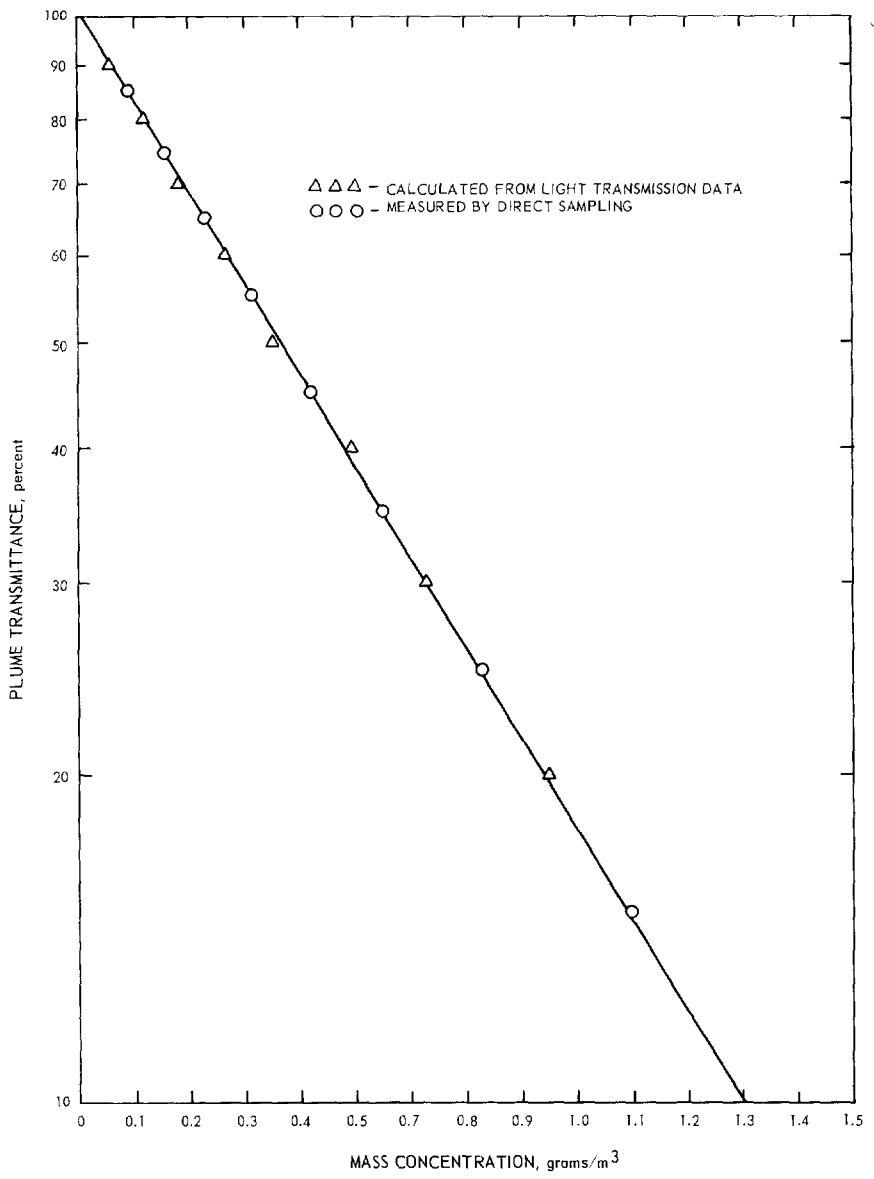


Figure 32. Mass concentration of black plume as calculated from transmittance and measured by direct sampling.

## **Transmittance-Wavelength Characteristics and Particle-Size of the Oil-Burning Power Station Plume**

The solid particles in the smoke consist primarily of metal sulfates with an indeterminate degree of hydration. An estimate of 0.14 micron diameter, based on electron microscopy, has been reported.<sup>23</sup> Inspection of the refractive indices of various sulfates suggests values of 1.45 to 1.5, with hydration making little difference.<sup>24</sup> A refractive index of 1.5 was therefore used in this analysis, since especially good Mie-theory tables for this refractive index have been published by Giese and others.<sup>25</sup> In the analysis of the transmittance measurements of the white experimental plume it was remarked that smoothing the Mie curve over a 2:1 range in particle size did not greatly change the shape of the initial rise in the curve, on which the present observations also fall. The experimental extinction ratios for the power station plume were therefore fitted by the same procedure to the unsmoothed Mie extinction curve for refractive index 1.5 (Figure 33), and yielded an estimate of 0.3 micron for the area-mean particle diameter.

Because of the very wide range in particle size suggested by the analysis of the scattering patterns (Appendix A) and the overwhelming preponderance by number of the finest particles, which because of their very small extinction coefficients contribute less than half of the total extinction by the model aerosol, fitting the transmittance measurements on the power plant smoke plume to the Mie-theory extinction curve gives an estimate of area-mean particle size considerably larger than the actual size. Nevertheless, such an estimate is of value; it is the mean size of the particles that chiefly contribute to the attenuation and the scattering and therefore is useful as a description of these properties. When we bear in mind the ignoring of the smaller particles, this estimate of 0.3 micron is reasonably consistent with the model size-distribution inferred from the scattering measurements (Table A1) as described in Appendix A. If any of the larger particles present were in fact condensed droplets, then their sizes might have been affected by the different air flow conditions at the exit of the smoke stack in the transmittance and scattering measurements.

## **INSTRUMENTAL TECHNIQUES FOR EVALUATING SMOKE PLUMES**

The experimental data accumulated on plume visual effects confirm theoretical expectations of great variability. Vision obscuration by smoke plumes and the visual appearance of smoke plumes are far too dependent on environmental conditions of plume illumination to be reliable measures for characterizing the plume as an aerosol. A plume that is assessed by a visual effect could be condemned when viewed on one day and accepted on another, or condemned when viewed from one direction and accepted from another, even when its contents had not changed.

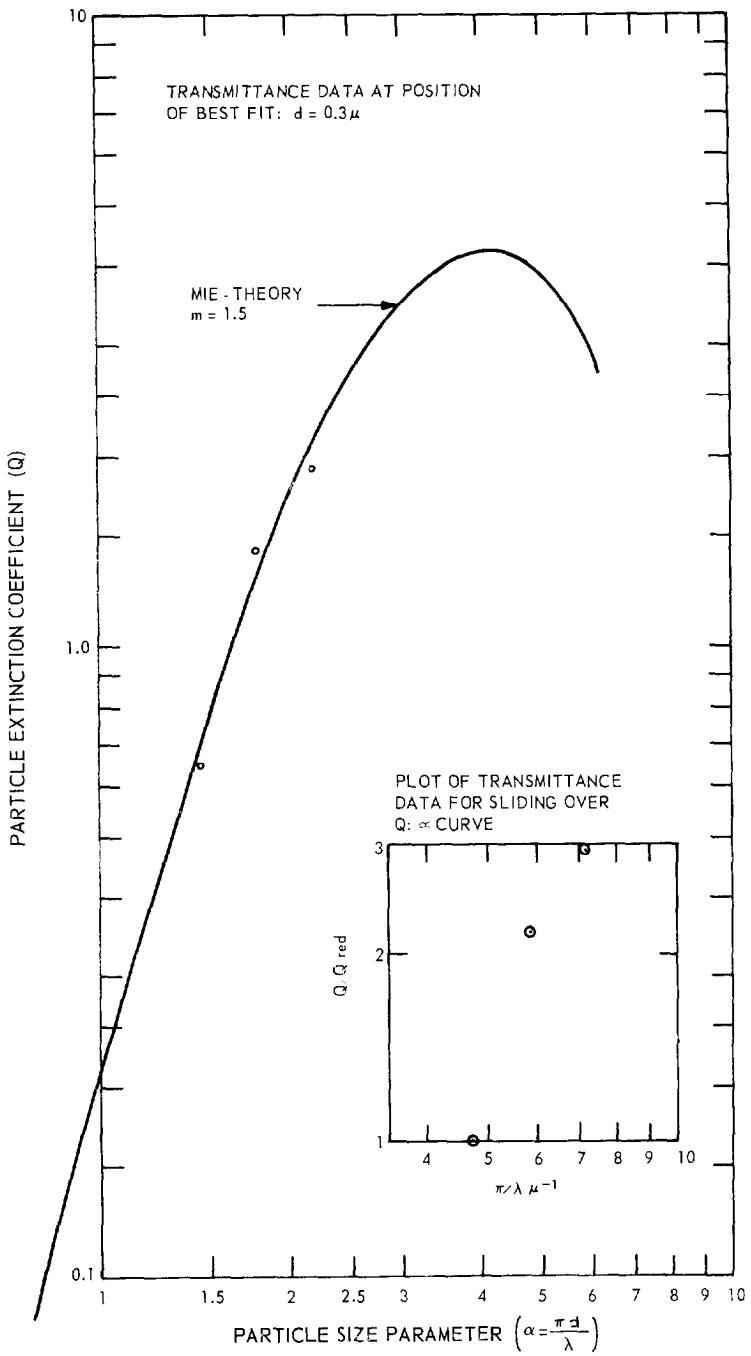


Figure 33. Experimental power-station plume: transmittance measurements fitted to Mie-theory extinction curve.

The solid and liquid particles in a plume may be characterized by two intrinsic optical properties, their angular scattering pattern and their extinction coefficients. However, the light transmittance of a plume is more simply related to concentration, particle size, composition, and plume dimensions, and is more readily measurable than a plume scattering pattern. Plume evaluation according to the angular scattering pattern would require not only measurements of the relative angular distribution of scattered light which, as evidenced by such measurements described here, are cumbersome, but also a quantitative comparison of the illuminating and scattered light.

We have indicated that, under conditions in which a measure of aerosol concentration can be derived from a determination of the plume transmittance, this measure is the projected-area of the solid and liquid particulate material per unit volume of air, termed the projected-area concentration. Conversely, the light-transmitting and light-scattering properties of the plume are in general related more closely to this measure of concentration than to any other, such as the number concentration (e. g. , particles per  $\text{cm}^3$ ) or the mass concentration (e. g. , grams per  $\text{m}^3$ , or loading as grain per cu ft). The mass concentration of solid particles is the only one that has been used routinely as a criterion of the maximum permissible level of particulate material in a smoke plume. Its relation to the area concentration depends on the particle mean-size and size distribution. Thus a given mass concentration of a given substance can correspond to a wide range of plume transmittances depending on the particle size. It is partly for this reason that the mass concentration is an incomplete criterion for assessing the particle content of a plume, although it is a useful subsidiary criterion; in the past it has often been the sole criterion because it was the simplest quantitative measure of particulate concentration that could be obtained.

### **Transmittance Measurement by Means of Contrasting Targets**

The transmittance of a plume can be obtained, even when it is scattering much light from other sources, by measuring the luminance difference between a pair of contrasting targets through the plume ( $B_1' - B_2'$ ) and clear of the plume ( $B_1 - B_2$ ). The transmittance is calculated from the relation

$$T = \frac{B_1' - B_2'}{B_1 - B_2}$$

With this procedure, interference from light scattered by the plume cancels out. Luminance difference ratios between contrasting targets viewed through and clear of a plume may be obtained by direct telephotometry of targets or by photographing the targets and obtaining the measurements from the negative in the laboratory with a densitometer.

For the photographic method, a series of neutral density filters would be positioned along one side of the camera film plane to produce

a calibration scale on the negative. For the photograph, the camera is orientated to position the filters in the brightest part of the scene, usually the sky. A calibration curve is obtained from the negative by plotting the optical density of the images as a function of the filter transmittance (relative negative exposure). Then by measuring the densities of the contrasting targets, their relative luminances are obtained from the calibration curve.

Contrasting targets that may be viewed through plumes from the ground may be a portion of blue sky and white cloud, or, where available, high ground or a building and a portion of sky.

Contrasting targets on the ground may also be used to measure plume transmittance by use of a helicopter. The contrasting targets may be distant land and horizon, plowed field and wooded areas, water and sandy beaches, etc. If the density of the smoke or ambient lighting conditions are unstable, the photographic technique is preferred because it gives a permanent and instantaneous record of the measurements. The camera must be equipped with lenses that will produce images of sizes suitable for densitometer measurements. Direct telephotometry of the targets has the advantages of greater simplicity and faster data reduction.

The technique of obtaining plume transmittance by direct telephotometry of contrasting targets has been illustrated in all the contrast reduction experiments on panel targets viewed through the black and white experimental plumes. Computations of transmittance from these measurements are compared with in-stack transmittance measurements in Appendix B.

The transmittance of plumes was also measured with a telephotometer by viewing distant hills and horizon skies through the plumes. Table 4 shows transmittances of the white experimental plume measured by sighting on a distant hill and adjacent sky. The measurements were made on a clear day and the viewing direction was northwest. The agreement between the two sets of transmittance measurements is acceptable.

Table 5 shows transmittance of a coal-burning power plant plume measured by sighting on a distant hill and adjacent sky. The measurements were made at various times over a 5-day period. Illuminating conditions were highly variable throughout the entire period because of the varying overcast conditions that persisted. A coal-cleaning operation located in the area also caused variable luminance measurements and was probably responsible for the particularly high luminance of the wooded hillside when viewed clear of the plume. The viewing direction was southwest.

Figure 34 illustrates the photographic technique of measuring the transmittance of a smoke plume. The coal-burning power plant plume was used for the test and the contrasting objects were the distant hill and adjacent sky. The sky was overcast. In Figure 34 the calibration

**Table 4. TRANSMITTANCE OF WHITE PLUME MEASURED BY SIGHTING ON HILL AND SKY THROUGH THE PLUME WITH A TELEPHOTOMETER**

(luminances are in candles/meter <sup>2</sup> )						
B <sub>s</sub>	B <sub>h</sub>	B <sub>s</sub> '	B <sub>h</sub> '	T'	T	E <sub>t</sub>
2900	600	3100	2600	22	22	0
2900	600	2800	2000	45	36	9
2650	600	3050	2400	32	28	4
2600	600	2800	1800	50	48	2
2600	600	2700	1600	55	58	3
2600	600	2650	1250	70	68	2
2550	600	2600	950	85	82	3
2650	600	3600	3250	17	14	3
2650	550	3100	2400	34	29	5
2700	600	3000	2600	19	24	5

$\bar{E}_t = 3.7$

T' = calculated plume transmittance

$$= \frac{B_s' - B_h'}{B_s - B_h}$$

T = in-stack plume transmittance  
(measured with transmissometer)

E<sub>t</sub> = error in the calculated transmittance

curve of density versus relative exposure is shown in upper right and the calibration scale is shown in the upper left. The calibration curve was obtained from densitometer readings of the negative image of the calibration scale. Densitometer readings of the negative images of the targets indicated a plume transmittance of 28 percent. Direct telephotometry of the targets indicated the transmittance of the plume was varying between 23 and 30 percent.

### Transmittance Measurement by Means of Single Targets

If the target is so bright that light scattered by the plume is negligible when compared to the transmitted light, the transmittance can be obtained directly as the ratio of the target intensity when viewed through the plume to the target intensity when viewed clear of the plume.

At night almost any light source behind the plume that is bright enough to be measured with a telephotometer is suitable, since the plume is not scattering light from its surroundings. The targets may be the moon, light scattered from an intense searchlight beam behind the plume, light reflected from illuminated objects behind the plume, or similar sources. In the daytime, the sun offers a suitable target. A simple sun photometer sighted on the sun, first clear of the plume and then through the plume, gives the transmittance directly, since any

**Table 5. TRANSMITTANCE OF A COAL-BURNING POWER PLANT PLUME MEASURED BY SIGHTING ON HILL AND SKY THROUGH THE PLUME WITH A TELEPHOTOMETER**

(luminances in candles/meter <sup>2</sup> )						
	Time (EDT)	B <sub>s</sub>	B <sub>h</sub>	B <sub>s</sub> '	B <sub>h</sub> '	T'
5/24/65	1115	10000	3100	10000	7200	23
	1120	11000	3200	8600	7200	18
	1136	10000	3400	8200	6700	23
	1200	12000	2800	7900	6400	16
	1235	10000	2200	6200	4600	21
	1240	9300	2600	6400	5100	19
5/25/65	0935	5500	1800	5500	4600	24
	0940	5700	1800	5500	4600	23
	0942	6000	1800	5800	4500	31
	0947	6900	2100	6900	5500	29
	0951	6500	2100	6700	5500	27
5/27/65	0950	7400	1500	5100	3600	25
	1030	8100	2400	5800	4500	23
	1059	8600	2100	6500	5500	15
	1130	5000	1000	3400	2700	18
	1300	8200	1500	5300	3900	21
	1314	7500	1500	5500	4300	20
	1342	7400	1400	5500	4100	23
	1432	8200	1400	6200	4500	25
	1514	11500	1400	6900	4100	18
1530	14500	2100	10000	8200	15	
5/28/65	0923	5800	1000	2700	2100	13
	0930	5200	1000	3400	2700	17
	0943	3200	510	2000	1500	19
	1000	4600	1000	2400	1700	19
	1015	6900	1000	4300	3400	15
	1045	5800	860	2900	2200	14

scattered light is faint compared to the brightness of the sun. Figure 35 shows two modified Volz sun photometers<sup>26</sup> that have been combined to permit simultaneous measurement of the transmittance of blue and red light through plumes. The spectral responses of the photometers are shown in Figure 36.

Table 6 shows the transmittances of red and blue light through the experimental white plume measured with the sun photometers. The measurements have been corrected for the angle of view through the rectangular plume, about 45 degrees. The results are compared with the in-stack transmissometer readings and the transmittance measurements of red and blue light as measured with the telephotometer and lamp (Figure 26).

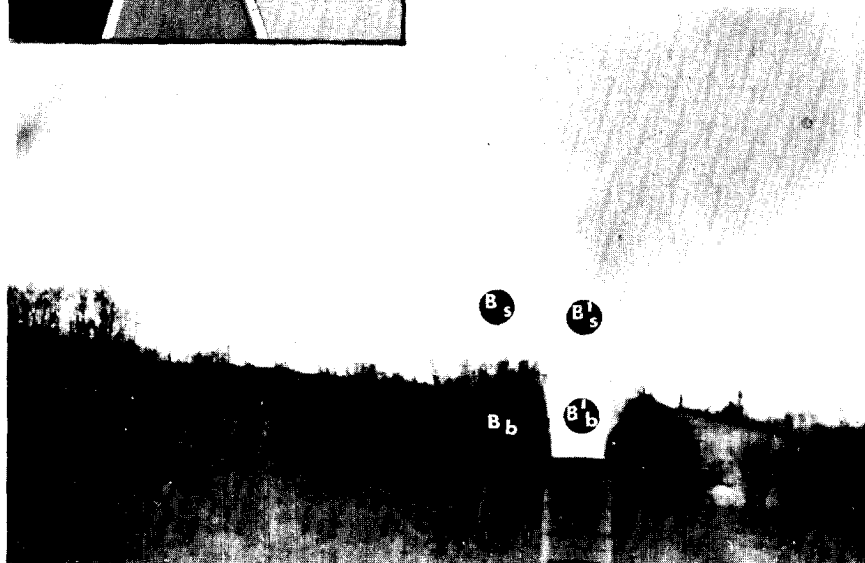
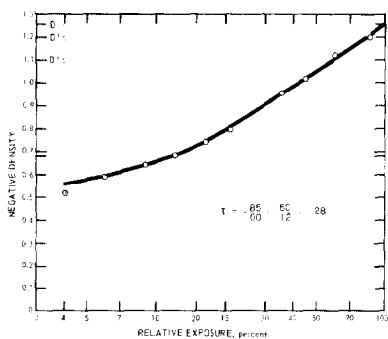
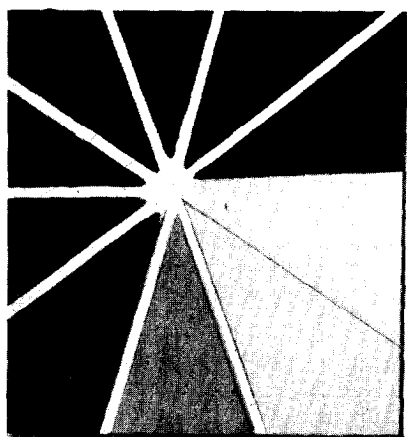


Figure 34. Transmittance of power-plant plume, measured by photography of contrasting targets.

Table 6. TRANSMITTANCES OF RED AND BLUE LIGHT THROUGH THE WHITE EXPERIMENTAL PLUME MEASURED WITH A SUN PHOTOMETER

In-stack transmittance, %	Transmittance with sun photometer, %			Transmittance with telephotometer and lamp, %		
	Red	Blue	Extinction ratio, $Q_b/Q_r$	Red	Blue	Extinction ratio, $Q_b/Q_r$
40	52	31	1.78	48	26	1.85
44	57	33	1.97	53	28	1.97
49	61	36	2.07	58	34	1.97
63	69	50	1.90	70	46	2.16
65	74	54	2.03	72	48	2.22
90	87	84	1.25	90	75	2.90

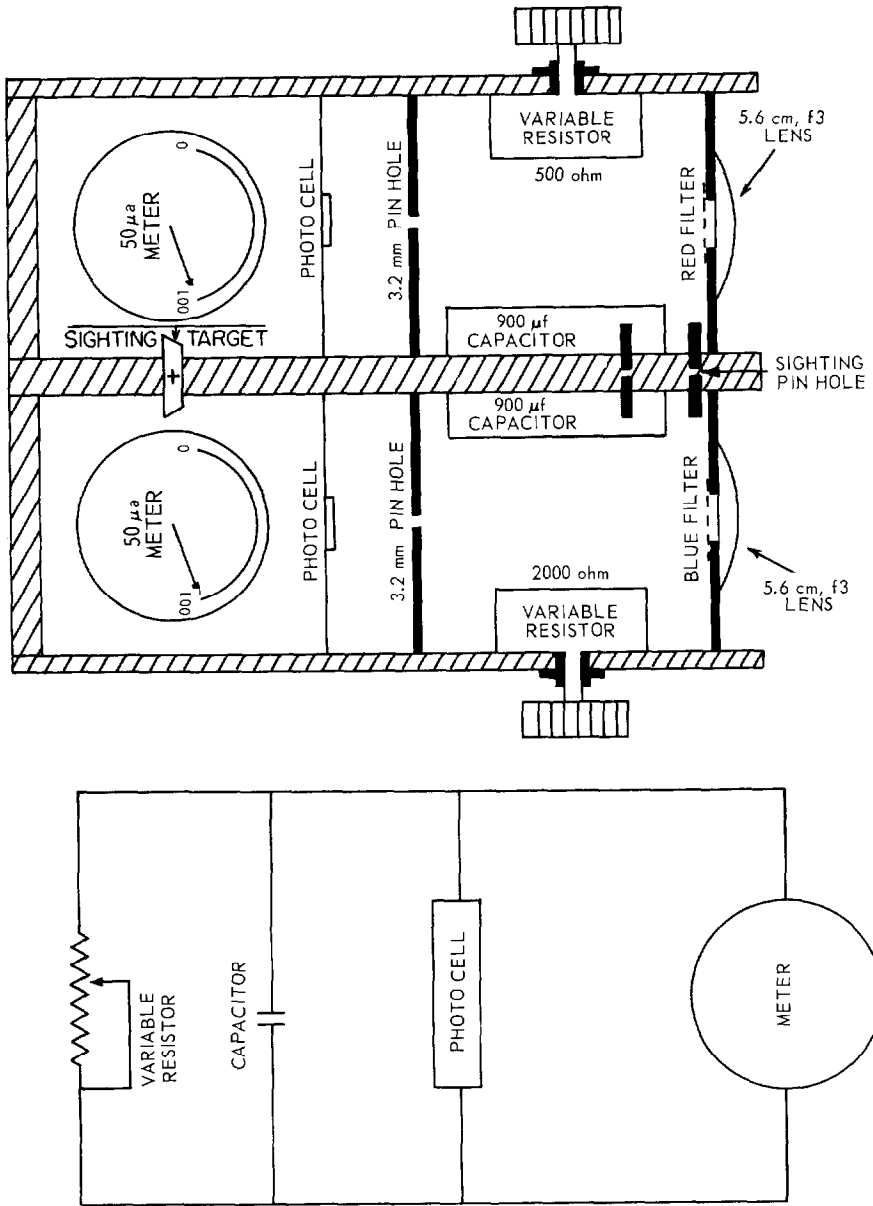


Figure 35. Modified sun photometer for measuring light-transmission characteristics of smoke plumes.

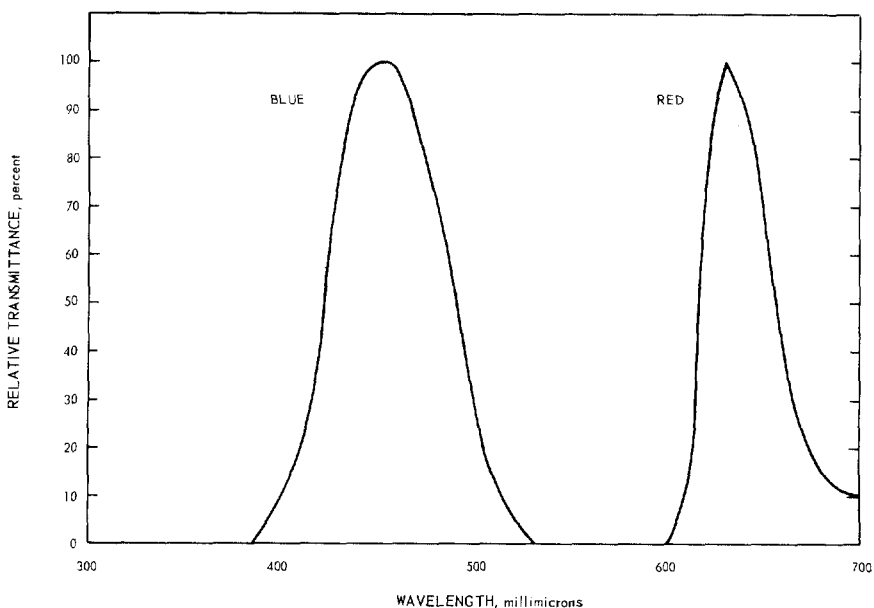


Figure 36. Spectral responses of dual sun photometer.

### Transmittance Measurement by Means of Comparators

Comparators may be used by an observer to estimate the transmittance of smoke plumes. For a comparator to be effective, it must contain particles with scattering properties similar to those of the plume being assessed; then when the comparator and plume are viewed under the same lighting conditions, their luminances should also be the same.

Black smoke comparators or transparent neutral filters for assessing the transmittance of black smoke only have already been developed in the form of the Public Health Service Smoke Guide. White smoke comparators might consist of small cells containing liquid suspensions of fine transparent particles of different concentrations and sizes.

### Transmittance Measurement by Means of Lasers

A laser technique for measuring the transmittance of smoke plumes appears feasible. The method is based on a relative measure of backscatter signals of a pulsed laser beam by aerosols in the air beyond a plume. A plume's transmittance is obtained by measuring the backscatter signal from the air behind the plume when the beam is directed through the plume relative to the backscatter signal obtained from the air when the beam is directed beside the plume.

The laser technique of measuring smoke plume transmittance was tested at the oil-burning power plant at Morro Bay. The tests were conducted by the Stanford Research Institute with their Mark I "lidar".<sup>27</sup> The measurements were made on the number one stack, which carries the effluent from two of the four generating units of the plant. The generating units can burn oil or gas. When the effluent contained 50 percent oil combustion products from one unit and 50 percent gas combustion products from the other unit, laser measurements indicated that the transmittance of the plume was around 82 percent. A slightly higher transmittance of 85 percent was indicated when the gas-burning unit was shut down and the plume contained only oil combustion products.

Sun photometer measurements on the plume when it was composed of equal parts of oil and gas combustion products indicated a transmittance of 85 percent for red and blue light. Sun photometer measurements on the plume when the plume contained only oil combustion products indicated a transmittance of 92 percent for red light and 89 percent for blue light.

Although field testing of instrumental techniques for measuring plume transmittance has been limited, the tests have served to illustrate the techniques and demonstrate their feasibility. The methods that require targets behind the plume, although completely objective, are not always applicable. They may be classified as two-ended techniques of measuring plume transmittance. The sun photometer method is most applicable in areas where overcast conditions are few and the sun may be viewed through the plume. The telephotometer method is most applicable in mountainous or metropolitan areas where a hill or building may be viewed through the plume or in areas with a large number of days where the sky offers areas of sufficiently contrasting brightness. The telephotometer, sun-photometer, and neutral filter method for black smoke could be combined in a single, inexpensive field instrument. A schematic for such an instrument is shown in Figure 37. The accuracy with which a nonblack plume may be assessed by use of a comparator has not been demonstrated, though the method is promising in principle. The laser method represents an objective, single-ended, general technique for measuring the transmittance of plumes, and may offer a standard for evaluating smoke plumes with which other less expensive methods can be compared.

## CONCLUSIONS

The visual appearance of smoke plumes and vision obscuration by smoke plumes are closely related to the amount of light the plumes scatter in the direction of the viewer from their surroundings and the sun. Consequently, evaluations of plumes by a visual effect are more stringent for nonblack plumes than for black plumes and depend on plume illuminating and viewing conditions. Because of this, nonblack plumes could be evaluated differently when viewed on different days or viewed from different directions, though their aerosol content had not changed.

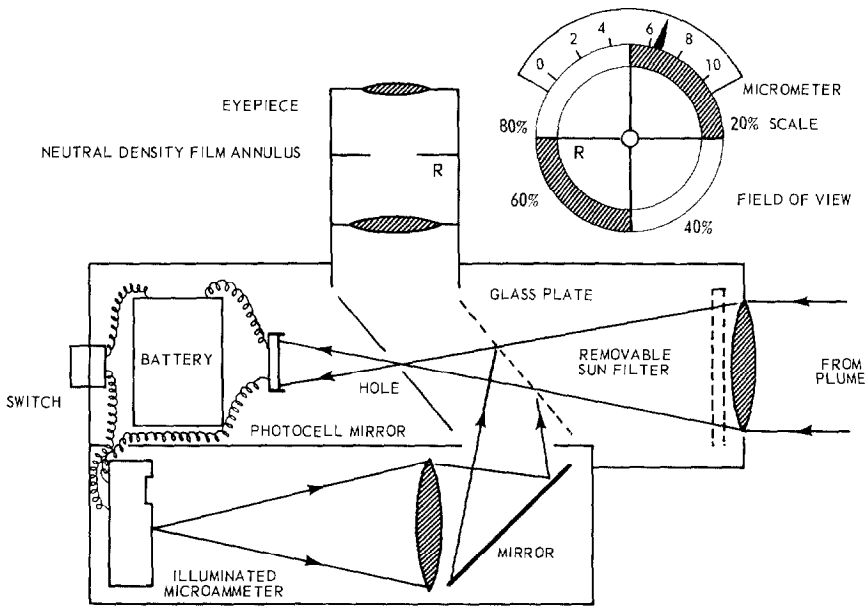


Figure 37. Schematic for combination smoke meter.

If a plume is regarded as contributing to an air pollution problem mainly by virtue of the nature and amount of its aerosol content, it would be desirable to evaluate the plume by an intrinsic property that can be related to that content, independent of environmental lighting conditions. Then the plume could be evaluated according to emission standards based on the composition, diameter, and velocity of the plume, the prevailing meteorological conditions, and other pollution sources in the area.

If the main objection to the plume is its appearance and the decrease in visibility that it will cause, it would still be desirable to evaluate the plume by an intrinsic property. In such a case emission limits in terms of some intrinsic property of the plume (e.g., transmittance) will have to be formulated from a consideration of the visual effects of plumes under the most unfavorable conditions. Then plumes meeting this emission limit would also be acceptable under all illuminating and viewing conditions.

Also, if plumes are evaluated by a property that can be related to the composition, size, and concentration of particles in the plume and a measurement technique is available, the operator of a stack can determine more readily for himself when his emission is excessive and he can better define specifications for control equipment to make the emission acceptable.

The optical property of a plume that is easiest to measure and most simply related to concentration, particle size, composition, and

dimensions of the plume is its light transmittance. Although no general, inexpensive instrumental technique is available for objectively measuring the transmittance of plumes, there are several special techniques which collectively under most circumstances will provide an objective means of measuring the transmittance of a plume.

It appears that an observer may be trained to estimate the transmittance of a plume from its visual appearance. Results presented in this report indicate, however, that plume illuminating, background, and viewing conditions must be considered in training of the inspector and by the inspector when he is assessing plumes in the field. The evaluations of a nonblack plume by observers even with training, may vary significantly if they assess plumes without regard to plume illuminating, background, and viewing conditions. A valuable aid to the inspector of a nonblack plume would be comparators with light-scattering characteristics similar to those of the plume being assessed. Such comparators would help the observer compensate for variations in the appearance of a plume due to illumination and viewing conditions.

A completely general technique that uses a pulsed laser beam for measuring the transmittance of plumes appears feasible. A laser may offer a standard technique for measuring the transmittance of plumes with which less expensive methods can be compared.

## ACKNOWLEDGMENTS

We wish to express our thanks to the Steering Committee of the study for their support and interest, especially to Mr. V. F. Estcourt of the Pacific Gas and Electric Co. and Dr. J. H. Ludwig and Mr. J. S. Nader of the Public Health Service. We extend thanks for valuable scientific discussions to Mr. E. S. Johnson of the Pacific Gas and Electric Co. and Dr. Werner Stoeber (now at the Max Planck Institute, Goettingen, Germany), who was a consultant to the Edison Electric Institute for this study. One of us (Dr. J. R. Hodkinson) was a consultant to the Public Health Service for the study. It is also a pleasure to thank Mr. C. F. Smith of the Public Health Service for his participation in all experiments and the construction of apparatus, and the late Mr. J. A. Tash of the Duquesne Light Co. and Mr. W. L. Crider of the Public Health Service for the development of the experimental smoke stack facilities. Finally, the authors wish to gratefully acknowledge the assistance of the personnel of the Bay Area Air Pollution Control District, California in obtaining the data involving trained observers.

## REFERENCES

1. Ringelmann, M., "Method of Estimating Smoke Produced by Industrial Installations," Rev. Technique, 268 (June 1898).
2. Marks, L. S., "Inadequacy of the Ringelmann Chart," Mech. Eng., 681 (September 1937).
3. Rose, A. H., J. S. Nader, and P. A. Drinker, "Development of an Improved Smoke Inspection Guide," J. Air Poll. Control Assoc. 8, 112-116 (August 1958).
4. Rose, A. H. and J. S. Nader, "Field Evaluation of an Improved Smoke Inspection Guide," J. Air Poll. Control Assoc. 8, 117-119 (August 1958).
5. State of California, Health and Safety Code Chapter 2, Division 20, Section 24242 (1947).
6. Yocum, J. E., "Problems in Judging Plume Opacity," J. Air Poll. Control Assoc. 13, 36-39 (January 1963).
7. Coons, J. D., et al, "Development, Calibration, and Use of a Plume Evaluation Training Unit," J. Air Poll. Control Assoc. 15, 199-203 (May 1965).
8. Crider, W. L. and J. A. Tash, "Study of Vision Obscuration by Non-Black Plumes," J. Air Poll. Control Assoc. 14, 161-167 (May 1964).
9. Curtis Automotive Devices, Inc., Westfield, Indiana.
10. Photovolt Multiplier Photometer Model 520-M, Photovolt Corporation, New York, New York.
11. Photo Research Corp., Hollywood, California.
12. General Electric lamp No. 6.6A/T4Q/1CL-200W.
13. Middleton, W. E. K., "Vision Through the Atmosphere," pp. 83-102, University of Toronto Press (1963).
14. Eppley Laboratories, Inc., Newport, Rhode Island.
15. Private communication, Dr. Werner Stoeber, Max Planck Institute, Goettingen, Germany.
16. Hodkinson, J. R., "The Refractive Index and Extinction Efficiency Factor of Carbon," J. Opt. Soc. Amer., 54, 846 (1964).

17. Van de Hulst, H. C., "Light Scattering by Small Particles," John Wiley & Sons, Inc., New York (1957).
18. Hodkinson, J. R., "The Optical Measurement of Aerosols," in "Aerosol Science," ed. C. N. Davies, Academic Press, London (1966).
19. Hodkinson, J. R., "Dust Measurement by Light Scattering and Absorption," Ph.D. thesis, University of London (1962).
20. Hodkinson, J. R., "The Theory of the Tyndahlscope," Staub (March 1966).
21. Penndorf, R. B., New Table of Mie Scattering Functions Part 6, Geophysical Research Paper No. 45, AFCRC-TR-56-204/6, Air Force Cambridge Research Laboratory, Bedford, Mass. (1956).
22. McDonald, J. E., "Visibility Reduction due to Jet-Exhaust Carbon Particles," J. Appl. Met., 1, 391 (1962).
23. Private communication, Mr. Elmer Johnson, Pacific Gas and Electric Company, San Francisco, California.
24. Handbook of Chemistry and Physics, Chemical Rubber C Publishing Company, Cleveland, Ohio.
25. Giese, R. H., E. deBary, K. Bullrich, and C. D. Vinnemann, Tables of Scattering Functions,  $M = 1.50$ . Abhand, Deutch. Akad. Wissenschaft. Berlin No. 6 (1961).
26. Volz, F., "A Photometer for Measurement of Solar Radiation," Arch. Met. Geophys. & Bioklimat. B 10, 100-131 (1959).
27. Collis, Ronald T. H., "Lidar Observation of Cloud," Science 149, 978-981 (August 1965).
28. Penndorf, R. B., Research on Aerosol Scattering in the Infra-Red, Final Report, AFCRL-63-668, Air Force Cambridge Research Laboratory, Bedford, Mass. (1963).
29. By courtesy of Dr. Bertram Dorin, NASA Space Flight Center, Greenbelt, Maryland.
30. Bush, A. S., "Municipal Incineration," Sanitary Engineering Research Project, Technical Bulletin No. 6, University of California, Los Angeles, California (1951).

## **APPENDICES**



# APPENDIX A: ANALYSES OF THE ANGULAR SCATTERING PATTERNS OF THE EXPERIMENTAL PLUMES

## Angular Scattering Characteristics and Particle-Size of the White (Oil) Plume

A second estimate of the particle size of the white (oil) plume was obtained by comparing its angular scattering pattern with theoretical patterns for different particle sizes plotted from Mie-theory computations (Figure A1). The experimental pattern was compared with Mie-theory patterns calculated by Penndorf<sup>28</sup> for refractive index  $m = 1.44$ , available at intervals in  $\alpha$  of 0.5. The best fit was given by the pattern for  $\alpha = 2.5$ , which at a mean wavelength of 0.5 micron, corresponds to a particle diameter of 0.4 micron. This agrees very well with the diameter estimates of 0.43 and 0.39 micron at 60 and 70 percent transmittance derived from the extinction data. At transmittances of 60 percent, an appreciable proportion of the light is scattered a second time before it leaves the plume. This secondary scattering tends to decrease the strong forward scattering and increase the weaker sideways scattering. At higher plume transmittances, this secondary scattering is less, but the particle-size is also less because of the smoke generator characteristics, and smaller particle-size gives a less forward-directed pattern. Thus, the similarity of the observed patterns at 60 and 90 percent transmittance is attributed to a fortuitous compensation of the effects of decreasing secondary scattering and decreasing particle size.

## Angular Scattering Characteristics and Particle-Size of the Black (Carbon) Plume

The angular scattering pattern of the black plume was compared to Mie-theory patterns for refractive index  $m = 2.0-i$  (Figure A2). Patterns of rms values of  $\alpha$  interpolated over consecutive ranges of 1.414 to 1 in  $\alpha$  were available.<sup>29</sup> An average of 1.414 to 1 is essentially equivalent to the averaging of the scattering pattern of an aerosol when measured experimentally with white light. Unlike the scattering pattern of the white plume, no single Mie-theory pattern would match the experimental scattering pattern of the black plume. Instead the pattern was fitted best by a composite of patterns for  $\alpha = \pi d/\lambda = 0.86, 1.72, \text{ and } 6.86$ . In Figure A2, the individual patterns are plotted with the absolute Mie-theory intensities for both polarizations combined ( $i_1 + i_2$  in the usual notation) and the compounded curve is plotted relative to the scattering at  $7^\circ$  for comparison with the experimental pattern. Thus, the scattering pattern of the black experimental plume may be represented by a model aerosol composed of spherical carbon particles of refractive index 2.0-i with diameters of 0.1, 0.3, and 1 micron in equal proportions by number.

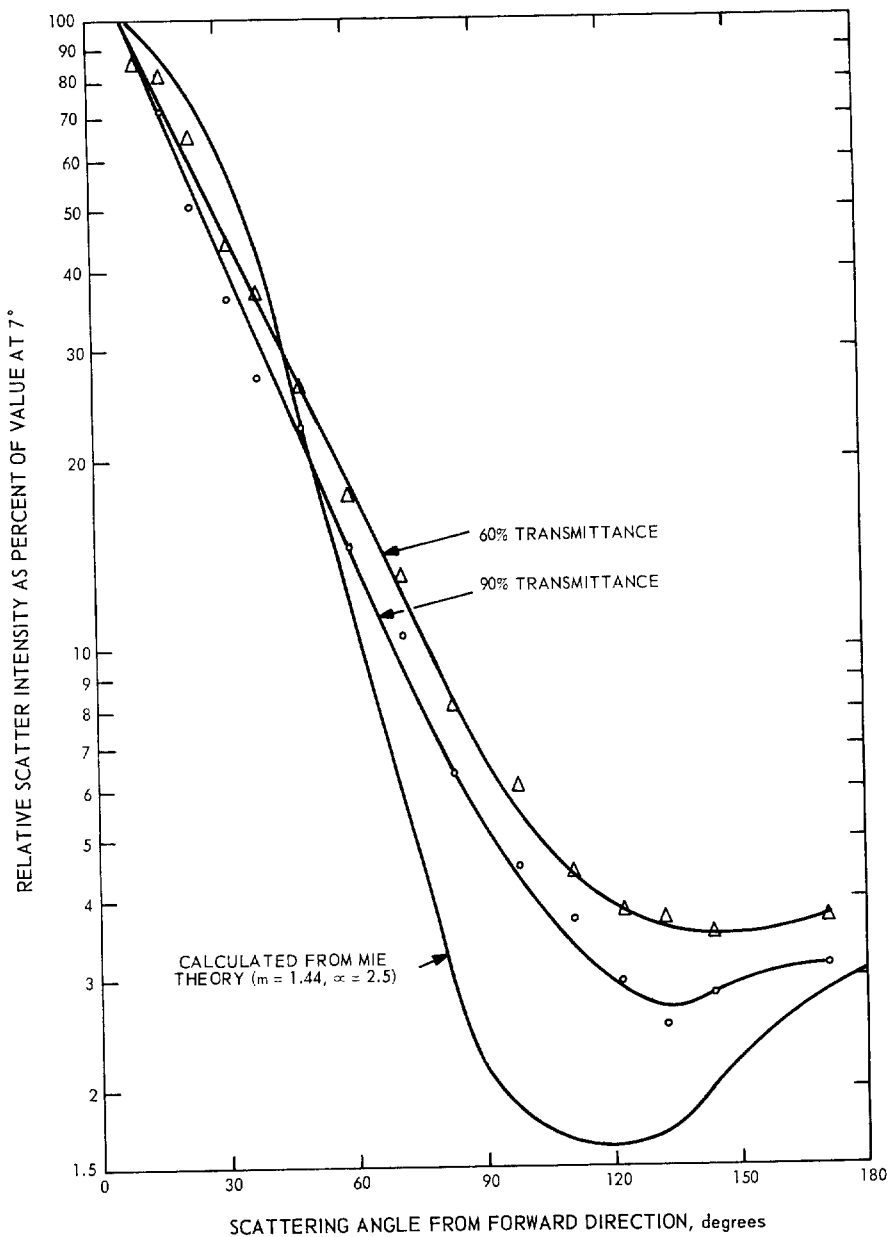


Figure A1. White plume: comparison of angular scattering measurements and Mie-theory patterns.

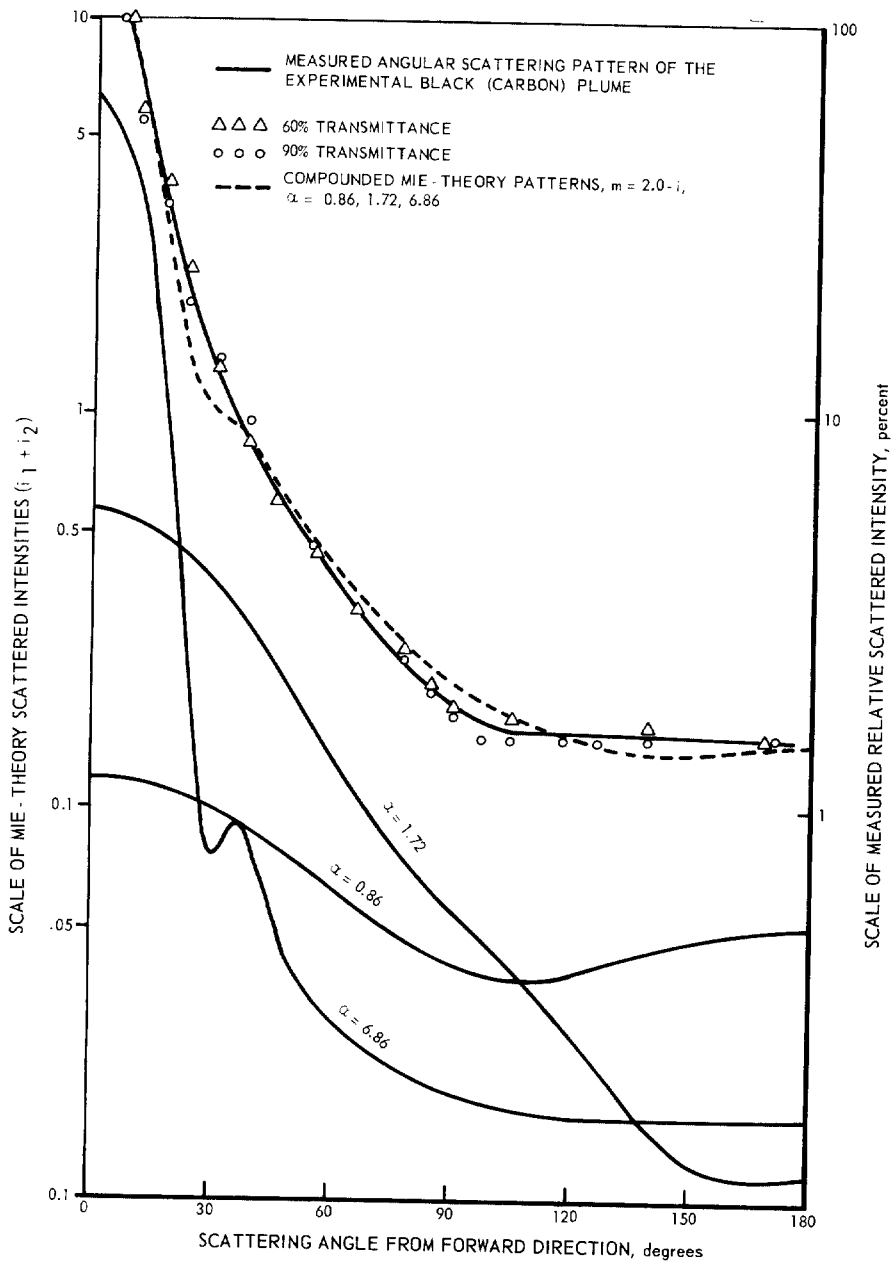


Figure A2. Black plume: comparison of angular scattering measurements and Mie-theory patterns.

The average particle size of such a model aerosol would be 0.47 micron, which is twice the particle size estimate of 0.23 micron obtained from the analysis of the plume's transmittance characteristics. The discrepancy is probably due to the particle shape. Electron-micrographs of the particles collected by diffusion onto the top and bottom surfaces of a microscope slide held in the effluent with its plane horizontal and normal to the direction of the effluent showed that the particles were composed of extended chains of particles with diameters of about 0.05 micron. Figure A3 shows a photograph of the particles collected on the upper surface of the slide. The appearance of the lower surface was the same.

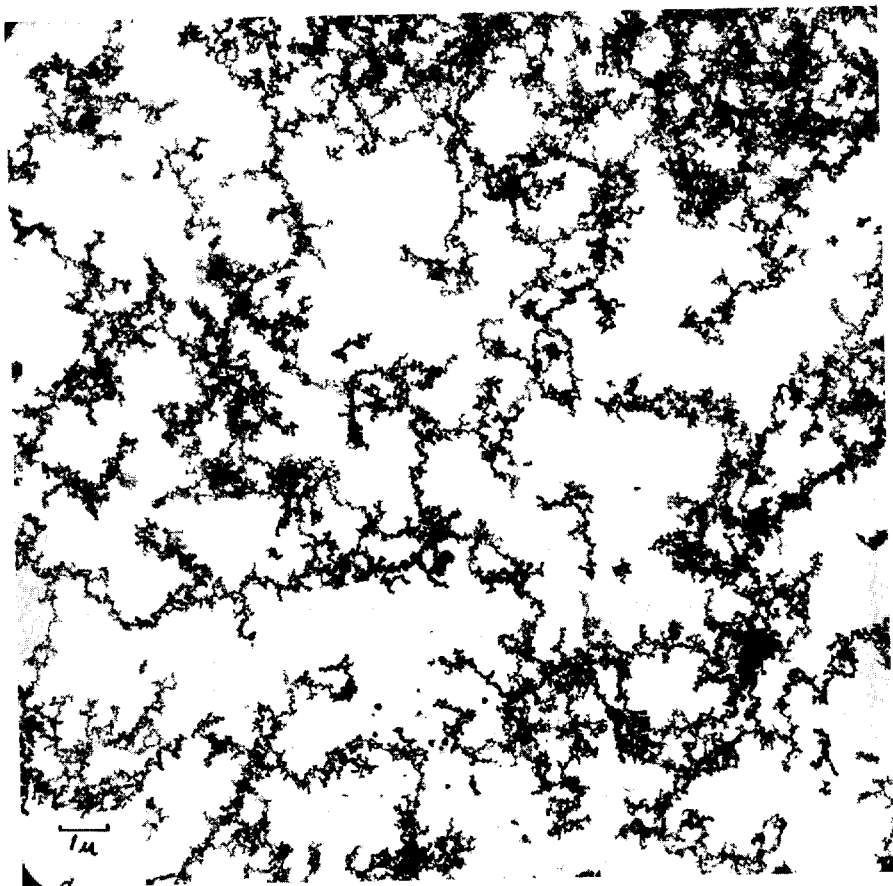


Figure A3. Electronmicrograph of particles in experimental black plume.

#### **Angular Scattering Characteristics and Particle-Size of the Oil-Burning Power Station Plume**

The experimental scattering curve of the power station plume, like the pattern of the black experimental plume, could be fitted only

by compounding three Mie-theory curves. The three distinctive angular regimes discernible were 0 to 25 degrees, 25 to 80 degrees, and 80 to 170 degrees, and they were best fitted respectively by a composite of the Mie patterns for  $\alpha = 5.0, 1.2,$  and  $0.4$  (Figure A4). Patterns were available at intervals of  $0.2$  in  $\alpha$ .<sup>25</sup> The logarithmic ordinate for the

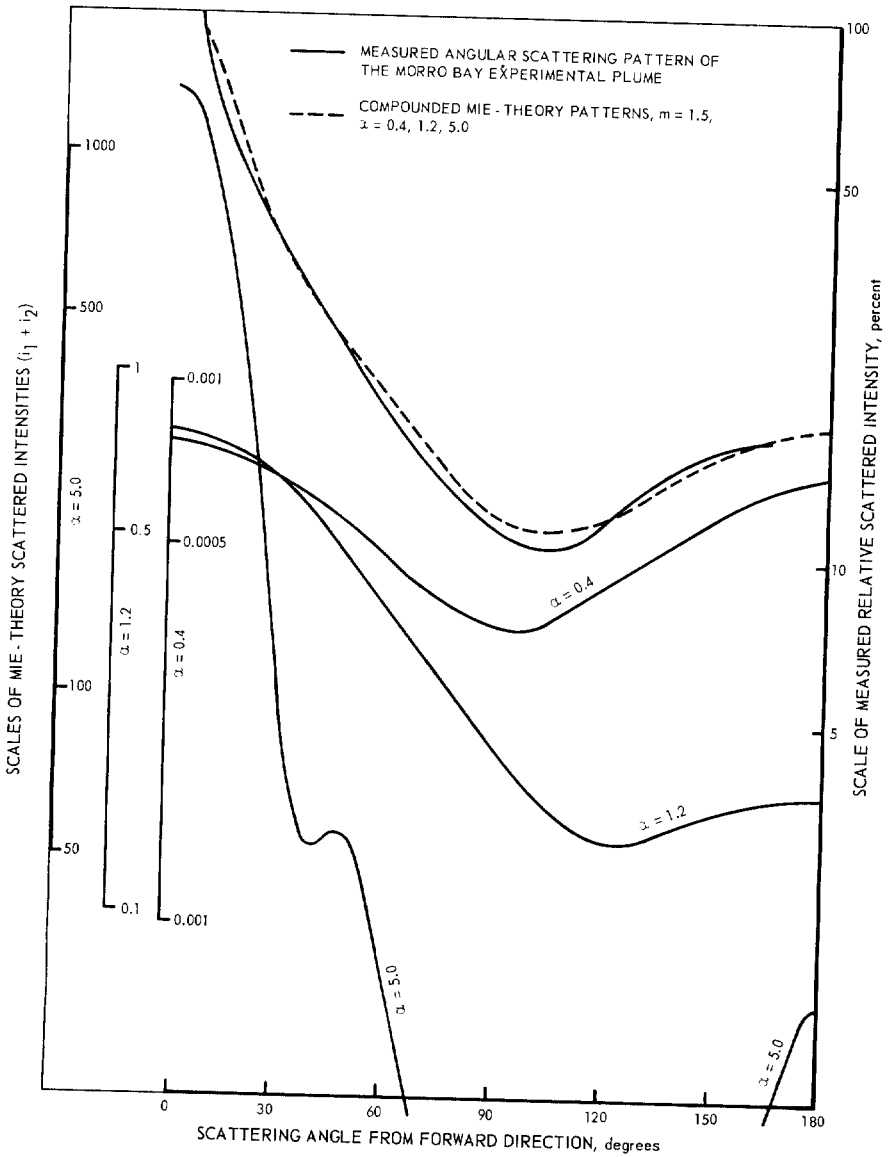


Figure A4. Power-plant plume: comparison of angular scattering measurements and Mie-theory patterns.

relative scattered intensity of the experimental curve was for convenience given the value 100 percent at the smallest angle measured, 7 degrees. To facilitate fitting them to the experimental pattern, the Mie patterns were plotted on three separate sheets with the same logarithmic ordinate scale in units of the absolute Mie-theory intensities for both polarizations combined, which are proportional to the intensity per particle scattered through a particular angle. These scales, for each of the Mie patterns, are shown in Figure A4 and allow for comparison of these patterns with one another.

The absolute ordinate 1 for the  $\alpha = 1.2$  pattern falls at the ordinate 390 for the  $\alpha = 5.0$  pattern. This relative positioning of the two patterns implies a model aerosol with 390 particles of size  $\alpha = 1.2$  for every one particle of size  $\alpha = 5.0$ . Similarly, since the 0.001 ordinate for the  $\alpha = 0.4$  patterns falls at the 370 ordinate for the  $\alpha = 5.0$  pattern, there would be 370,000 particles of size  $\alpha = 0.4$  for every one of size  $\alpha = 5.0$ . If the wavelength is taken as the mean of the green and blue, i.e., of 0.531 and 0.438 – or 0.485 micron – the aerosol model that gives a scattering pattern that resembles the experimental patterns has spherical transparent particles of refractive index 1.5 with diameters 0.8, 0.2, and 0.06 micron in the proportions 1:390:370,000 by number.

These particle diameters and relative number of particles in the model aerosol, also the relative areas and volumes of particles, are set out in the upper division of Table A1. Because of the preponderance of the smallest particles, the number, area, and volume mean diameters for this model aerosol are all not significantly different from 0.06 micron.

Although few accurate size analyses of submicron particulate material in smoke stacks of any kind seem to have been reported, particle-sizes as fine as those in the present plume are not infrequently encountered. For example, measurements by Bush<sup>30</sup> on municipal incinerator stacks give median particle-sizes ranging from 0.017 to 0.082 micron.

The corresponding values of  $\lambda$  and  $Q$  for the red, green, and blue wavelengths, 0.651, 0.531, and 0.438 micron, are given in the lower three divisions of the table. Multiplying each value of  $Q$  by the appropriate proportion of particle-area of each of the three particle-sizes and adding the products gives a number proportional to the total extinction coefficient of the whole aerosol for each of the three wavelengths (right column), provided there is no absorption of light within the particles.

From these three numbers we see that the extinction coefficients of the whole model aerosol for the red, green, and blue wavelengths used would stand in the ratios 1:1.5:3.0.

These do not differ greatly from the measured ratios of 1:2.2:2.9 for the plume extinction coefficients at the red, green, and blue wave-

lengths. Note that, although the scattering pattern at angles larger than 25 degrees seems to be the most conspicuous feature in Figure A4, this is a consequence of the logarithmic scale and of the absence of measurements at angles smaller than 7 degrees. In fact, the total flux scattered between 0 and 25 degrees is comparable with that scattered between 25 and 180 degrees.

It must be emphasized that we have devised a model aerosol that would have the same scattering pattern as observed. This is not the same thing as saying this is the aerosol in the plume. It is conceivable that in such a plume there might actually be three populations of particles, e.g., solids, condensed oil droplets, and water droplets condensed on solid nuclei. Equally, there might be a continuous size distribution from, say, 1 down to 0.1 micron, the frequency increasing

**Table A1. PARAMETERS OF MODEL AEROSOL (OF TRANSPARENT SPHERICAL PARTICLES OF REFRACTIVE INDEX 1.5) WITH SAME SCATTERING PROPERTIES AS AEROSOLS IN THE OIL-BURNING STREAM-ELECTRIC POWER STATION PLUME**

		Particle Diameter, $\mu$		
		0.8	0.2	0.06
Blue-Green Wavelength 0.485 $\mu$	$\alpha$	5.0	1.2	0.4
	Relative numbers of particles	1	: 390	: 370,000
	Relative areas of particles	1	: 22	: 2,350
	Relative volumes of particles	1	: 5.4	: 190
Red Wavelength 0.651 $\mu$	$\alpha$	: 3.7	0.95	0.30
	Q	: 4.1	0.18	0.0019
	$Q_r \times$ relative area	: 4.1	4.0	4.5
	Total			12.6
Green Wavelength 0.531 $\mu$	$\alpha$	: 4.6	1.1	0.35
	Q	: 4.2	0.30	0.0035
	$Q_g \times$ relative area	: 4.2	6.6	8.2
	Total			19.0
Blue Wavelength 0.438 $\mu$	$\alpha$	: 5.5	1.3	0.45
	Q	: 3.3	0.50	0.010
	$Q_b \times$ relative area	: 3.3	11.0	23.5
	Total			37.8
		Hence $Q_r : Q_g : Q_b = 12.6 : 19.0 : 37.8 = 1 : 1.5 : 3$		
		By direct measurement, $Q_r : Q_g : Q_b = 1 : 2.2 : 2.9$		

rapidly as the particle size diminishes; the successful approximation of the scattering by a mixture of three distinct particle sizes could be explained equally well as a consequence of the very considerable changes in the amount and angular distribution of light scattered as the particle size changes from  $1/10$  to 1 or 2 wavelengths of light, in fact, passing through three distinct regimes of light-scattering.

## APPENDIX B: DATA ON PLUME CONTRAST AND OBSCURATION OF CONTRAST FOR THE EXPERIMENTAL BLACK AND WHITE PLUMES

Data on the visual effects of smoke plumes are presented here because of the interest shown in the variety of ways that such data may be reduced and interpreted. These are not necessarily the data used in the figures of the report. The following symbols and relationships have been used:

$B_1$  and  $B_2$  = the inherent luminances\* of the targets

$B_1'$  and  $B_2'$  = the apparent luminances of the targets

$B_a$  = the luminance of the plume air-light

$B_s$  = the luminance of the sky behind the plume

$B_p$  = the luminance of the plume

$C_a$  = the apparent contrast between targets

$$= \frac{B_1' - B_2'}{B_1'} \times 100$$

$C_p$  = the contrast between plumes and their sky background

$$= \frac{B_p - B_s}{B_s} \times 100$$

$T'$  = the calculated plume transmittance

$$= \frac{B_1' - B_2'}{B_1 - B_2} \times 100 \quad \text{or} \quad \frac{B_p - B_a}{B_s} \times 100$$

$E_t$  = error between calculated transmittance and corrected in-stack transmittance

$E_G$  = intensity of solar radiation on a horizontal surface as indicated by an Eppley globe pyrheliometer. A full-scale reading of 100 represents a radiation intensity of 2.5 gram-calories per minute per square centimeter.

---

\*All luminance measurements are in candelas/meter<sup>2</sup>.

**Table B1. VARIATION OF APPARENT CONTRAST BETWEEN PANEL TARGETS VIEWED FROM THE EAST THROUGH AN EXPERIMENTAL WHITE PLUME; 60 PERCENT TRANSMITTANCE, CLEAR DAY**

TIME	$B_1$	$B_2$	$B_1'$	$B_2'$	$C_a$	$T'$	$E_t$	$E_G$
0842	18000	600	12000	2100	83	56	+ 2	30
0847	18400	600	12800	2200	83	72	+18	
0908	19400	600	14000	2400	83	62	+ 8	33
0918	18000	600	14000	2600	81	66	+12	
0934			13000	2600	80			41
0950			13400	2500	81			
1010	17200	600	13500	3000	78	63	+ 9	
1024			11000	2900	74			
1041	15000	600	11000	3000	73	56	- 2	49
1107	12500	600	10000	3200	68	57	+ 3	51
1119	10500	500	8400	3000	64	54	- 1	
1129	9100	450	7600	3100	59	52	- 3	
1143	8800	500	7800	3300	58	54	- 1	54
1300	3800	320	5600	3600	36	57	+ 3	54
1317	3800	320	5800	3600	38	63	+ 9	
1332	3500	320	6100	4100	33	63	+ 9	
1352	3400	320	6400	4600	28	58	+ 4	50
1421	3300	400	7100	5400	24	59	+ 5	
1440	3300	350	8000	6300	21	58	+ 4	
1503			9200	7300	21			42
1531			11000	8800	20			
1548			11500	9600	17			35
1613			12500	11000	12			

**Table B2. VARIATION OF APPARENT CONTRAST BETWEEN PANEL TARGETS VIEWED FROM THE EAST THROUGH AN EXPERIMENTAL WHITE PLUME; 40 PERCENT TRANSMITTANCE, CLEAR DAY**

TIME	$B_1$	$B_2$	$B_1'$	$B_2'$	$C_a$	$T'$	$E_t$	$E_G$
0840	17000	600	9800	3000	69	41	+5	30
0846	18000	600	9800	3000	69	39	+3	
0904			11000	3200	71			32
0916			11000	3500	68			
0930	18000	400	10000	3700	63	36	+1	41
0946			10000	3800	62			
1007			12000	4000	67			
1022	16000	600	9900	4000	60	38	+2	49
1040			9800	4500	54			51
1105			9000	4600	49			
1118			7900	4100	48			
1126			7100	4000	44			
1141			7600	4600	39			54
1152			6600	4400	33			
1300			6300	4800	24			54
1316			6500	5000	23			
1329			6800	5600	18			50
1350			7400	6100	18			
1425	3500	300	8900	7900	11	31	-6	
1445	3400	400	9600	8300	14	43	+7	
1505	3400	480	11000	10000	9.1	34	-3	42
1533	3800	400	13000	12000	7.7	29	-8	
1554	3600	400	14000	13000	7.0	31	-6	
1616	3600	450	13000	12000	7.7	32	-5	

**Table B3. VARIATION OF APPARENT CONTRAST BETWEEN PANEL TARGETS VIEWED FROM THE EAST THROUGH AN EXPERIMENTAL BLACK PLUME; 60 PERCENT TRANSMITTANCE, CLEAR DAY**

TIME	$B_1$	$B_2$	$B_1'$	$B_2'$	$C_a$	$T'$	$E_t$	$E_G$
1000	19000	760	13000	1500	88	63	+ 1	41
1015	18000	790	12000	1400	88	62	0	43
1040	17000	650	11000	1400	87	59	- 3	48
1150	7600	430	5500	860	84	65	+ 3	56
1210	5900	290	4100	750	82	60	- 2	56
1235	3400	170	3000	820	73	67	+ 5	57
1250	3400	160	2900	790	73	65	+ 3	
1315	3200	150	2600	820	68	58	- 4	56
1330	2900	170	2500	860	66	60	- 2	56
1345	3000	170	2500	820	67	59	- 3	55
1400	2800	210	2500	1100	56	54	- 8	50
1420	2900	190	2600	910	65	62	0	48
1435	2900	210	2600	1200	54	52	- 10	46
1510	2800	210	2700	1200	56	58	- 4	41
1515	2900	210	2900	1400	52	56	- 6	40
1530	2900	210	3000	1300	57	63	+ 1	38

**Table B4. VARIATION OF APPARENT CONTRAST BETWEEN PANEL TARGETS VIEWED FROM THE EAST THROUGH AN EXPERIMENTAL BLACK PLUME; 40 PERCENT TRANSMITTANCE, CLEAR DAY**

TIME	$B_1$	$B_2$	$B_1'$	$B_2'$	$C_a$	$T'$	$E_t$	$E_G$
1000	19000	760	10000	1700	83	46	+ 3	41
1015	18000	790	9600	1800	81	45	+ 2	43
1040	17000	650	8200	1700	79	40	- 3	48
1115	13000	600	6900	1500	78	44	+ 1	
1150	7600	430	4300	1200	72	43	0	56
1210	5900	290	3400	1300	62	37	- 6	56
1250	3400	160	2400	1100	54	40	- 3	
1315	3200	150	2400	1100	54	43	0	56
1330	2900	170	2400	1300	46	40	- 3	56
1345	3000	170	2100	1100	48	35	- 8	55
1400	2800	210	2300	1400	39	35	- 8	50
1420	2900	190	2400	1300	46	41	- 2	48
1435	2900	210	2600	1400	46	45	+ 2	46
1500	2800	210	2500	1600	36	35	- 8	41
1515	2900	210	2900	1800	38	41	- 2	40
1540	2900	210	3100	1900	39	45	+ 2	37

**Table B5. VARIATION OF APPARENT CONTRAST BETWEEN PANEL TARGETS VIEWED FROM THE WEST THROUGH AN EXPERIMENTAL BLACK PLUME; 60 PERCENT TRANSMITTANCE, CLEAR DAY**

TIME	$B_1$	$B_2$	$B_1'$	$B_2'$	$C_a$	$T'$	$E_t$	$E_G$
0930	2700	450	3400	1900	44	67	+ 5	25
0950	2800	380	3400	1900	44	62	0	28
1010	2900	340	3400	1800	47	63	+ 1	
1020	2900	290	3300	1700	48	61	- 1	
1035	2900	290	3100	1400	55	65	+ 3	36
1045	2900	270	3100	1400	55	65	+ 3	
1105	3000	260	3000	1200	60	66	+ 4	38
1120	3000	260	2900	1100	62	66	+ 4	43
1135	3100	260	2900	1000	66	67	+ 5	43
1150	3300	240	2800	930	67	61	- 1	43
1245	4300	220	3100	720	77	58	- 4	44
1315	4800	270	3400	690	80	60	- 2	41
1330	5800	310	4100	790	81	60	- 2	
1400	8200	290	6000	750	88	66	+ 4	35
1435	10000	480	7200	890	88	60	- 2	30
1500	12000	510	8600	860	90	67	+ 5	27
1520			8200	860	90			26

**Table B6. VARIATION OF APPARENT CONTRAST BETWEEN PANEL TARGETS VIEWED FROM THE WEST THROUGH AN EXPERIMENTAL BLACK PLUME; 40 PERCENT TRANSMITTANCE, CLEAR DAY**

TIME	$B_1$	$B_2$	$B_1'$	$B_2'$	$C_a$	$T'$	$E_t$	$E_G$
0930	2700	410	3300	2200	33	48	+ 5	25
0950	2800	380	3200	2200	31	41	- 1	28
1010	2900	340	3200	2100	34	43	0	
1020	2900	290	3100	2000	35	42	- 1	
1035	2900	290	3000	1800	40	46	+ 3	36
1045	2900	270	2900	1700	41	46	+ 3	
1105	3000	260	2700	1500	44	44	+ 1	38
1120	3000	260	2600	1400	46	44	+ 1	43
1135	3200	240	2600	1300	50	44	+ 1	43
1150	3300	240	2600	1200	54	46	+ 3	43
1254	4300	220	2600	1000	62	39	- 4	44
1315	4800	270	2700	1000	63	38	- 5	41
1330	5800	310	3600	1000	72	47	+ 4	
1400	8200	290	4200	1000	76	40	- 3	35
1435	10000	480	5100	1000	80	39	- 4	30
1500	12000	510	6100	1000	84	44	+ 1	27
1520			5900	960	84			26

**Table B7. VARIATION OF APPARENT CONTRAST BETWEEN PANEL TARGETS VIEWED FROM THE EAST THROUGH AN EXPERIMENTAL WHITE PLUME; 60 PERCENT TRANSMITTANCE, OVERCAST DAY**

TIME	$B_1$	$B_2$	$B_1'$	$B_2'$	$C_a$	$T'$	$E_t$
0951	500	20	540	240	56	63	+8
0955	680	40	740	380	49	56	+1
1047	2880	200	2800	1160	59	61	+6
1051	2520	160	2360	1000	58	58	+3
1118	2760	200	2560	1200	53	53	-2
1121	2600	200	2660	1200	55	61	+6
1151	1880	200	2120	1160	45	57	+2
1155	1880	160	1960	1080	45	51	-4
1227	2240	200	2400	1160	52	55	0
1230	2640	240	2760	1280	54	62	+7
1316	3040	240	3240	1600	51	59	+4
1325	2400	150	2700	1350	50	60	+5
1358	2360	160	2560	1290	50	58	+3
1400	2520	160	2840	1600	44	53	-2
1430	1800	200	1960	1020	48	59	+4
1432	1600	120	1800	920	49	59	+4
1508	1720	120	1960	1160	41	50	-5
1510	1840	120	2040	1020	50	59	+4
1534	1200	60	1270	620	51	57	+2
1536	1200	60	1280	620	52	58	+3

**Table B8. VARIATION OF APPARENT CONTRAST BETWEEN PANEL TARGETS VIEWED FROM THE EAST THROUGH AN EXPERIMENTAL WHITE PLUME; 40 PERCENT TRANSMITTANCE, OVERCAST DAY**

TIME	$B_1$	$B_2$	$B_1'$	$B_2'$	$C_a$	$T'$	$E_t$
0947	500	20	580	380	35	42	+5
0953	680	40	660	470	29	30	-7
1045	2800	200	2660	1560	41	42	+5
1050	2720	200	2520	1480	41	41	+4
1116	2600	160	2400	1440	40	39	+2
1120	2880	200	2680	1600	40	40	+3
1148	2120	200	2400	1640	32	40	+3
1153	1720	160	1960	1320	33	41	+4
1225	2240	200	2400	1600	33	39	+2
1228	2480	200	2560	1680	34	39	+2
1315	2920	240	3120	2000	36	42	+5
1322	2550	200	2900	1900	35	43	+6
1356	2320	160	2600	1760	32	39	+2
1359	2440	160	2800	1800	36	44	+7
1428	1800	200	2040	1360	33	43	+6
1431	1680	120	1920	1240	35	44	+7
1506	1640	120	2080	1480	29	40	+3
1509	1800	160	2120	1400	34	44	+7
1533	1220	60	1300	860	34	38	+1
1535	1200	80	1300	800	38	45	+8

Table B9. VARIATION OF APPARENT CONTRAST BETWEEN PANEL TARGETS VIEWED FROM THE EAST THROUGH AN EXPERIMENTAL BLACK PLUME; 60 AND 40 PERCENT TRANSMITTANCE, OVERCAST DAY

TIME	B <sub>1</sub>	B <sub>2</sub>	B <sub>1</sub> '	B <sub>2</sub> '	C <sub>a</sub>	T'	E <sub>t</sub>	E <sub>G</sub>
			(60% transmittance)					
0912	316	28	240	62	74	62	0	1
1032	1510	120	1100	274	75	59	-3	6
1140	1170	103	926	258	72	63	+1	8
1252	1480	137	1170	434	63	55	-7	9
1417	1060	96	840	206	75	68	+6	4
1426	1270	114	1030	274	73	65	+3	5
1535	960	96	755	189	75	66	+4	3
1543	825	76	650	182	72	62	0	3
			(40% transmittance)					
0913	315	17	206	69	67	46	+3	1
1030	1370	103	875	310	65	45	+2	6
1145	1680	137	1060	412	61	42	-1	8
1256	2100	165	1310	550	58	39	-4	9
1422	1060	96	705	275	61	45	+2	4
1428	1370	138	928	360	61	46	+3	5
1538	930	86	620	223	64	47	+4	3
1540	840	69	600	224	63	49	+6	3

**Table B10. VARIATION OF APPARENT CONTRAST BETWEEN SELF-LUMINOUS TARGETS VIEWED FROM THE EAST THROUGH AN EXPERIMENTAL WHITE PLUME; 60 PERCENT TRANSMITTANCE, CLEAR DAY**

TIME	B <sub>1</sub>	B <sub>2</sub>	B <sub>1</sub> '	B <sub>2</sub> '	B <sub>a</sub>	C <sub>a</sub>	T'	E <sub>t</sub>
0929	10700	800	7400	2400	2100	68	51	-4
0951	10900	800	7600	2500	2150	67	50	-5
1015	10700	800	7800	2800	2500	64	51	-4
1034			8100	3000	2400	63		
1054	10700	800	8200	3000	2800	63	53	-2
1119	10600	800	8300	3100	2900	63	53	-2
1204	10700	800	8500	3600	3200	58	49	-6
1229	10700	720	8700	3700	3300	57	50	-5
1254	10800	800	8900	4100	3700	54	48	-7
1321	10900	800	9500	4200	4150	56	52	-3
1344	10600	800	9800	5000	4850	49	49	-6
1412	10600	800	10700	5800	5440	46	50	-5
1414	10600	800	11200	6200	5920	45	51	-4
1506	10800	640	12000	7200	6880	40	47	-8
1526	10800	800	13300	8000	7520	40	53	-2
1551	10600	800	13400	9000	8800	33	45	-10

**Table B11. VARIATION OF APPARENT CONTRAST BETWEEN SELF-LUMINOUS TARGETS VIEWED FROM THE EAST THROUGH AN EXPERIMENTAL WHITE PLUME; 40 PERCENT TRANSMITTANCE, CLEAR DAY**

TIME	B <sub>1</sub>	B <sub>2</sub>	B <sub>1</sub> '	B <sub>2</sub> '	B <sub>a</sub>	C <sub>a</sub>	T'	E <sub>t</sub>
0928	10700	800	6400	3400	3200	47	30	-7
0950	10900	800	6600	3400	3300	48	32	-5
1014	10700	800	7000	3700	3500	47	33	-4
1033			7400	4100	4000	45		
1053	10700	800	7700	4300	4100	44	34	-3
1118	10600	800	7700	4300	4100	44	35	-2
1203	10700	800	7800	4850	4700	38	30	-7
1227	10700	720	8250	5000	4900	39	33	-4
1253	10900	800	8200	4800	4800	41	34	-3
1320	10900	800	9150	5800	5700	37	33	-4
1343	10600	800	9550	6400	6200	33	32	-5
1410	10600	800	10000	6900	6800	31	32	-5
1443	10600	800	11000	8000	7760	27	31	-6
1505	10600	640	11800	8880	8500	25	29	-8
1525	10800	800	13400	10600	10500	21	28	-9
1550	10600	800	14200	11000	10600	23	33	-4

**Table B12. VARIATION OF APPARENT CONTRAST BETWEEN SELF-LUMINOUS TARGETS VIEWED FROM THE EAST THROUGH AN EXPERIMENTAL BLACK PLUME; 60 PERCENT TRANSMITTANCE, CLEAR DAY**

TIME	$B_1$	$B_2$	$B_1'$	$B_2'$	$B_a$	$C_a$	$T'$	$E_t$
1000	10700	800	7000	1200	650	83	59	-3
1030	10700	800	7500	1200	700	84	64	+2
1045	10700	800	7500	1200	700	84	64	+2
1110	10700	800	7000	1200	720	83	59	-3
1130	10700	800	7500	1200	750	84	64	+2
1230	10700	800	7500	1300	750	83	63	+1
1240	10700	800	7400	1300	820	82	62	0
1300	10700	800	7100	1400	830	80	58	-4
1315	10700	800	7300	1400	1050	81	60	-2
1340	10700	800	7200	1500	1050	79	58	-4
1400	10700	800	6700	1500	1150	78	53	-9
1430	10700	800	7100	1400	1050	80	58	-4
1445	10700	800	7200	1500	1100	79	58	-4
1510	10700	800	7400	1800	1450	76	57	-5
1530	10700	800	7500	1900	1550	75	57	-5
1545	10700	800	8000	2100	1700	74	60	-2

**Table B13. VARIATION OF APPARENT CONTRAST BETWEEN SELF-LUMINOUS TARGETS VIEWED FROM THE EAST THROUGH AN EXPERIMENTAL BLACK PLUME; 40 PERCENT TRANSMITTANCE, CLEAR DAY**

TIME	$B_1$	$B_2$	$B_1'$	$B_2'$	$B_a$	$C_a$	$T'$	$E_t$
1000	10700	800	5500	1300	900	76	42	-1
1030	10700	800	6000	1300	1000	78	47	+4
1045	10700	800	5800	1300	900	78	45	+2
1110	10700	800	5000	1200	800	76	38	-5
1130	10700	800	5300	1300	1000	75	40	-2
1230	10700	800	6000	1500	1100	75	45	+2
1240	10700	800	5500	1600	1100	71	39	-4
1300	10700	800	5500	1600	1200	71	39	-4
1315	10700	800	5800	1800	1400	69	40	-3
1340	10700	800	5800	1800	1400	69	40	-3
1400	10700	800	5300	1800	1400	66	35	-8
1430	10700	800	6000	2000	1500	67	40	-3
1445	10700	800	5800	2000	1600	66	38	-5
1510	10700	800	6400	2300	2000	64	41	-2
1530	10700	800	6700	2500	2200	63	42	-1
1545	10700	800	6600	2700	2400	59	39	-4

**Table B14. APPARENT CONTRAST BETWEEN SELF-LUMINOUS TARGETS VIEWED THROUGH AN EXPERIMENTAL WHITE PLUME ON A CLEAR DAY FROM THE EAST AND WEST BETWEEN 3:30 AND 4:15 P.M. AS A FUNCTION OF TRANSMITTANCE**

In-stack trans (T), %	B <sub>1</sub>	B <sub>2</sub>	B <sub>1</sub> '	B <sub>2</sub> '	B <sub>a</sub>	C <sub>a</sub>	T'	E <sub>t</sub>
			(from east)					
20	11000	1000	12000	11000	11000	8	10	-11
30	11000	1000	13000	10000	9800	23	30	+2
40	11000	1000	13000	9300	9100	28	37	+1
50	11000	1000	13000	8700	8500	33	43	-2
60	11000	1000	12000	7400	7200	38	46	-9
70	11000	1000	12000	6300	5800	48	57	-8
80	11000	1000	12000	4700	4400	61	73	-3
			(from west)					
20	10600	700	4600	3000	3000	35	16	-5
30	10600	700	5000	2600	2500	48	24	-4
40	10600	700	5600	2400	2200	57	32	-4
50	10600	700	6300	2100	1800	67	42	-3
60	10600	700	7000	1800	1600	74	53	-2
70	10600	700	7600	1600	1200	79	60	-5
80	10600	700	8400	1300	900	85	72	-4

**Table B15. APPARENT CONTRAST BETWEEN PANEL TARGETS VIEWED THROUGH AN EXPERIMENTAL WHITE PLUME ON A CLEAR DAY FROM THE EAST AND WEST BETWEEN 3:30 AND 4:15 P.M. AS A FUNCTION OF TRANSMITTANCE**

In-stack trans (T), %	B <sub>1</sub>	B <sub>2</sub>	B <sub>1</sub>	B <sub>2</sub> '	C <sub>a</sub>	T'	E <sub>t</sub>
			(from east)				
20	3000	360	15000	14000	6	38	+17
30	3000	360	14000	13000	7	38	+10
40	3000	360	13000	12000	8	38	+2
50	3000	360	12000	10000	17	76	+21
60	3000	360	11000	9100	17	72	+17
70	3000	360	8700	7100	18	61	-4
80	3000	360	6900	5200	25	64	-12
			(from west)				
20	6800	400	3800	2600	32	19	-2
30	6800	400	4000	2300	43	27	-1
40	6800	400	4400	2000	55	38	+2
50	6800	400	4800	1700	65	48	+3
60	6800	400	5000	1500	70	55	0
70	6800	400	5500	1200	78	67	+2
80	6800	400	5800	1000	83	75	-1

**Table B16. APPARENT CONTRAST BETWEEN PANEL TARGETS VIEWED THROUGH AN EXPERIMENTAL BLACK PLUME ON A CLEAR DAY FROM THE EAST AND WEST BETWEEN 3:30 AND 4:15 P.M. AS A FUNCTION OF TRANSMITTANCE**

In-stack trans (T), %	B <sub>1</sub>	B <sub>2</sub>	B <sub>1</sub> '	B <sub>2</sub> '	C <sub>a</sub>	T'	E <sub>t</sub>
			(from east)				
90	2800	350	2900	560	81	96	+5
78	2800	350	2700	720	73	81	+3
69	2800	350	2700	1000	63	69	-2
53	2800	350	2600	1400	46	49	-6
45	2800	350	2600	1500	42	45	-2
33	2800	350	2600	1700	35	37	+1
20	2800	350	2500	2000	20	20	-3
10	2800	350	2200	1700	23	20	+10
			(from west)				
90	12000	500	11000	520	95	91	0
82	12000	500	11000	620	94	90	+7
78	12000	500	10000	620	94	82	+5
68	12000	500	9600	650	93	78	+12
59	12000	500	8400	690	92	67	+6
48	12000	500	7400	740	90	58	+8
40	12000	500	5700	970	83	41	-2
29	12000	500	5500	1000	82	39	+7
19	12000	500	4100	1100	73	26	+4
10	12000	500	3100	1100	65	17	+7

**Table B17. APPARENT CONTRAST BETWEEN SELF-LUMINOUS TARGETS VIEWED THROUGH AN EXPERIMENTAL BLACK PLUME ON A CLEAR DAY FROM THE EAST AND WEST BETWEEN 3:30 AND 4:15 P.M. AS A FUNCTION OF TRANSMITTANCE**

In-stack trans (T), %	B <sub>1</sub>	B <sub>2</sub>	B <sub>1</sub> '	B <sub>2</sub> '	B <sub>a</sub>	C <sub>a</sub>	T'	E <sub>t</sub>
			(from east)					
90	10700	800	10000	1100	400	89	90	-1
80	10700	800	9500	1300	700	86	83	+2
70	10700	800	8500	1600	1100	81	70	-2
60	10700	800	8000	2100	1700	74	60	-2
50	10700	800	7300	2500	1950	66	48	-4
40	10700	800	6600	2700	2400	59	39	-4
30	10700	800	5900	2900	2600	50	30	-3
20	10700	800	4300	3150	2900	27	12	-11
			(from west)					
90	10700	800	9500	930	230	90	87	-4
80	10700	800	8500	1000	300	88	76	-5
70	10700	800	7900	1100	500	86	69	-3
60	10700	800	7100	1300	650	82	59	-3
50	10700	800	6000	1300	800	78	47	-5
40	10700	800	5500	1300	900	76	42	-1
30	10700	800	4500	1300	1000	71	32	-1
20	10700	800	3500	1300	1100	63	22	-1

**Table B18. PLUME-TO-SKY CONTRAST AND AIR-LIGHT OF A WHITE EXPERIMENTAL PLUME WITH 60 PERCENT TRANSMITTANCE WHEN VIEWED THROUGHOUT A CLEAR DAY FROM EAST**

TIME	$B_s$	$B_p$	$B_a$	$C_p$	$T'$	$E_t$	$E_g$
0923	6700	6500	3100	-3	51	-4	
0928	6200	6500	3100	5	55	0	
1110	6400	7200	3100	13	64	+9	58
1123	6200	7400	4100	19	53	-2	60
1215	7000	8200	4300	17	56	+1	62
1219	7300	8200	4200	12	55	0	62
1231	7200	8400	4600	17	53	-2	62
1247	7500	8900	5000	19	52	-3	62
1251	7500	8700	5500	16	43	-12	63
1317	7900	9600	5000	22	58	+3	59
1322	8200	9900	5100	21	59	+4	59
1327	8600	10000	5500	16	52	-3	59
1348	8200	10000	6900	22	38	-17	58
1354	8200	11000	6900	34	50	-5	58
1418	8900	12000	7900	35	46	-9	55
1420	9100	12000	7400	32	51	-4	55
1446	10000	14000	9100	40	49	-6	53
1449	10000	14000	8900	40	51	-4	
1524	13000	18000	12000	38	46	-9	48
1528	12000	18000	12000	50	50	-5	

**Table B19. PLUME-TO-SKY CONTRAST AND AIR-LIGHT OF A WHITE EXPERIMENTAL PLUME WITH 60 PERCENT TRANSMITTANCE WHEN VIEWED THROUGHOUT A CLEAR DAY FROM WEST**

TIME	$B_s$	$B_p$	$B_a$	$C_p$	$T'$	$E_t$	$E_g$
0940	19000	24000		26			45
0942	19000	24000		26			
1030	14000	19000	11000	36	57	+2	52
1037	13000	17000	9900	31	55	0	
1040	13000	19000	12000	46	54	-1	54
1107	11000	15000	8900	36	55	0	
1110	11000	15000	8600	36	58	+3	
1129	9600	13000	7900	35	53	-2	58
1131	9600	12000	7900	25	43	-12	
1215	8400	9900	6300	18	43	-12	
1220	8200	10000	6200	22	46	-9	60
1249	7900	8900	4800	13	52	-3	
1251	8200	9800	5500	20	52	-3	60
1316	7900	8900	4500	13	56	+1	
1318	7900	8900	5000	13	49	-6	59
1347	7600	8500	4600	12	51	-4	
1351	7500	8200	4100	9	55	0	55
1417	7300	8100	4100	11	55	0	
1419	7600	7900	3900	4	53	-2	
1443	7200	7600	3800	6	53	-2	
1445	7200	7600	3800	6	53	-2	
1529	6700	6900	3400	3	52	-3	45
1531	6700	7000	3600	4	51	-4	
1550	6600	6700	3200	2	53	-2	40
1553	6700	6700	3200	0	52	-3	

**Table B20. PLUME-TO-SKY CONTRAST AND AIR-LIGHT OF A BLACK EXPERIMENTAL PLUME WITH 60 PERCENT TRANSMITTANCE WHEN VIEWED THROUGHOUT A CLEAR DAY FROM EAST**

TIME	$B_s$	$B_p$	$B_a$	$C_p$	$T'$	$E_t$	$E_g$
0955	6500	4800	860	-26	61	-1	43
1027	6700	5000	860	-25	62	0	50
1038	6700	5000	860	-25	62	0	
1125	6900	4800	960	-30	56	-6	55
1200	7200	5500	850	-24	65	+3	59
1235	7500	5500	930	-27	61	-1	59
1258	8400	6200	1000	-26	62	0	60
1330	9600	7500	1100	-22	67	+5	59
1410	10000	8200	1400	-18	68	+6	54
1440	11000	8600	1700	-22	63	+1	49
1515	14000	10000	1800	-29	59	-3	45
1550	17000	12000	2300	-29	57	-5	
1600	17000	12000	2400	-29	56	-6	38

**Table B21. PLUME-TO-SKY CONTRAST AND AIR-LIGHT OF A BLACK EXPERIMENTAL PLUME WITH 60 PERCENT TRANSMITTANCE WHEN VIEWED THROUGHOUT A CLEAR DAY FROM WEST**

TIME	$B_s$	$B_p$	$B_a$	$C_p$	$T'$	$E_t$	$E_g$
0910	18500	14400	2120	-22	67	+5	21
0915	18500	14000	1950	-24	65	+3	22
0935	18500	13700	1950	-26	64	+2	26
1000	14700	11000	1710	-25	63	+1	33
1005	15100	11300	1680	-25	64	+2	34
1015	14100	10300	1610	-27	62	0	36
1030	13400	10300	1580	-23	65	+3	39
1045	12700	9250	1410	-27	62	0	42
1100	11700	8900	1230	-24	66	+4	43
1115	10600	7700	1230	-27	61	-1	46
1130	10300	7700	1030	-25	65	+3	48
1145	9400	7200	1030	-23	66	+4	50
1200	8740	6500	960	-26	63	+1	51
1230	7700	5830	855	-24	65	+3	53
1315	6330	5130	720	-19	70	+8	53
1330	6330	4620	735	-27	61	-1	50
1350	5800	4620	720	-20	67	+5	46
1420	5480	3760	635	-31	57	-5	41
1450	5480	3940	547	-28	62	0	34
1510	5120	3760	582	-27	62	0	31
1525	4720	3760	548	-20	68	+6	30

**Table B22. PLUME-TO-SKY CONTRAST AND AIR-LIGHT OF THE WHITE EXPERIMENTAL PLUME WHEN VIEWED FROM THE EAST BETWEEN 3:30 AND 4:15 P.M. AS A FUNCTION OF TRANSMITTANCE**

In-stack trans (T), %	$B_s$	$B_p$	$B_a$	$C_p$	$T'$	$E_t$
96	13000	15000	2700	15	95	-1
93	13000	14000	2100	8	92	-1
88	13000	19000	4800	46		
80	13000	17000	8700	31	64	-12
67	13000	19000	11800	46	55	-7
62	13000	20000	12400	54	58	-1
59	13000	19000	12800	46	48	-6
53	12000	19000	13800	58	43	-5
44	12000	20000	16200	67	32	-8
38	13000	21000	18200	62	22	-12
31	13000	21500	17600	65	30	+1
22	13000	22000	19100	69	23	+1
17	13000	22000	20400	69	12	-7
11	13000	21000	20000	62	8	+3
4	12500	19000	18000	52	8	+4

**Table B23. PLUME-TO-SKY CONTRAST AND AIR-LIGHT OF THE WHITE EXPERIMENTAL PLUME WHEN VIEWED FROM THE WEST BETWEEN 3:30 AND 4:15 P.M. AS A FUNCTION OF TRANSMITTANCE**

In-stack trans (T), %	$B_a$	$B_p$	$B_a$	$C_p$	$T'$	$E_t$
89	6800	6500	1700	-4	71	-18
84	6700	6500	1200	-3	79	-3
82	6500	6300	1400	-3	75	-4
72	6500	6300	1700	-3	71	+4
67	6500	6300	2600	-3	57	-5
58	6600	6400	3100	-3	50	-3
52	6500	6300	3400	-3	45	-2
44	6800	6800	4200	0	38	-2
39	6700	6700	4600	0	31	-5
32	6500	6700	5000	+3	26	-4
24	6700	7400	6000	+10	21	-3
22	6800	7400	6000	+9	21	-1
13	6700	7900	7200	+18	10	-6
4	6700	9600	9200	+43	6	+2

**Table B24. PLUME-TO-SKY CONTRAST AND AIR-LIGHT OF BLACK PLUMES WHEN VIEWED FROM EAST AND WEST BETWEEN 3:30 AND 4:15 P.M. AS A FUNCTION OF TRANSMITTANCE**

In-stack trans (T), %	B <sub>s</sub>	B <sub>p</sub>	B <sub>a</sub>	C <sub>p</sub>	T'	E <sub>t</sub>
		(from east)				
90	16500	15800	450	-4	93	+2
80	17200	15500	1030	-10	84	+3
70	17200	14500	1720	-16	74	+2
60	17500	14100	2300	-19	67	+5
50	17900	13400	3430	-25	56	+4
40	18200	13000	3600	-29	52	+9
30	18500	11700	4120	-37	41	+8
20	18900	10300	4300	-46	32	+9
10	18900	8600	4620	-54	21	+11
		(from west)				
90	6500	6200	103	-5	94	+3
80	6500	5840	343	-10	85	+4
70	6500	5500	480	-15	77	+5
60	6500	5140	650	-21	69	+7
50	6500	4300	755	-34	55	+3
40	6500	4100	857	-37	50	+7
30	6500	3600	960	-45	41	+8
20	6500	2920	1030	-55	29	+6
10	6500	2580	1100	-60	23	+13

**Table B25. AIR-LIGHT AND PLUME-TO-SKY CONTRAST OF THE EXPERIMENTAL WHITE PLUME WHEN VIEWED ON AN OVERCAST DAY AS A FUNCTION OF TRANSMITTANCE**

In-stack trans (T), %	B <sub>s</sub>	B <sub>p</sub>	B <sub>a</sub>	C <sub>p</sub>	T'	E <sub>t</sub>
90	1030	1050	190	+2	83	-7
89	1070	1120	170	+5	89	0
87	1090	1070	140	-2	85	0
83	1600	1560	290	-3	79	-1
83	2000	1950	330	-3	81	+1
78	1080	1030	270	-5	70	-4
70	1220	1060	380	-13	56	-9
68	1080	1080	330	0	69	+6
67	1290	1210	310	-6	70	+8
50	1030	1000	520	-3	47	+2
46	1580	1300	620	-18	43	+1
45	1100	1170	760	+6	37	-4
37	1440	1270	820	-12	31	-3
37	1070	960	620	-10	32	-2
35	1610	1245	690	-23	34	+2
30	1340	1170	860	-13	23	-5
15	1580	1300	1000	-18	19	+2
15	1500	1050	720	-30	20	+3

**Table B26. AIR-LIGHT AND PLUME-TO-SKY CONTRAST OF THE EXPERIMENTAL BLACK PLUME WHEN VIEWED ON AN OVERCAST DAY AS A FUNCTION OF TRANSMITTANCE**

In-stack trans (T), %	$B_s$	$B_p$	$B_a$	$C_p$	$T'$	$E_t$
88	1430	1300	260	-9	73	-16
85	5800	4900	310	-16	79	-7
80	1560	1300	340	-17	62	-19
78	2470	2120	220	-14	78	-1
75	1250	1070	340	-14	58	-16
70	3080	2540	340	-18	71	0
70	3760	2940	380	-22	68	-3
65	3430	2800	450	-18	69	+2
60	2230	1720	310	-23	63	0
58	2820	2060	330	-27	61	+1
55	4100	2940	550	-28	58	+1
50	3150	2200	570	-30	52	0
50	2260	1480	410	-35	47	-5
48	2200	1560	380	-29	54	+4
47	3130	2240	600	-28	52	+3
47	4620	3040	720	-34	50	+1
35	4460	2190	650	-51	35	-2
33	3280	1920	790	-41	34	-1
25	2680	1440	720	-46	27	-1
22	3130	1510	720	-52	25	0
15	2880	1200	690	-58	18	0
13	2880	1310	720	-55	20	+7

## GLOSSARY OF PHOTOMETRIC TERMS

<u>Term</u>	<u>Symbol</u>	<u>Description</u>	<u>Units (MKS)</u>
Luminous energy	$Q_e$	Quantity of light (energy)	Talbot
Luminous density	$q$	Energy per volume	Talbots/meter <sup>3</sup>
Luminous flux	$F$	Energy per time (flux)	lumen
Luminous emittance	$L$	Flux per area	lumens/meter <sup>2</sup>
Luminous intensity	$I$	Flux per solid angle	candle
Luminance	$B$	Flux per solid angle per area	candles/meter <sup>2</sup>
Illuminance	$E$	Flux per area	lumens/meter <sup>2</sup>